Universidade do Minho
Escola de Engenharia

Filipe André Oliveira Barroso

Influence of the robotic exoskeleton Lokomat on the control of human gait: an electromyographic and kinematic analysis

Setembro de 2011

Influence of the robotic exoskeleton Lokomat on the control of human gait: an electromyographic and kinematic analysis
Filipe André Oliveira Barroso
UMinho | 2011

Universidade do Minho
Escola de Engenharia

Filipe André Oliveira Barroso

Influence of the robotic exoskeleton Lokomat on the control of human gait: an electromyographic and kinematic analysis

Dissertação de Mestrado

Ciclo de Estudos Integrados Conducentes ao
Grau de Mestre em Engenharia Biomédica

Trabalho efectuado sob a orientação da
Professora Doutora Cristina P. Santos
Universidade do Minho

Co-Orientador
Juan C. Moreno
CSIC - Madrid

Setembro de 2011

Acknowledgements

I would like to express all my gratefulness to my advisor Cristina Santos, for her continuous and opportune supervising, always paying attention to the detail and giving me important advices to work out this dissertation.

A special word goes to my other advisor Juan C. Moreno. His knowledge and experience in the area were fundamental to this work. He guided me along this period and it was a real pleasure to work with him.

I also want to show gratitude to Anselmo Frizera and Jose Luis Pons, for the opportunity they gave me to work in such an important Research Center as CSIC (Consejo Superior de Investigaciones Cientificas), as well as their supervising during the period before starting this work, which was fundamental to me.

There are no sufficient words to express my gratitude to my friends and colleagues working on CSIC, which were the individuals studied on this work and performed the experiences very well. Without their collaboration, it would be impossible to do the experiments.

Finally, I want to thank to my family and friends all the support they have given me during the life, especially because they always believe in my work.

Abstract

Nowadays there is an increasing percentage of elderly people and it is expected that this percentage will continue increasing. This aging of the population carries huge costs to the government, especially in the provision of health care. Among those health care, there is the motor rehabilitation after a stroke. The recent robotic devices for gait training are pointed out as an excellent solution to solve this problem, because besides the cost savings they can provide longer and more innovative trainings. All the advantages presented by such devices can trigger more research in this area as well as more government investments.

There are already some control strategies implemented in these devices, which should be improved to create new motor rehabilitation interventions. One strategy that can be used in the future is to provide the amount of motor assistance as the patient really needs to achieve certain goals. Lokomat is one of these rehabilitation devices, which allows changing the percentage of assistance provided to the user. However, it is necessary to study the effects of such strategy in the physiological response of the users.

There is more and more consensus about the need to obtain muscular activation patterns and kinematic patterns during walking in devices as Lokomat very similar to those obtained by healthy subjects during non-assisted walking. Recent scientific investigations make us to believe that the nervous system controls human gait via a simple modular structure. It is important to understand how this structure works when the walking is assisted by robotic devices.

Thus, this work had three main objectives: to study the muscular electric activity during walking in Lokomat, by varying the total assistance provided by the device, as well as the walking speed; to analyze kinematic changes obtained during Lokomat-assisted walking, as well as the interaction forces between each user and the robotic device; to understand how this modular organization of the nervous system involved in synchronization of the muscular activity works during walking assisted by robotic devices. Only healthy subjects participated in our study. Therefore, our work generated a basis of comparison for future control strategies to be implemented in motor rehabilitation.

We obtained quite encouraging results, which allow us to formulate new strategies for motor rehabilitation. In the future, these strategies will be implemented and it expected that post-stroke people can restore their normal gait more quickly.

Resumo

Actualmente verifica-se um aumento crescente da percentagem de pessoas idosas e prevê-se que essa percentagem continue a aumentar. Este envelhecimento da população acarreta enormes custos para o estado, sobretudo na prestação dos cuidados de saúde. Entre esses cuidados, está a reabilitação motora após um AVC (acidente vascular cerebral). Os novos dispositivos robóticos de treino da marcha são apontados como uma excelente solução para este problema, pois além da poupança de custos poderão proporcionar treinos de maior duração e mais inovadores. Todas as vantagens apresentadas por este tipo de dispositivos podem servir para o despoletar de cada vez mais investigação nesta área e investimentos governamentais.

Existem já algumas estratégias de controlo implementadas nestes dispositivos, que devem ser melhoradas para se criarem novas intervenções de reabilitação motora. Uma estratégia que se poderá utilizar futuramente nesses dispositivos consiste em providenciar somente a ajuda motora necessária para que o paciente atinja determinados objectivos. O Lokomat é um destes dispositivos, que permite variar a percentagem de ajuda providenciada. É no entanto necessário estudar os efeitos de tal estratégia na resposta fisiológica dos utilizadores.

Cada vez se verifica maior consenso acerca da necessidade de se obterem padrões de activação muscular e padrões cinemáticos durante a marcha em dispositivos como o Lokomat muito similares aos obtidos por indivíduos saudáveis em marcha não assistida. Recentes investigações científicas levam-nos a crer que o sistema nervoso controla a marcha humana através de uma estrutura modular simples. É importante saber como actua essa estrutura quando a marcha é assistida por dispositivos robóticos.

Assim, este trabalho teve três objectivos principais: estudar a actividade eléctrica muscular durante a marcha em Lokomat, variando a ajuda total providenciada pelo dispositivo, bem como a velocidade da marcha; analisar as diferenças cinemáticas obtidas durante a marcha em Lokomat, bem como as forças de interacção entre cada usuário e o dispositivo robótico; perceber como actua a organização modular do sistema nervoso envolvida na sincronização da actividade muscular durante a marcha em dispositivos robóticos. Apenas indivíduos saudáveis participaram neste estudo. Assim, este estudo gerou uma base de comparação para futuras estratégias de controlo utilizadas em reabilitação motora.

Os resultados foram bastante animadores e permitam-nos formular novas estratégias de reabilitação motora. No futuro, estas estratégias serão levadas a cabo de modo a que pessoas afectadas por AVCs possam restabelecer mais rapidamente a sua marcha normal.

Contents

List of Figures

List of Tables

Chapter 1

Introduction

This dissertation presents the work developed in the second semester of the 2010-2011 year, in the scope of the fifth year of the Integrated Master in Biomedical Engineering.

To introduce the reader to this dissertation, it is important to briefly explain four concepts of the title: an *exoskeleton* is a mechanical device externally attached to the user's body that operates according to the user's movements or intentions thereby assisting or increasing the user's performance; *gait* is the way of moving the body from one place to another, by moving on feet in a synchronized order or rhythm; *electromyography* is the recording of the electric activity of the muscles; *kinematics* is the branch of Classical Mechanics that describes the movement of objects or groups of objects. In our study, kinematics were used to describe the gait in terms of joints angles.

The main goal of this work is to study the muscular electric activation and kinematic patterns obtained during the walking in the rehabilitation device Lokomat, changing the speed and the guidance force (the amount of aid the patient receives during the walking). Changing the guidance force applied by a rehabilitation device can be a new control strategy to be implemented in motor rehabilitation. After statistically analyze the data from the experiments, the aim was to try to study the organization of the nervous system involved in the synchronization of muscular activation during human walking.

All the procedures, analysis and conclusions are detailed in this dissertation.

1.1 Motivation and Objectives

The number of people with disabilities in the lower limbs is increasing. Nowadays, about 20% of the world population is over the age of 65 and this percentage is expected to increase

above 35% by 2050. This demographic variation will impose a higher overload in health care to deal with the risks associated with the aging [4]. Robotic devices are a great solution that can solve the majority of those issues thereby allowing the elderly to recover their independence, maintaining the life style. The interest in using robotic devices to assist people after neurologic injuries is increasing, but control strategies of these devices must be improved in order to provide better therapy trainings to the patients [56].

Lokomat is a worldwide commercialized robotic device for therapy training. Due to the knowledge and experience acquired by Bioengineering Group in CSIC working with Lokomat, it was proposed to start a new research with Lokomat in the second semester of 2010-2011, in the scope of the European Project BETTER (Brain-Neural Computer Interaction for Evaluation and Testing of Physical Therapies in Stroke Rehabilitation of Gait Disorders). We started an analysis of the muscular function during human walking in Lokomat in order to define new interventions for rehabilitation. This was done by acquiring and studying electromyographic patterns of lower limb muscles, as well as the joints mechanical performance (kinematics and forces) during the gait assisted by this rehabilitation device. Parameters like the guidance force and the speed provided by the machine to the user were changed. Only healthy individuals were studied. The last goal of this work was to analyze the modular organization of nervous system involved in the synchronization of muscular activation during human walking assisted by a robotic exoskeleton designed for therapy. The results of this study developed during the second semester are exposed on this dissertation.

In the future, the objective is to apply all the knowledge and experience obtained during this work to develop novel means to ambulatory monitor and rehabilitate people with gait disabilities by means of improved wearable sensing and exoskeletons technologies that are suitable for gait retraining.

Because we want this work to be read by people around the world interested in this area and also continue it in the future, we decided to publish this dissertation in English, the worldwide used language to publish scientific articles, and not in Portuguese, which is my mother language.

1.2 Outline

This dissertation is composed by nine chapters.

Chapter 1 describes the motivation of this work and introduces the reader to the basic

concepts and the objectives of this dissertation.

Chapter 2 presents the state of the art in measuring muscular electric activity and kinematics. The most recent rehabilitation devices and orthoses are also introduced, including the one used on this work. Finally, it is referred the theory about the existence of a modular control of the nervous system to coordinate the human gait.

The physiological mechanisms involved in the production of movement are detailed in Chapter 3. The generation of action potentials, which encode orders from the nervous system that results in muscular contractions, are also explained.

Muscular activity can be recorded by electromyography systems. In Chapter 4, the recommendations for the best procedures to be taken in order to record the muscular electric activity are mentioned. According to electromyographic recordings, it is possible to make conclusions about the physiological mechanisms occurring in different conditions of gait walking.

Chapter 5 is devoted to the analysis of the typical electromyographic activity and kinematics during normal gait, as well as when the gait is assisted by robotic rehabilitation devices.

Chapter 6 introduces the theory that supports the existence of synergistic control of muscles for generation of limb movement, as well as the possible existence of low-dimension organizational structure of the nervous system, which may be the basis of the neuromechanical output during walking and some other different tasks.

The followed protocol to measure muscular electric activity and kinematics from the participants along the trials is referred in Chapter 7. The applied signal processing techniques are also mentioned.

Data analysis and results are presented in Chapter 8. In particular, special emphasis is given to the results with respect to the average group, complemented with the statistical tests. The achieved results of this work are also discussed in detail in this chapter.

The conclusions of this work are made in Chapter 9. Finally, the proposals to continue this work in the future are written in this chapter too.

1.3 Publications

During this year, it was possible to publish two different articles in International Conferences, both of them related with this dissertation:

Barroso, F. O.; Moreno, J. C.; Santos, C.; Pons, J. L.; "*Preliminary evaluation of mechanical effects of robotic guidance during walking*"; International Bionic Engineering Conference 2011; Boston, USA; 18-20 September 2011

Barroso, F.; Frizera, A.; Santos, C.; Ceres, R.; "*Revisão crítica das ortóteses activas para membros inferiores* (Critical review of active orthoses for lower limbs)"; VI Congresso Iberoamericano de Tecnologías de Apoyo a la Discapacidad, Palma de Mallorca, Spain; 16-17 June 2011

Together with my advisors and other researchers from BETTER project, we are also preparing the submission of a scientific paper called '*Effects of robotic guidance on the activation and organization of muscle synergies during robot-aided treadmill walking*' for *Journal of NeuroEngineering and Rehabilitation*.

Chapter 2

State of the art

First, it is important to refer the procedures and the employed equipment to record electric activity from the muscles, as well as the kinematics during the human walking. Then, the most recent rehabilitation devices are presented, especially Lokomat, which was the one used during the experimental trials. Recent studies indicate that a relatively low-dimensional organizational structure may be the basis for the complexity of the neuromechanical output of the human walking. Theoretical formulations and experimental evidences in this regard are presented in the last section of this chapter.

2.1 Electromyography

The Human motor system is controlled by different mechanisms in the Nervous System, which results in all the movements people can perform during their daily life. The Nervous System is divided in the Central Nervous System (CNS), constituted by the brain and the spinal cord, and the Peripheral Nervous System (PNS), constituted by the nerves. Motor commands generated in the CNS are sequences of electric signals, called action potentials, which travel through the nerves in direction to the effectors (muscles or glands).

Muscle tissue conducts actions potentials in a similar way nerves do, resulting in the muscular contractions. These potentials propagated along the muscular tissues are signals that can be recorded by a method called electromyography (EMG). Mainly, two types of electrodes are used to record muscle signals: invasive (needle) and non-invasive (surface). Surface electromyography (sEMG) is electromyography using surface electrodes, a method worldwide used nowadays [75].

Electromyography has many possible clinical and biomedical applications [75], like for

example the exploration of the physical integrity of the motor system and the study of muscle activation during walking. It can also be used to study motor control, neuromuscular physiology, gait disorders and postural control, among other applications. The first study about the use of sEMG for treatment of specific disorders was done in 1966 by Hardick and his researchers [17]. In the early 1980s, Cram and Steger introduced a clinical method to study muscle activations using an EMG device [17]. Nowadays, electromyography is used mainly to study muscles performance, for rehabilitation purposes, training and biofeedback (feedback using biological signals) for patients [57].

Raw EMG signal is usually processed to be a useful way of information. Several signal processing techniques can be applied on raw EMG, depending on the purpose of the analysis. These methods can be Wavelet analysis (a suitable method for the classification of EMG signals [49]); some artificial intelligence techniques based on neuronal networks [71]; techniques to extract the common features of EMG signals [40] [12]; compute EMG envelopes [18], a technique that allows researchers to understand the level of activity of each studied muscle; and many other techniques.

EMG signals usually contain noise and movement artifacts. It is necessary to implement advanced methodologies to record the correct signals. The most recent devices for recording EMG information can atenuate such a noise, even the interference from the 50 Hz power line interference and its harmonics. It is also important to use a very powerful equipment of acquisition and to do the correct signal processing, in order to obtain better EMG signals. Nowadays, users can handle the recording device and upload the recordings to a PC later. These devices can also transmit data online via wireless. Many of them have also touch screen, acting as a form of interaction with the patient.

Examples of sEMG systems available on the market are *BTS Bioengineering* (Milan, Italy), *Biometrics Ltd* (Newport, United Kingdom), *NORAXON* (Scottsdale, USA), among others. For the experiments performed on this work, it was used the Pocket EMG equipment from BTS Bioengineering (see Figure 2.1), an equipment with 16 electromyograph channels that allows to record sEMG from 16 body locations at the same time.

2.2 Kinematics

Kinematics is the branch of Classical Mechanics that describes the movement of objects or groups of objects. The knowledge of human kinematics during gait walking is very im-

Figure 2.1: Pocket EMG equipment used in the trials

portant and it has been done using different techniques [46]. There are several equipments to measure human movement. Electrogoniometers are probably the simplest and cheapest method, but the one with more limitations to obtain accurate results. The most basic consists in a potentiometer mounted on two brackets strapped to the body segments either side of the joint. Each voltage value obtained in the potentiometer corresponds to an angular value of movement. Biometrics Ltd sells flexible electrogoniometers, without the need for alignment with joint center (see Figure 2.2). Biometrics electrogoniometers were used on this work. It is possible to obtain three-dimensional information with these devices, but they are mainly used for two-dimensional analysis. Electrogoniometers cannot record absolute motion of the body segments, but simply the relative motion of body segments.

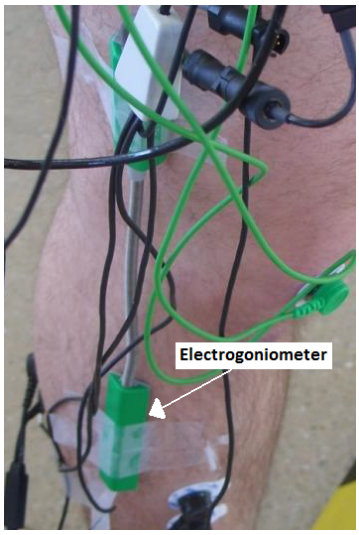

Figure 2.2: Electrogoniometer used during the trials

If the purpose of research is to measure absolute motion of body segments, measurements must be taken with respect to a fixed global reference system. There are four basic ways to achieve this goal and it is to use one of the following systems that captures motion:

- Optical: *Vicon Motion Systems* (Oxford, UK), *BTS* (Milan, Italy), *Motion Analysis Corp.* (Santa Rosa, CA, USA).
- Ultrasonic: *Zebris* (Zebris Medizintechnik GmbH, Tuebingen, Germany).
- Inertial: *Technaid* (Madrid, Spain).
- Electromagnetic: *FasTrack* (Polhemus, USA).

Throughout this dissertation, it is sometimes referred or presented results from kinetic analysis, in order to complement kinematic analysis. Kinetics is the study of the forces acting on a system, as the human body for example [29]. Kinetic movement analysis is the study of the forces that cause movement (such as those working in the joints of the hip, knee or ankle to allow the human walking, for example) and it is more difficult to perform than a kinematic analysis and it is also more difficult to understand because the forces are not visible. We can only see the effects of the application of a force. The determination of the forces acting during walking is usually performed by estimation[1] and it can be inaccurate [29]. Kinetic analysis is usually performed through parameters like forces, torques[2] or moments acting in the body's joints. In this study, we didn't performed kinetic analysis during treadmill walking. However, the forces of interaction between the subjects and Lokomat at the knee and hip joints were recorded from the analog output of Lokomat.

2.3 Rehabilitation and Assistive Devices

Strokes or spinal cord injuries that people may sometimes have, generate lesion to their nervous system that disrupts the normal motor commands for limb movement. Even though this phenomenon kills nervous cells, nervous system can reorganize itself, an event called plasticity [81]. Motor rehabilitation after an event like a stroke, for example, can spark

[1] There are software that calculate joint kinetics by inverse dynamics analysis [44] [45]

[2] Torque (also called moment or moment of force) is the tendency of a force to rotate an object around an axis. If we imagine a force as being a push or a pull, we can think a torque as being a twist

plasticity, modulating cortical organization, and in the most successful cases leading to a total recovery of the damaged/lost functions.

The number of people with disabilities in the lower limbs is growing. This demographic change will impose a higher overload in health care to deal with the risks associated with the aging [4]. Robotic devices are a solution that can solve the majority of those issues and allow the older people to maintain their independence and their quality of life. Therefore, there is a huge potential on using robotic devices for motor rehabilitation purposes. Individuals who received body-weight supported treadmill training after a stroke or spinal cord injury got better electromyographic activity during locomotion and also obtained better recovery results than the others who received conventional gait training [34] [95]. Robotic devices can automate and repeat the trainings, and with unlimited duration of time, representing a more effective and a cheaper form of rehabilitation.

Robotic devices for rehabilitation purposes can be divided in static devices and portable exoskeletons or orthoses.

2.3.1 Static devices

During the last years, the use of manual-assisted treadmill training in neurorehabilitation programs is increasing. Manual-assisted treadmill training has a major disadvantage: it usually requires many therapists to perform the training, which results in increased costs. Besides, these trainings are short in time due to the effort therapists need to do. Therefore, robotic devices that automate these trainings, allowing for extended trainings and providing a body-weight support system have been created. These robotic devices are usually static (placed in motor rehabilitation clinics), guaranteeing safety, repeatability, unlimited duration of training and adapting the gait to the type of patient and pretended training [36]. Lokomat and LOPES are examples of such devices.

Hocoma AG created Lokomat (see Figure 2.3), a robotic exoskeleton to automate the motor training of lower limbs, which is commercialized all over the world. Lokomat is composed by a treadmill and a body-weight support system. It has four degrees of freedom, allowing the movement control of hip (one degree of freedom in the left hip and other in the right hip) and knees (one degree of freedom in the left knee and other in the right knee) in the sagittal plane (see human body planes of reference on section 4.3.1) [13]. During the trainings, the feet stay in neutral position because of the footlifters[3] that the patient needs to

[3]Footlifter consists in a loop fastened around the foot during Lokomat walking, keeping the foot in a neutral

put on (see figure 2.3-(B)). Footlifters have to be correctly fastened to the feet in order to guarantee that they will pull the feet up sufficiently in the swing phase so that the feet do not touch the treadmill. The trajectory, the speed and the percentage of assistance used in Lokomat is totally programmable.

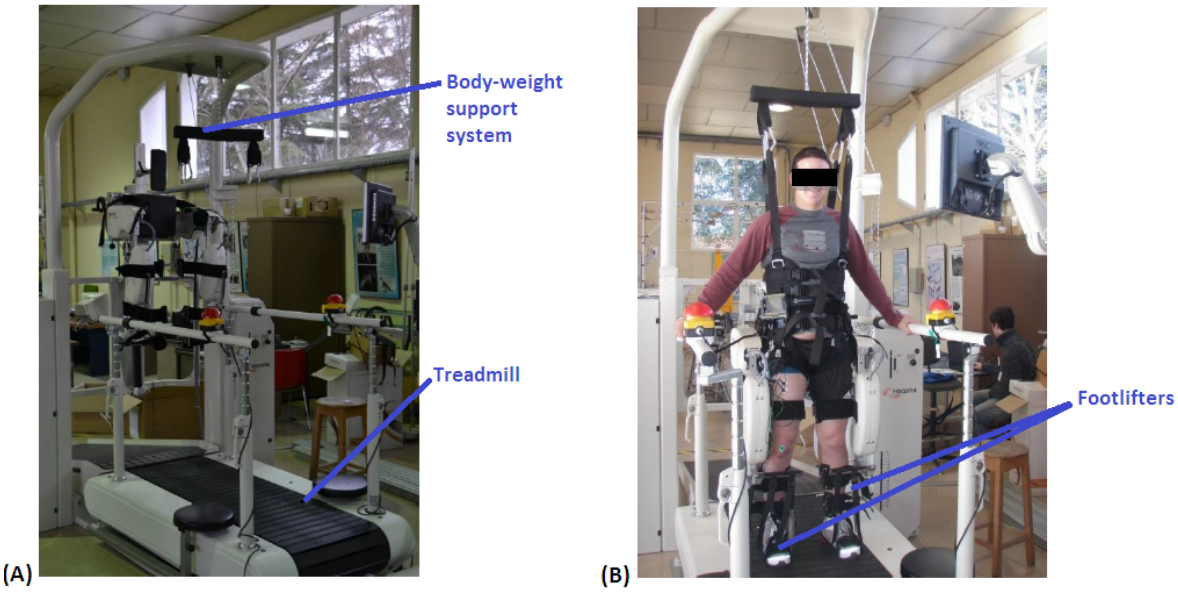

Figure 2.3: (A) Lokomat and its treadmill and body-weight support system; (B) Subject performing a trial on Lokomat

One important feature of Lokomat is the applied guidance force (the amount of aid the patient receives during the walking). A value of 100% of guidance force corresponds to a strict guiding (position control with stiff Lokomat joints) of the exoskeleton. A value of 0% corresponds to free run mode (easily moveable Lokomat joints). Reducing the guidance force allows the user to move more freely and actively, *i.e.*, the user can move away from the defined gait pattern. Providing too much assistance (or guidance force) can have negative consequences for motor learning [56]. What may be important for rehabilitation purposes is to provide assistance as needed or in other words, to assist the patent only as much as is needed to accomplish the tasks. Results of a pilot study [96] suggested that Lokomat training may have advantages over manual-assisted treadmill training following a modest intervention dose in chronic hemiparetic persons. There is the need of more research studies to prove if actual robotic therapy is effectively more efficient than manual-assisted treadmill training in persons with gait disorders. There is a lack in actual robotic therapy, because it is not designed and adapted according to the muscular coordination of the patient. Therefore,

position and preventing it from getting caught in the treadmill while walking

future robotic therapy exoskeletons will certainly include this principle and will probably result in better therapy results. Lokomat was the robotic exoskeleton chosen for this work and we changed the guidance force during the trials. We also changed the speed to study its influence in muscular activation.

LOPES (LOwer extremity Powered ExoSkeleton) is another exoskeleton that was recently developed. It differs from Lokomat in the sense that it has more degrees of freedom [92]. Beyond the same four degrees of freedom existing in Lokomat, LOPES allows the translation of pelvis in the transverse plane and also the abduction and adduction of the hip in the coronal plane. These extra degrees of freedom can be important to this kind of training, because the addition of pelvic motion can be benefic for rehabilitation [3] [38].

2.3.2 Portable Exoskeletons and Orthoses

Exoskeletons and orthoses can be defined as mechanical devices worn by the user and fit to the body, working according to the user's movements or intentions. Generally, the term *exoskeleton* is used to describe a device capable of increasing the performance of the user, whereas the term *orthoses* is typically used to describe a device used to assist people with pathologies associated with the limbs. These devices differ from the static orthoses, essentially because they allow training to take place any where (at home for example) and at any time, allowing the training to be more effective and takes less time to complete [4]. The greatest handicap of the use of exoskeletons for rehabilitation purposes is still the autonomy, because the battery needs to be very large to allow many hours of durability.

The research group of University of Michigan led by Daniel Ferris has been examining the biomechanics and energetics of human locomotion with powered (by artificial pneumatic muscles) lower limb exoskeletons, controlled by myoelectric signals [25] [80] [9] [45]. These exoskeletons allow the selective manipulation of artificial flexor and extensor strength and relate their force to the changes in metabolic energy consumption. The results can give a new insight about the mechanical actions and functions of lower limb muscles during walking and running. This research group pretend to build bilateral hip-knee-ankle-foot orthoses to assist gait rehabilitation after stroke or spinal cord injury.

The Israeli company Argo Medical Technologies developed the Rewalk (figure 2.4), an exoskeleton that will allow walking in paraplegic people. Therefore, simple tasks for healthy people, like for example climb stairs, walk and drive could be possible for paraplegic people using this exoskeleton. This exoskeleton is light and composed by DC motors at the joints,

rechargeable batteries (placed in the back side of the body), a support for the upper limbs, an array of sensors interacting with the user and computer-based control system. Rewalk detects the upper-body motions and those movements are analyzed and used to program the gait patterns. In order to maintain the stability and safety of the procedure, the user has to use crutches to assist his gait. Rewalk presents a long battery life.

Figure 2.4: Rewalk^{TM}. Courtesy of Argo Medical Technologies Ltd

2.4 Modular organization of the motor system

Human walking presents considerable variability step to step and is highly complex in terms of neural activation and biomechanical output [12]. The correct execution of voluntary movements relies on the functional integration of many different parts of the CNS. Several cortical areas of the brain produce neural signals that travel along the spinal motorneurons, which activate several muscles, resulting in the purposeful motor behaviors [11] [76].

The importance of the cortical areas in motor control underlies the clinical observation that neurologic lesions after a stroke can severely affect the generation of voluntary movements. There is now evidence indicating that a low-dimensional modular organization may be the basis for the neuromechanical output [12] [11].

Recent studies have been trying to understand how the central nervous system produce the neuronal responses corresponding to the planned movements, coordinating a large num-

ber of degrees of freedom of the musculoskeletal system [12] [87] [50] [64] [19] [40] [10] [41] [39].

The concept of synergies was first proposed by Bernstein [6] in 1967, as a strategy for grouping output variables to simplify control. A muscle synergy (also referred as motor module) is a set of positive levels of muscle activation [88] and each synergy is activated by a positive activation signal. The total activation of each muscle along the time is the sum of the contributions from all the activation signals, weighted by synergies. This fact can be useful for movement restoration by using, for example, FES (functional electrical stimulation) if a limited set of synergies can describe several functional tasks. Although different names have been referred to describe this modular organization, the concept is similar for all the researchers.

In 1985, Patla [72] applied Principal Component Analysis (PCA) to investigate if the EMG patterns could be described by a few underlying components and concluded that an appropriate combination of few activity patterns could result in the observed motor activity.

Davis [20] used PCA to analyze EMG data and concluded that some combinations of four basic patterns could reconstruct EMG activity of 16 leg muscles during locomotion.

Some experimental studies have shown that muscle activation patterns during natural behaviors may be organized in motor modules during locomotor and postural tasks [69] [91] [39] [40]. Some other studies have shown direct correlations between the activity of motor modules with kinematic outputs [87] [89].

Clark et al [12] suggested a common modular organization of muscle coordination underlying walking in both healthy and post-stroke individuals. His research group found that the poorer walking performance in post-stroke survivors is related with damaged modules and that less healthy modules result in an overall reduction of the complexity of locomotor control.

Recent computer simulations [59] [63] [64] showed that walking can be produced through the coordinated activation of few motor modules, each one associated with specific biomechanical subtasks.

Robotic assisted walking can be used to induce synergistic activation patterns during walking that might be beneficial for the recovery of stroke survivors. After researchers identify all the activation signals and motor modules in healthy people, it will be possible to monitor locomotor impairments in patients with neurologic injuries and design specific training for those populations.

One of the goals of this study is to verify our hypothesis that walking under variations of robotic guidance force and gait speed can be represented by a reduced number of motor modules and activation signals. All the procedures performed to achieve that goal are detailed in Chapter 6.

The next chapter details the physiological mechanisms underlying the motor control.

Chapter 3

Human mobility

The correct execution of body movements, specially the walking, depends on the correct working of the Nervous System and the Muscular System. The physiological mechanisms involved in the production of movements are detailed in this chapter.

3.1 Nervous System

The nervous system is a vital system of the human body, which supports, maintains and regulates the body functions. It is divided in central nervous system (CNS) and peripheral nervous system (PNS), as we can see in the figure 3.1.

3.1.1 Central nervous system and Peripheral nervous system

The CNS is constituted by the brain and spinal cord, which are both protected by the involved bones. The brain is located inside the cranium box and the spinal cord is located inside the spinal channel, formed by the vertebras. The brain and the spinal cord are in continuity one with the other by the occipital hole [90].

The peripheral nervous system consists in sensorial receptors, nerves, ganglions and plexus. The sensorial receptors are terminations of the nervous cells or isolated cells, specialized, which detect temperature, pain, tact, pressure, light, sound, odors and other stimulus. These sensorial receptors are located on the skin, muscles, articulations, intern organs and specialized sensorial organs like the eyes and the ears. The nerves are sets of axons (the definition and description of an axon is done in section 3.1.2.) with their sheaths which link the CNS to the sensorial receptors, muscles and glandules. The ganglia are agglomerations of neural cellular bodies located in the exterior of the CNS. The plexus are extensive networks

of axons and, in some cases, neural cellular bodies located in the exterior of the CNS [90].

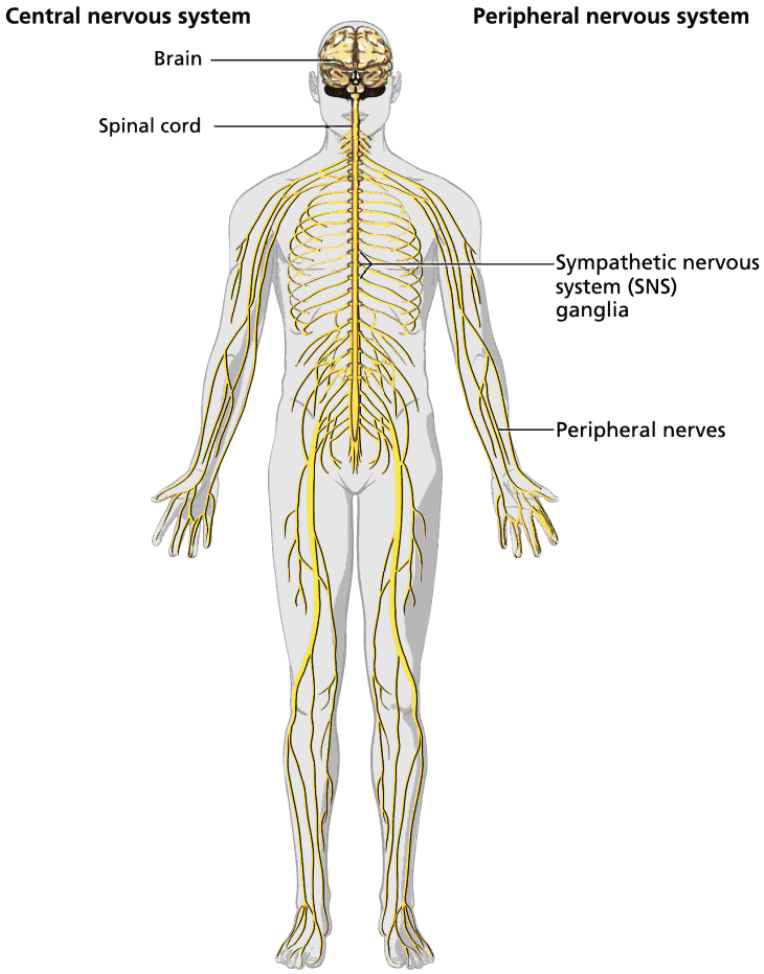

Figure 3.1: The central nervous system consists of the brain and spinal cord, whereas the peripheral nervous system consists on the peripheral nerves, nerves, ganglions and plexus. Used with permission from © Infobase Learning [23].

PNS can be functionally and structurally divided into somatic nervous system and autonomous nervous system. The somatic nervous system controls the voluntary movements whereas the subconscious control and the involuntary movements are controlled by the autonomous nervous system.

3.1.2 Neurons

The nervous system is constituted by neurons (see figure 3.2) and non-neural cells. The neurons receive stimulus and conduct electrical signals called action potentials (a complete definition and description of an action potential is done in section 3.2.). The non-neural cells are called neuroglia.

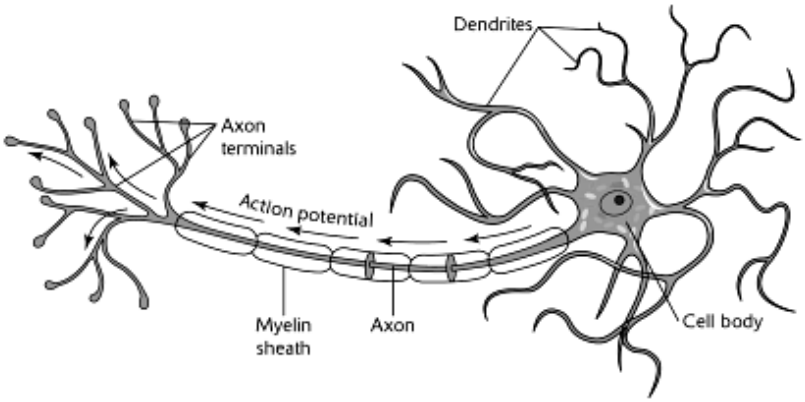

Figure 3.2: Representation of a neuron. Used with permission from [30]

A neuron is constituted by a cell body (or soma), dendrites and an axon. Dendrites are filaments of the neurons, specialized in the reception of nervous stimulus. The axon is the part of the neuron responsible for the conduction of the electric impulses generated in the cell body, to another place like another neuron or a muscle. Therefore, neurons receive stimulus and transmit action potentials to another neurons or to the effector organs. They are organized to form complex networks that perform the functions of the nervous system. They are classified according to their function, considering the direction of the action potentials they conduct. The afferent (or sensorial) neurons conduct the action potentials to the CNS and the efferent (or motor) neurons conduct the action potentials from the CNS to the muscles or glands. The interneurons conduct the action potentials from one neuron to other, inside the CNS (see figure 3.3) [84].

Motor neurons are neurons in the brain, brain stem (region in the brain that connects the brain with the spinal cord - see figure 6.1) and spinal cord that control movements of muscles. There are two types of motor neurons: upper motor neurons and lower motor neurons. The upper motor neurons are in the motor cortex of the brain. These neurons connect with the lower motor neurons in the brain and the spinal cord. Lower motor neurons connect with the muscles on face, chest and limbs, exerting direct control over muscle contraction. Therefore upper motor neurons are involved in the initiation of the voluntary movements and the maintenance of appropriate muscle tone. If the upper motor neurons are damaged, the limbs will become spastic (characterized by spasms or convulsions) and the reflexes will be exaggerated. If the lower motor modules are lost, the muscles will become weak and wasted and reflexes may disappear [60].

An action potential propagates quickly in a motor neuron, from the cell body within the CNS to the skeletal muscle along the axon of the neuron. As the axon approaches a muscle,

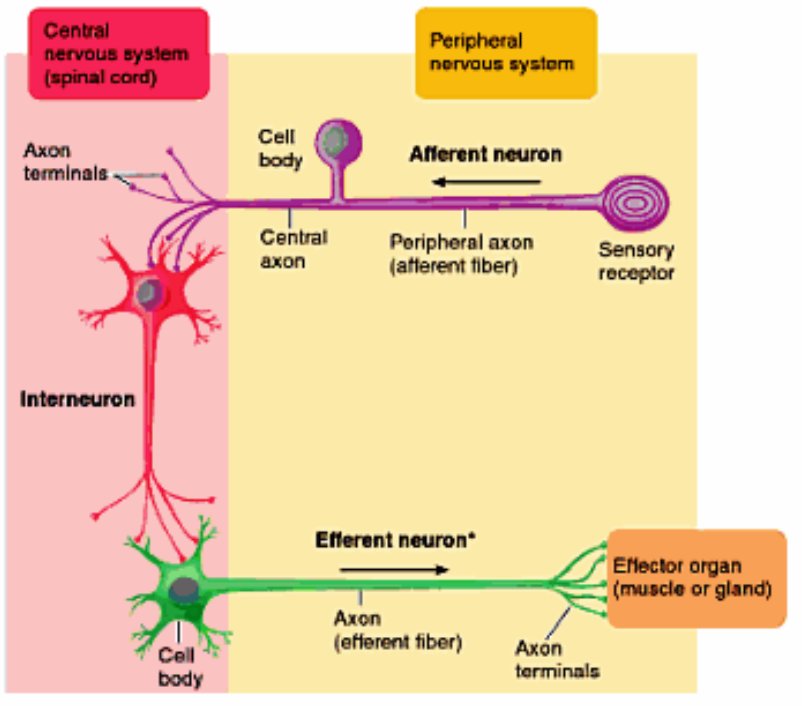

Figure 3.3: Location of the three types of neurons [84].
Reproduced by permission. www.cengage.com/permissions

it divides into several terminal branches (axon terminals). Each of these axon terminals forms a special junction, called neuromuscular junction, with one of the several muscle cells that compose the whole muscle (see figure 3.4). Some scientist refer to the neuromuscular junction as a 'motor end plate' [83]. Therefore, these two terms will be used interchangeably throughout this document. The following section explains what an action potential is and how it is propagated.

3.2 Creation of Action Potentials

Action potentials are electrical signals generated and propagated along the cells. The action potentials are important means by which the cells transmit information from one part of the body to another. For example, stimulus like the light, the sound and the pressure act on specialized sensorial cells in the eye, the ear and skin to produce action potentials, which are conducted from those cells to the spinal cord and the brain. The action potentials created in the brain and the spinal cord are conducted to muscles and some glands in order to regulate their activities [90].

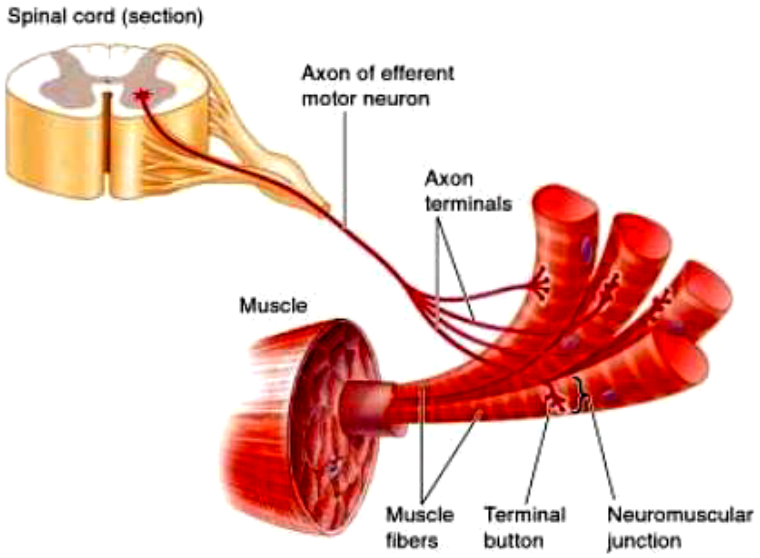

Figure 3.4: Motor neuron innervating skeletal muscle cells. The axon travels through a spinal nerve to the skeletal muscle it innervates. When the axon reaches a skeletal muscle, it divides into many axon terminals, each of which forms a neuromuscular junction with a single muscle cell [84]. Reproduced by permission. www.cengage.com/permissions

3.2.1 Membrane Resting Potential

A typical neuronal cell membrane is represented in figure 3.5. The membrane is semipermeable because it is selective, just allowing some ions to pass through it [79]. The composition of the extracellular fluid is different from the intracellular fluid. The intracellular fluid has a high concentration of potassium (K^+) ions and molecules with negative charge (A^-), like proteins and others with phosphate. The K^+ ions are small enough to pass through the channels in the membrane, but the A^- ions are large to pass the membrane. The extracellular fluid has a high concentration of sodium (Na^+) and chloride (Cl^-) ions. The Cl^- ions are small enough to pass through the membrane channels, but the Na^+ ions are larger and have difficulty in passing through the channels.

Intracellular and extracellular fluid are almost neutral, because they have a similar number of anions and cations. However, there is an unequal charge distribution between the immediately adjacent region to the interior and exterior of the cell membrane. This electric charge difference between the interior and the exterior of the membrane is called potential difference. In non-stimulated or resting cells, this potential is about -70 to -90 mV and it is referred as membrane resting potential.

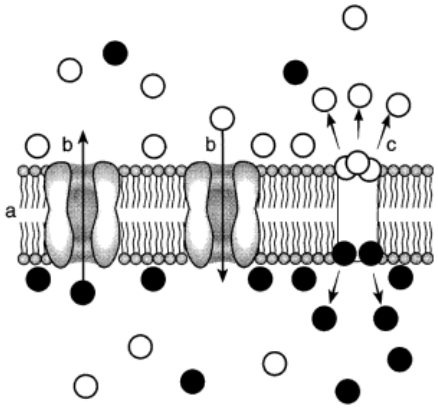

Figure 3.5: Two essential components of a neuronal cell membrane are (a) the phospholipid bilayer and two classes of macromolecular proteins: (b) ion channels and (c) ion transporters. (b) A difference in concentration of an ion across the plasma membrane will result in a net movement through ion channels away from the side of higher concentration to the side of lower concentration by passive transport know as diffusion. (c) An ion transporter is a pump working in the opposite direction of the concentration gradient. Inserted from [14], with kind permission of Springer Science+Business Media

3.2.2 Ion channels

The transmission of information along neuronal axons is mediated by instantaneous changes in membrane potential called action potentials. These changes in membrane potential occur when the charge gradients maintained by the membrane are allowed to flow unimpeded through ion channels. Ion channels are selective for specific ions, not allowing the others to pass. In the resting state, these ions channels are closed.

Ion channels only open when ligands bind to receptors - *ligand-gated ion channels* - or in response to changes in membrane potential - *voltage-gated ion channels*. Among ligand-gated ion channels, certain ligands, called *excitatory neurotransmitters*, open cation channels that depolarize (increase the potential difference) the membrane and increase the probability of the generation of an action potential. Other ligands, called *inhibitory neurotransmitters*, open Cl^- channels that hyperpolarize (decrease the potential difference) the membrane and decrease the probability of generation of an action potential. The combined activation of several ligand-gated channels is needed to trigger an action potential [79].

3.2.3 Action potentials

When an action potential occurs, the membrane potential changes (see figure 3.6). The first step to generate an action potential is the moment when ligand-gated ion channels open, letting the Na^+ ions to enter in the cell and gradually make the inner surface of the membrane to be less negatively charged in relation to the outside. When this charge is approximately

-50 mV, the adjacent voltage-gated Na^+ channels open. The inward flow of Na^+ quickly depolarizes the membrane and initiates an action potential, which propagates itself along the membrane by sequentially triggering adjacent voltage-gated Na^+ channels. The action potential is a brief wave of membrane potential that moves along an axon (figure 3.6).

At the peak of the action potential (approximately +30 mV), the Na^+ channels quickly close. After this peak, voltage-gated K^+ channels open. K^+ ions flow out of the axon because they are much more concentrated inside than outside. Once these K^+ channels are still opened, K^+ ions leave the inside and drive the membrane to a temporary hyperpolarization (figure 3.6 - (8)). Finally, K^+ channels close, the sodium-potassium pump restores the original distribution of K^+ and Na^+ ions and the membrane returns to its resting potential [42].

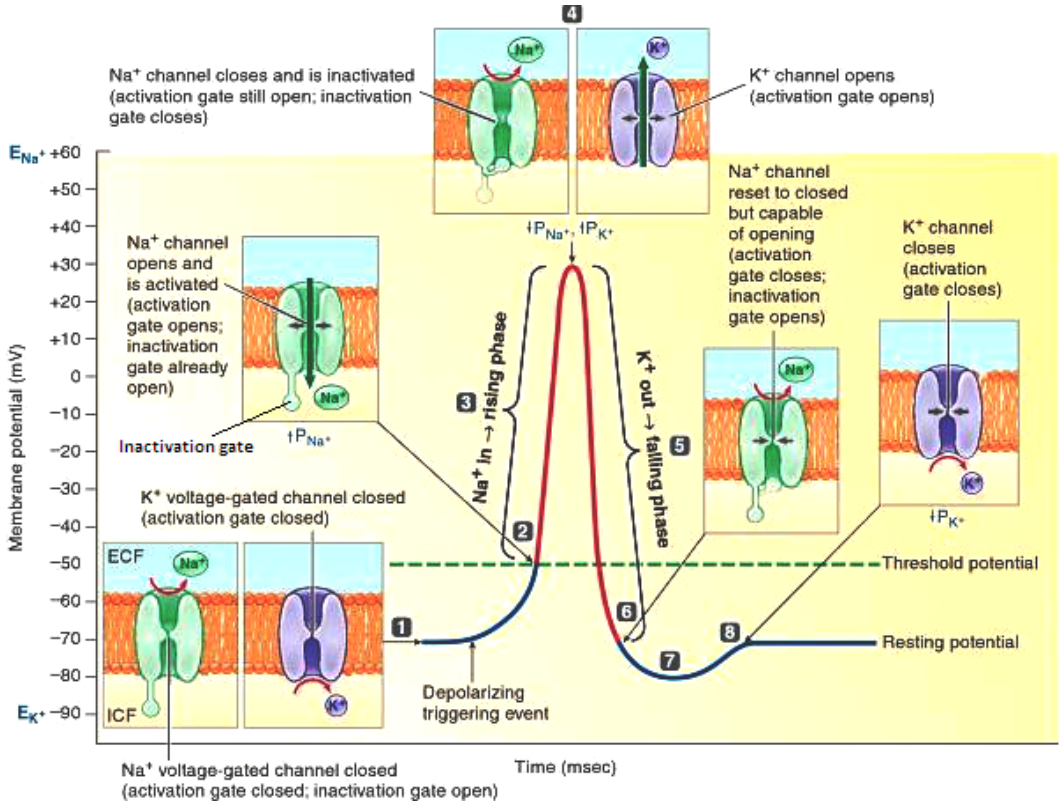

Figure 3.6: Permeability changes and ion fluxes during an action potential. (1) Resting potential: all voltage-gated channels closed; (2) At threshold, Na^+ activation gate opens and permeability to Na^+ rises; (3) Na^+ enters in the cell, causing depolarization to +30 mV, which generates rising phase of action potential; (4) At the peak of action potential, Na^+ inactivation gate closes and permeability to Na^+ decreases, ending the net movement of Na^+ into the cell. At the same time, K^+ activation gate opens and permeability to K^+ rises; (5) K^+ leaves cell, causing its repolarization to resting potential; (6) Na^+ activation gate closes and inactivation gate opens, resetting channel to respond to another depolarization triggering event; (7) Further outward movement of K^+ through the still open K^+ channels briefly hyperpolarization membrane, which generates after hyperpolarization; (8) K^+ activation gate closes and membrane returns to the resting potential. [84]. Adapted with permission. www.cengage.com/permissions

3.2.4 Propagation of an action potential

Once an action potential is initiated, no more triggering events are necessary to activate the remainder of the nerve fiber because the impulse is automatically conducted throughout the neuron. This mechanism of propagation is illustrated in figure 3.7. The membrane of the axon hillock (specialized part of the cell body that connects with the axon) is at the peak of an action potential (about +30 mV). The inside of the cell is positively charged on this area, because Na^+ ions have already rushed in. The remainder of the axon, still at resting potential and negative inside, is considered inactive. Therefore, a local current flow between the area already undergoing an action potential and the adjacent inactive area, because opposite charges attract each other. This depolarizing effect quickly brings the involved inactive area to threshold and, at that time, the voltage-gated Na^+ channels in this region of the membrane are all open, leading to an action potential on this area. Meanwhile, the original active area returns to resting potential as a result of K^+ efflux. Beyond the new active area is another inactive area, so the same thing happens again. This cycle repeats itself in a chain reaction until the action potential spread the end of an axon, where there are synapses (figure 3.8).

The synapse, which is a junction between two cells, is the place where an action potential of a cell can cause the production of action potentials in another cell. The cell that transports the action potential to the synapse is called presynaptic cell and the cell that transports the action potential to far away from the synapse is called postsynaptic cell.

There are two types of synapses: electrical and chemical. However, this thesis simply refers to the process that takes place at the chemical synapses (figure 3.8), because muscular cells are controlled by chemical synapses. In the chemical synapses, the action potentials do not pass directly from the presynaptic terminal to the postsynaptic membrane. Instead, the action potentials trigger the release of neurotransmitters at the synaptic terminals of the axon. The neurotransmitters diffuse across the synaptic cleft and combines with receptors in the membrane of the postsynaptic cell. The receptors cause ion channels to open or close, resulting in either depolarization or hyperpolarization. When depolarization reaches the threshold level, an action potential is generated in the postsynaptic neuron.

3.3 The Human Muscular System

Muscles exert forces and therefore have a crucial role in the human movement. Muscles can be used, for example, to change speed during walking and to raise or lower a body segment

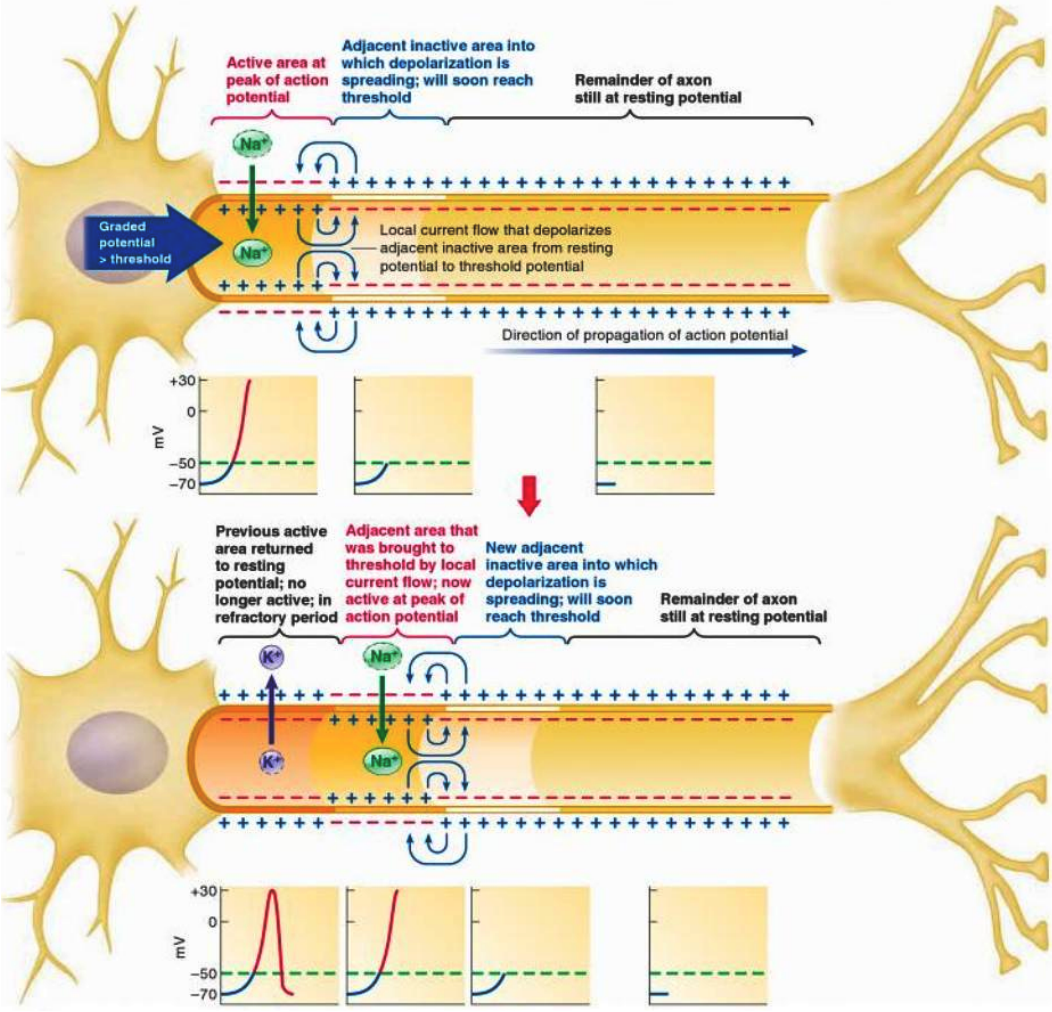

Figure 3.7: Contiguous conduction. Local current flow between the active area at the peak of an action potential and the adjacent inactive. This reduces the potential in this contiguous inactive area to threshold, which triggers an action potential in the previously inactive area. The original active area returns to resting potential and the new active area induces an action potential in the adjacent area by local current flow as the cycle repeats itself down the length of the axon [84]. Reproduced by permission. www.cengage.com/permissions

[29]. In this next section, it is detailed and explained the muscular physiology in order to better understand the final steps to produce movement.

3.3.1 Muscular Physiology

There are three types of muscular tissue: skeletal muscle, cardiac muscle and smooth muscle. Through their capacity to contract, groups of highly developed muscular cells working together can produce work and movement. Although the three types of muscles are structurally and functionally distinct, they can be classified in two different categories, according their common features (see figure **??**) [84].

The muscles can be classified as striated (skeletal and cardiac muscle) or unstriated

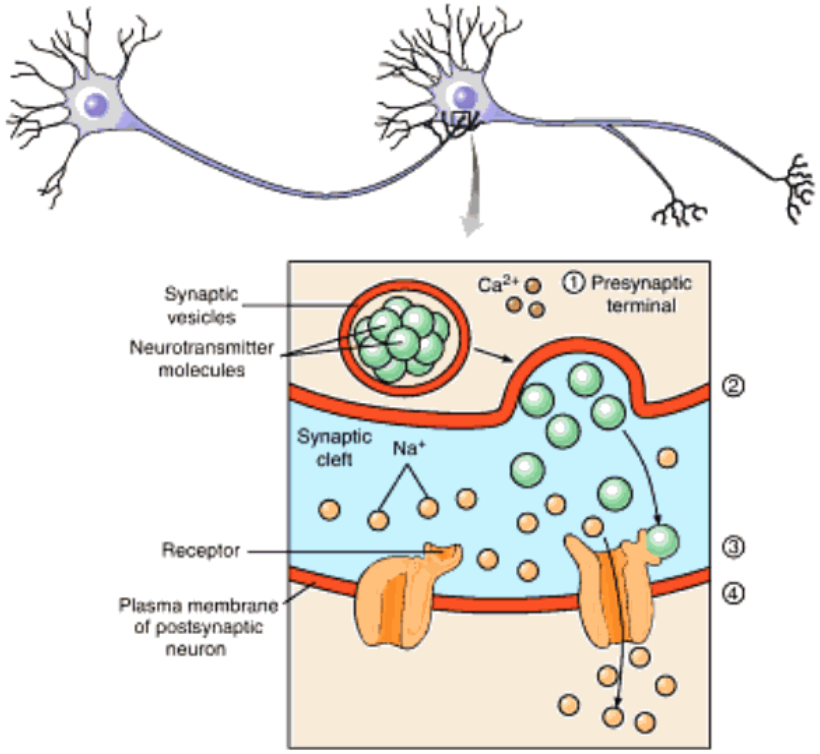

Figure 3.8: Transmission of a neural impulse across a synapse. (1) The action potential reaches the synaptic terminals at the end of the presynaptic neuron, which induces the calcium ions to enter the synaptic terminals from the extracellular fluid; (2) These calcium ions will cause the fusion of the synaptic vesicles with the plasma membrane and release a neurotransmitter into the synaptic clefs; (3) Neurotransmitter diffuses across the synaptic cleft and combines with the membrane of the postsynaptic neuron; (4) These receptors open or close ion channels, resulting in either depolarization or hyperpolarization. When the depolarization exceed the threshold, another action potential is generated in the postsynaptic neuron. Adapted from [86]

(smooth muscle). Another possible classification is to divide the muscles in the voluntary (skeletal muscle) or involuntary type (cardiac and smooth muscle), depending, respectively, if they are enervated by the somatic nervous system and submitted to voluntary control, or if they are enervated by the autonomous nervous system and not submitted to a voluntary control. Although the skeletal muscle is classified as voluntary, once it can be counsciently controlled, part of the muscle-skeletal activity is submitted to the involuntary control too, like the control related to the posture, balance and gait [84]. This thesis focuses on the skeletal muscle because it is the type of muscle studied throughout the experiments.

3.3.2 Skeletal Muscle Fiber

A simple skeletal muscular cell, known as muscle fiber, is relatively big and has a cylindrical shape, ranging from 10 to 100 μm in diameter and up to 750 mm in length. A skeletal muscle consists of several muscle fibers lying parallel to one another and linked through connective

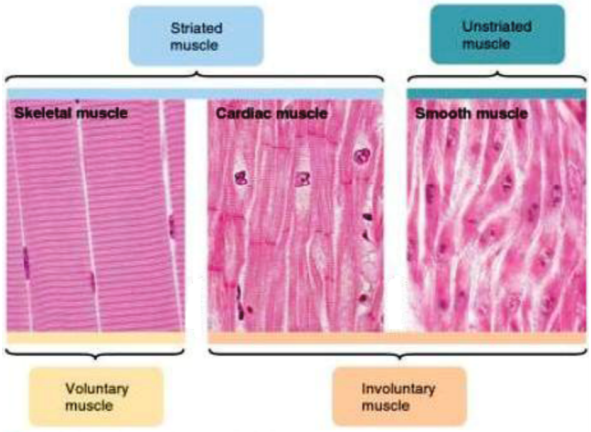

Figure 3.9: Classification of the three different types of muscle [84].
Reproduced by permission. www.cengage.com/permissions

tissue (sarcolemma), as it is represented in figure 3.10-(a). These fibers usually extend the entire length of the muscle [84].

A skeletal muscle fiber is mainly constituted of specialized contractile elements called myofibrils, which are cylindrical intracellular structures with one to two μm of diameter, extending the entire length of the muscle fiber (see figure 3.10-(b)). Each myofibril consists in a regular arrangement of cytoskeletal elements highly organized - the thick and thin filaments (see figure 3.10-(c)). The thick filaments, which have between 12 to 18 nm of diameter and a length of 1.6 μm, are sets of myosin protein, whereas the thin filaments, which have from 5 to 8 nm of diameter and a length of 1.0 μm, are composed by actin protein (see figure 3.10-(d)).

The levels of organization of the skeletal muscle are resumed in the figure 3.11.

3.3.3 Mechanism of contraction: the cross-bridge cycle

Myosin heads are also known as cross-bridges, because they can bind to and move along actin in the thin filaments. The interaction between actin and myosin heads is the basis for the contraction and movement of muscle cells (see figure 3.12).

The cross-bridge cycle starts with the myosin head attached to actin. The myosin head binds to ATP (Adenosine triphosphate, which transports chemical energy within cells for metabolism), which causes the dissociation of myosin from actin. Then, the myosin ATPase (enzyme that catalyzes the decomposition of ATP) hydrolyses (chemical process in which a certain molecule is split into two parts by the addition of a molecule of water) ATP and the products of this reaction (ADP and inorganic phosphate) remain bound to the ATPase.

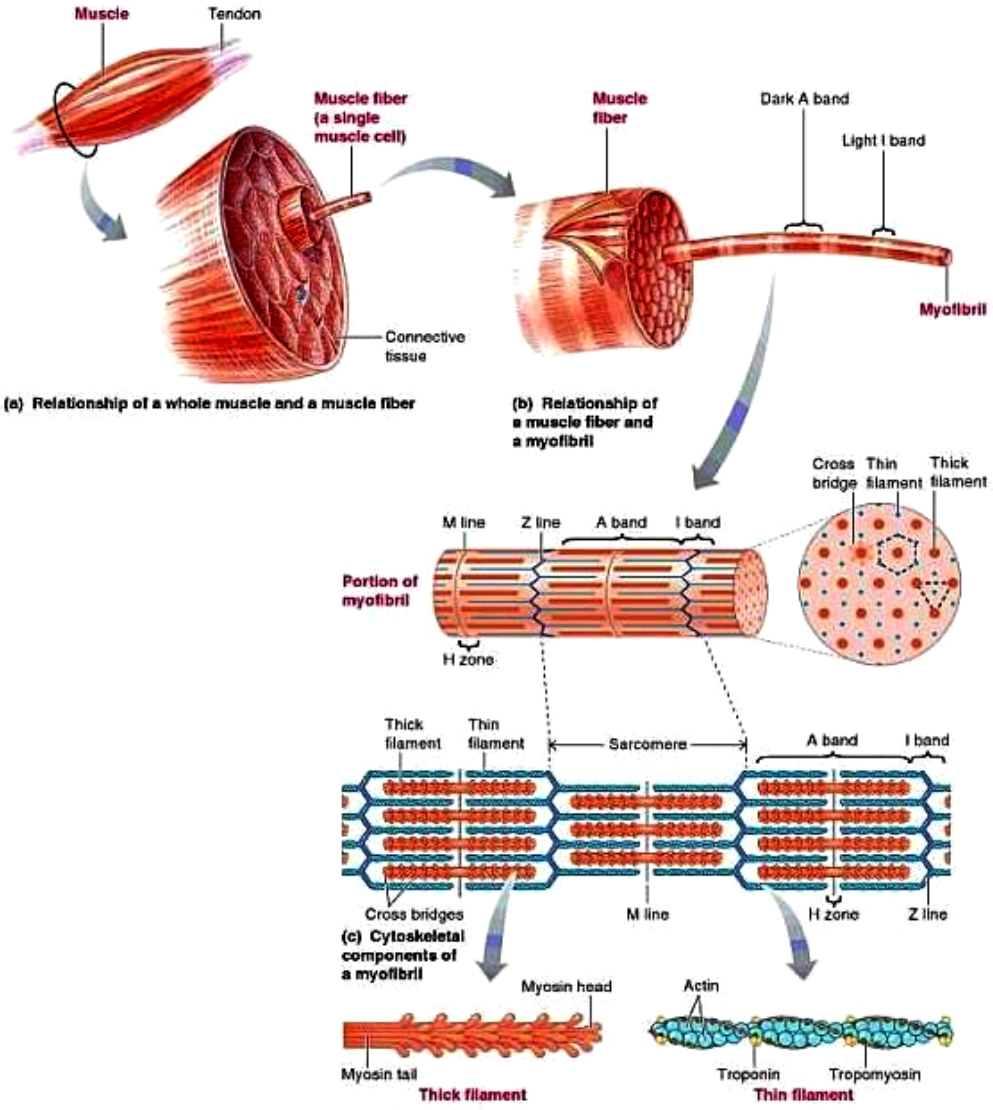

Figure 3.10: Detailed representation of the organization of the skeletal muscle [84]. Reproduced by permission. www.cengage.com/permissions

The phosphate (Pi) is released and the myosin head binds tightly to the actin. After that, a stronger binding triggers the powerstroke and the release of ADP. The powerstroke consists in the return of the myosin head to its low-energy conformation. The powerstroke generates force, pulling the thin filament toward the center of the sarcomere. The binding of another ATP molecule will cause the dissociation of myosin head from actin and the cycle repeats itself [65].

The number of active cross-bridges depends on the concentration of Ca^{2+} in the muscle fiber cytoplasm. At each instant during contraction, only about 50% of the cross-bridges are attached to actin. Therefore, only about 50% of the maximum possible force is produced.

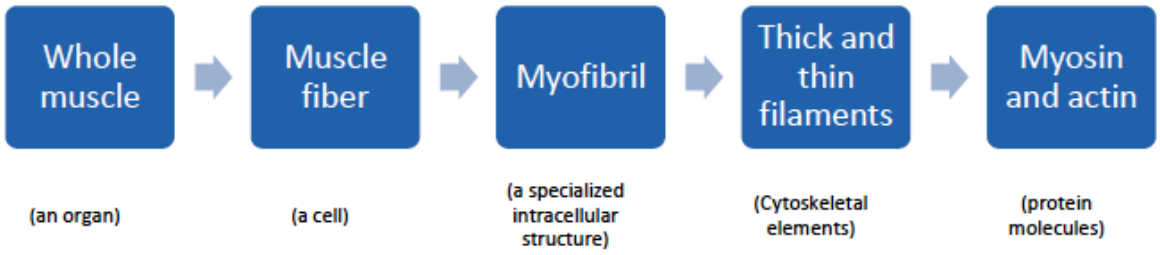

Figure 3.11: Levels of organization of the skeletal muscle

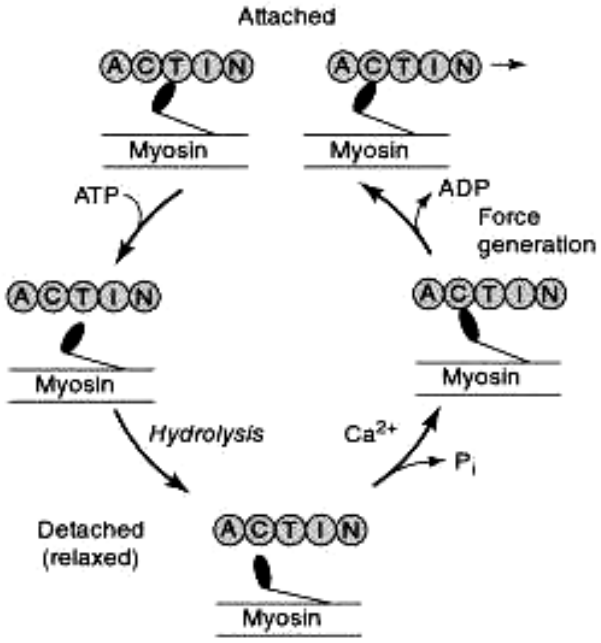

Figure 3.12: Cross-bridge cycle. Used with permission from [65]

3.3.4 Muscle Fiber Action Potential

Running parallel with myofibrils is the sarcolemma (see figure 3.13). Sarcolemma is an electrically excitable membrane that can activate the contractile actions in response to signals received from the motor nerve [43].

Several events must occur before a muscle fiber contracts, as explained during the previous sections. When the central nervous system initiates the depolarization in the motorneuron, this depolarization is conducted along the motorneuron to the neuromuscular junction. At the neuromuscular junction, a chemical substance called acetylcholine is released, stimulating the Na^+ ion channels in the muscle fiber. This fact increases the permeability to Na^+, which, together with the ion's concentration gradient, causes a sudden influx of Na^+ into the muscle fiber. A rapid depolarization of the muscle fiber occurs and continues until the fiber reverses its polarity and reaches about +30 mV positive inside with respect to the outside.

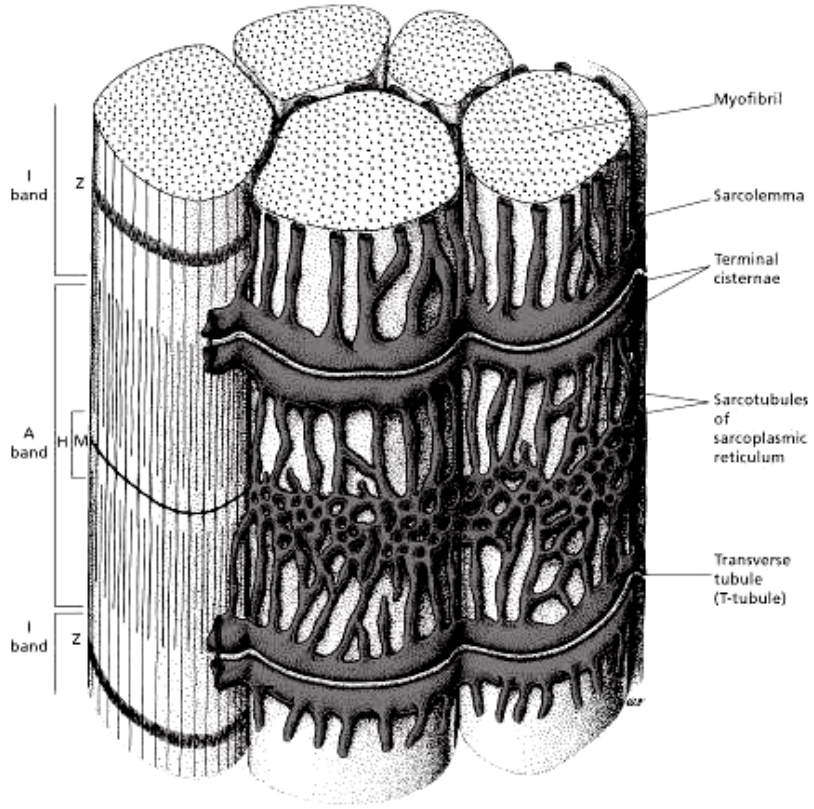

Figure 3.13: Skeletal muscle fiber, showing the sarcoplasmatic reticulum that surrounds myofibrills. Used with permission from [77]

Near the peak of the reverse polarity, the decreased influx of Na^+ and increased efflux of K^+ causes a rapid repolarization of the muscle fiber.

When a depolarization of the membrane under the neuromuscular junction occurs, a potential difference is established between the active and the inactive region of the muscle fiber. Therefore, ion current flows between those regions. This current decreases the membrane potential of the inactive region to a point where the membrane permeability to Na^+ rapidly increases in the inactive region and an action potential is generated. The action potential propagates away from the initial active region in both directions along the muscle fiber. The propagated action potential along the muscle fiber is a muscle fiber action potential.

The action potential spreads along sarcolemma and into the muscle fiber through the transversal tubules (see figure 3.13). In response to the action potential, the sarcoplasmatic reticulum (sarcotubules) releases stored calcium. Finally, a muscle contraction takes place due to the cross-bridge cycle.

Chapter 4

Measurement of muscle activity

This chapter begins with an explanation about how muscular electric activity can be recorded and the anatomical structures whose potential differences can be recorded. The chapter continues with the best procedures to perform the recordings of muscular activity and finishes describing the muscles that we focused on this work.

4.1 Electromyography

The recording of muscle's electric activity is called electromyography (EMG). EMG can be used as a test for exploring the physical integrity of the motor system, because it reflects the complex function of the motor system [57].

It is crucial to have a great knowledge of the physiological mechanisms underlying the normal muscular contractions to understand the large variety of abnormalities that characterize the various disorders of the nervous system.

Many factors, like the muscular properties, the electric specifications of the electrodes and the EMG recording instrumentation can largely affect the EMG recordings [74].

4.1.1 Motor unit action potential

The smallest functional unit of the neuromuscular system is called motor unit [85]. A motor unit is constituted by a motorneuron, its axon and the muscle fibers it innervates (see figure 3.4) [17]. When a motorneuron is activated, the conduction of its activation travels along its axon and neurotransmitters are released at the neuromuscular junctions. Finally, the action potentials run in both directions of the muscle fibers from each neuromuscular junction to the

tendinous attachments at both ends (see Figure 4.1). The sum of these muscle fibers action potentials forms the MUAP (motor unit action potential).

Although each muscle fiber just receive input from only one motor unit, different motor units overlap their fiber territories spatially (see figure 4.2).

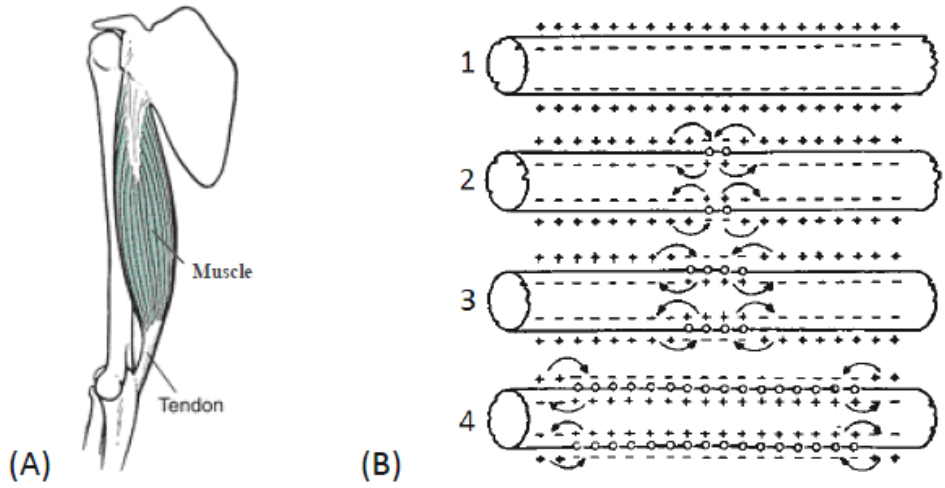

Figure 4.1: (A) A muscle can attach indirectly to the bone via a tendon. Adapted with permission from [29]; (B) Depolarization runs in both directions along a conductive fiber in direction to the tendinous attachments at both ends. Adapted with permission from [85]

4.1.2 Extracellular Recording of Action Potentials

Electromyography is the recording of electric activity in the muscles. This recording can be done using two types of electrodes: needle electrodes or surface electrodes. Electromyography with needle electrodes is called intramuscular electromyography (iEMG) and the electromyography with surface electrodes is called surface electromyography (sEMG). This thesis will rather focus on sEMG than iEMG, mainly because the experiments were performed with sEMG and also because sEMG is largely a more used method over the world [17]. The source of the sEMG signal is the spatial and temporal sum of the action potentials from each muscle fiber. The use of superficial electrodes creates the concept of detection volume, which is the volume of tissue from which the electrodes are capable of detecting an electric signal. The detected energy of the motor units depends on the depth of these motor units in the volume, because the energy is dissipated along the distance and the higher the depth the lower the energy reaching the electrodes (see figure 4.2). It is necessary to clearly understand the recording of a muscle fiber action potential to understand the MUAP and the correspondent sEMG detected signal.

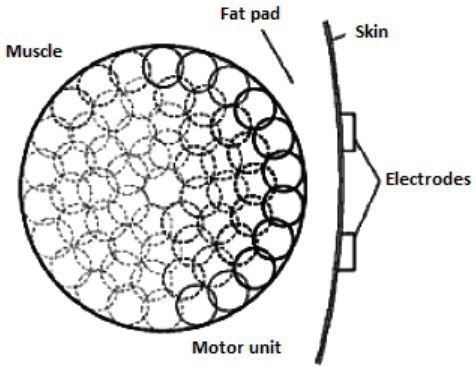

Figure 4.2: Motor unit recruitment territories. Only the 'dark' muscle fibers contribute substantially to the sEMG recordings. Used with permission from [17]

Consider the following example presented in figure 4.3. Two electrodes are placed at a considerable distance apart, on the surface of a muscle fiber and connected to an oscilloscope in order to measure the voltage changes. In the resting state, the fiber is electrically positive outside and negative inside (as explained in Chapter 3). Since both these electrodes are placed on areas with the same potential, the resulting potential difference between them is 0V (panel 1 of figure 4.3-(A)). In the second panel of figure 4.3-(A), an action potential is generated and runs from the left to the right of the fiber. When that action potential reaches the region under the electrode A, that region becomes negative in relation to the region below the electrode B and the oscilloscope deflects upward. Then, the action potential continues toward electrode B and the region under the electrode A repolarizes (returns to the normal potential) (panel 3 of figure 4.3-(A)). Therefore, the oscilloscope returns to baseline. The action potential continues and reaches the region under the electrode B. So, that region becomes negative in relation to the region below the electrode A and the oscilloscope deflects downward (panel 4 of figure 4.3-(A)). Finally, the repolarization occurs under the electrode B and the potential difference is again 0V (panel 5 of figure 4.3-(A)). The output of this model is two monophasic waves separated by a brief period of time when no potential difference is measured. But this time depends on the distance between the two electrodes and the conduction speed of the muscle fiber (see figure 4.3-(B)). For example, if the electrodes are placed very close together, the two waves temporally summate and form a biphasic wave.

These muscle fibers action potentials summate to form the motor unit action potential (see Figure 4.4-(A), where h(t) represents a MUAP). The majority of motor unit action potentials are biphasic or triphasic in shape. This shape depends on the characteristics of the muscle fibers, the spatial orientation of those muscle fibers and the tissues surrounding the active muscle fibers. The superposition of multiple MUAPs forms the sEMG signal (figure

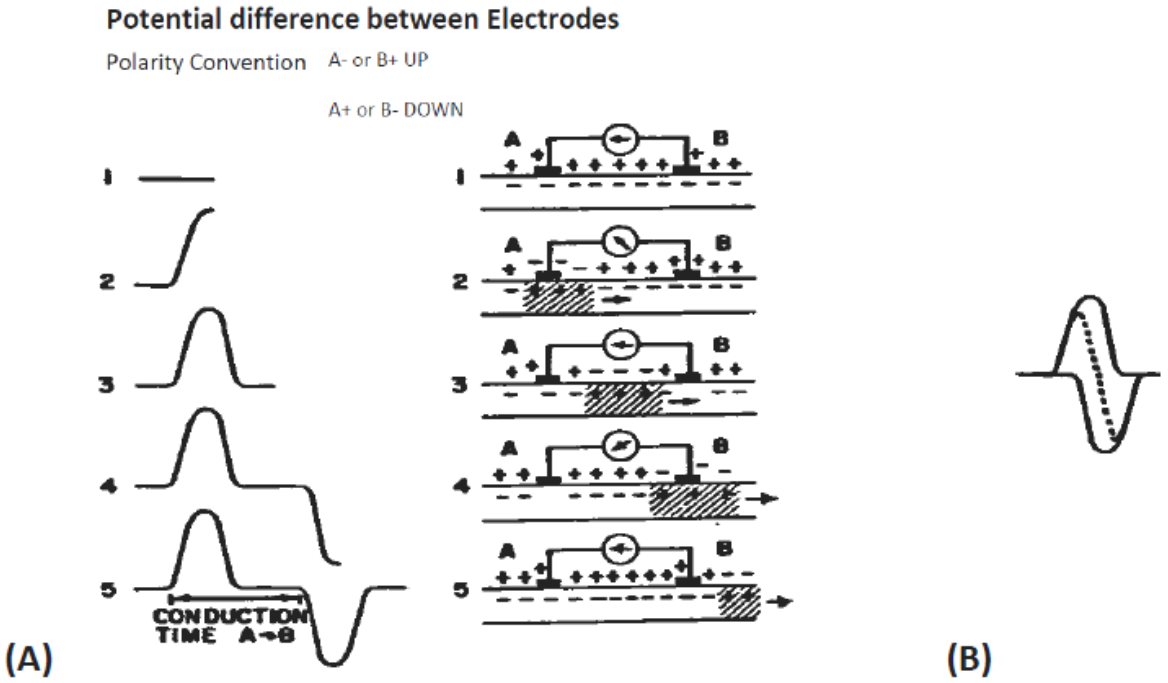

Figure 4.3: (A) Measurement of action potentials on a muscle fiber; (B) Time delay between two monophasic waves depends on the distance between the two electrodes and the conduction speed of the muscle fiber. Adapted with permission from [85]

4.4-(B)).

4.1.3 Differences between surface and intramuscular electromyography

This dissertation is focused in the used of sEMG. However, it is important to discuss some differences between sEMG (figure 4.5-(A)) and iEMG (figure 4.5-(B)).

Using iEMG, the magnitude of energy recorded is in the range of milivolts and the electrodes record a motor unit action potential. On the other hand, the energy recorded using sEMG is in the range of microvolt and the electrodes record action potentials from sets of motor units. The reduced amplitude recorded using sEMG is related to the loss of energy in the body tissue, because the tissue absorbs some electrical potential generated in the muscle.

Superficial electrodes have many advantages. For example, they are non-invasive, allow the global recording of muscle activity and there is no limitation to the time of recording. However, some disadvantages can be also pointed out, including the following: these electrodes just allow the study of superficial musculature; it requires a correct preparation of the skin; and the signals have a low frequency spectrum.

On the other hand, needle electrodes allow a more local recording of the muscle electric

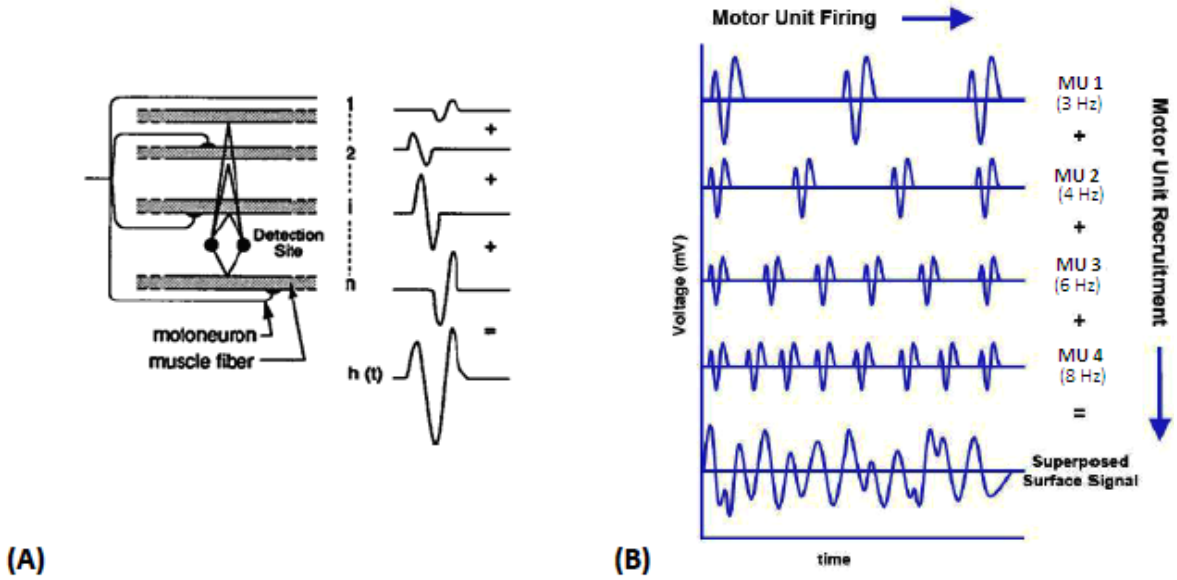

Figure 4.4: (A) Generation of a MUAP (motor unit action potential); (B) The sEMG signal is the superposition of multiple MUAPs

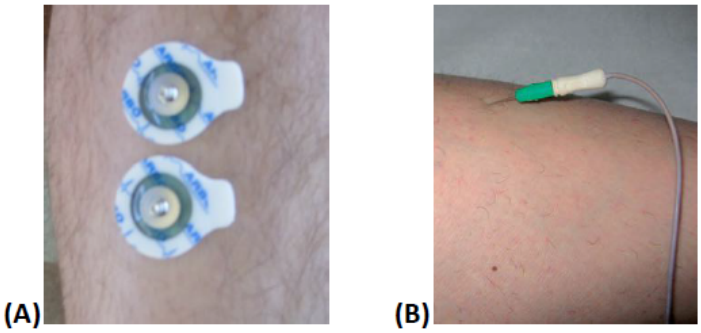

Figure 4.5: (A) Superficial electrodes; (B) Needle electrode

activity, which makes it possible to study both superficial and deep musculature. Needle electrodes also capture a higher frequencies spectrum and it is not necessary a great preparation of the skin. Being invasive is the main disadvantage that needle electrodes present [57].

In essence, the experiments were performed using surface electrodes mainly because they are non-invasive, cheap and used in many laboratories around the world.

4.2 Procedures for recording muscle activity

To do a correct surface electromyography, it is necessary to follow complex procedures and to use a very sophisticated instrumentation.

4.2.1 Recommendations for electrodes placement

In this study, all the SENIAM (Surface ElectroMyography for the Non-Invasive Assessment of Muscles) recommendations were followed [32] [31]. SENIAM is a European project concerned with Biomedical Health. Its recommendations are followed by many research groups around the world.

The first step to be taken in sEMG is to select the sEMG electrodes. The electrodes are chosen based on the shape (of the conductive area), size (of the conductive area), inter electrode distance (the center to center distance between the conductive area of two bipolar electrodes) and electrode material (which forms the contact layer with the skin). SENIAM recommendations about these features are:

- There are no clear and objective criteria for choose the electrode shape;

- The size of the electrodes in the direction of the muscle fibers should be 10 mm at maximum;

- Inter electrode distance of 20 mm;

- Use pre-gelled Ag/AgCl electrodes.

We used a bipolar derivation with pairs of circular electrodes (Ag-AgCl, Fiab S.p.A.) on this work (see figure 4.5-(A)).

The second step is to put the patient in a starting posture to determine the proper location of the electrodes on the muscle to be tested (see Appendix B). In this starting position, which varies from muscle to muscle, it is possible to determine via palpation the muscle and the anatomical landmarks. Anatomical landmarks are standard reference points in the body.

The third step is the preparation of the skin. If the area where the electrodes will be placed is covered with hair, it is necessary to shave the area (see figure 4.6-(A)). It is then necessary to clean the skin with alcohol and allow the alcohol to vaporize in order to dry the skin before placing the electrodes.

The fourth step is the correct determination of the electrodes location, *i.e.*, the centre of two bipolar electrodes on the muscle (see figure 4.6-(B)). Electrodes must be placed in the location where it is possible to obtain a good and stable sEMG, according to the SENIAM recommendations for each muscle.

The fifth step is the fixation of the electrodes, respecting the inter electrode distance of 20 mm and the recommendations for the orientation of electrodes (see figure 4.6-(C)). SENIAM also recommends using elastic band or double sided taped for fixation of the electrodes and cables in such a way that movement is not perturbed and cables don't pull the electrodes.

It is also necessary to place a reference electrode (section 4.2.2 explains what a reference electrode is and why it is necessary) in a location where the risk for signal disturbance is minimal [17].

The last step before starting to record EMG signals is the testing of the connection. SENIAM recommends doing a clinical test for each individual muscle and these clinical tests are described in the Appendix B.

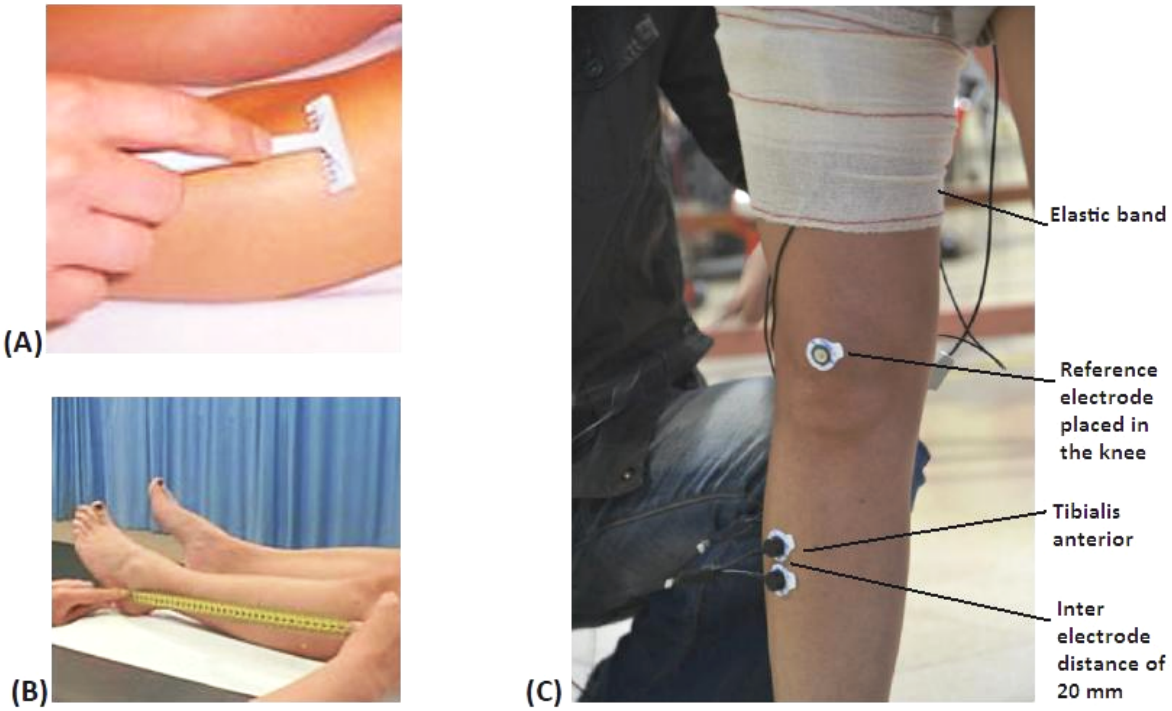

Figure 4.6: (A) SENIAM recommends to shave the place where the electrodes will be placed. Used, with permission, from [31]; (B) SENIAM recommends to draw a line between two landmarks Used, with permission, from [31]; (C) Fixation of the electrodes and cables

4.2.2 Recording EMG signal

In order to record a very good EMG signal, it is necessary to use a very sophisticated and sensitive instrumentation, because the energy generated by the muscles has a very small value (in order of mV).

Figure 4.7 shows a block diagram of the various components that can be implemented in sEMG instrumentation. The output of a general sEMG system is usually the raw sEMG signal. In this work, it was used the Pocket EMG system from BTS Bioengineering (features indicated in the Appendix). On this dissertation we will just describe some of the most important features of such sEMG instrumentation.

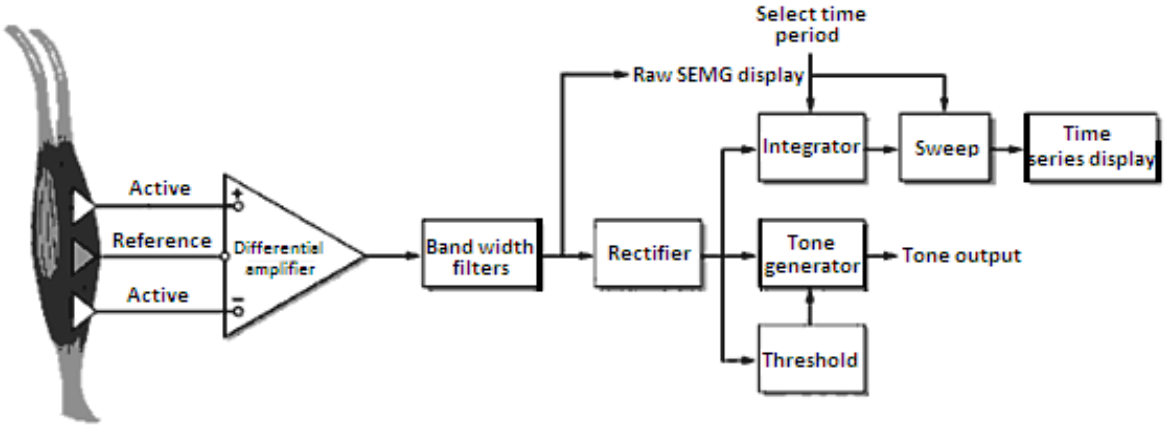

Figure 4.7: Block diagram of typical sEMG instrumentation. Used with permission from [17]

One important procedure is to guarantee a correct interface between the electrodes and the skin. The impedance (or resistance) of the skin (also described as resistance to a direct current) may vary as function of the superficial skin oil content, dead cell layer, the humidity of the skin, etc. In sEMG, it is necessary to keep this impedance as low as possible and similar at the two electrodes location. This is commonly accomplished by abrading the skin vigorously with alcohol. Although we can't measure it, the impedance at the electrode site should be less than 5 to 10 KΩ [17], so that the practitioner can get a clean sEMG signal.

The desired value for the skin impedance depends on the input impedance of the amplifier. In figure 4.8, it is represented the interface between the skin impedance and the input of the EMG amplifier. R_S represents the impedance of the skin and R_A represents the input impedance of the amplifier. The input impedance of the amplifier should be 10 to 100 times higher than the impedance of the skin-electrode interface. The Ohm's law says that

$$E = i.R \ (voltage = current \ x \ impedance) \tag{4.1}$$

For the schematic representation of figure 4.8,

$$E = E_S + E_A \Leftrightarrow E = i.R_S + i.R_A \tag{4.2}$$

where E is the energy (voltage) reaching the skin, E_S is the energy lost in skin impedance, E_A is the input voltage of the amplifier and i is the current.

If the input impedance of the amplifier is 100 times higher than the skin impedance, then

$$E = i.\ 0,01R_A + i.R_A \Leftrightarrow E - i.\ 0,01R_A = i.R_A \Leftrightarrow E - 0,01E_A = E_A \tag{4.3}$$

In this way, almost all the energy that reaches the skin can also reach the input of the amplifier. The Pocket EMG system has an input resistance of $10^{10}\Omega$, which is a very high value.

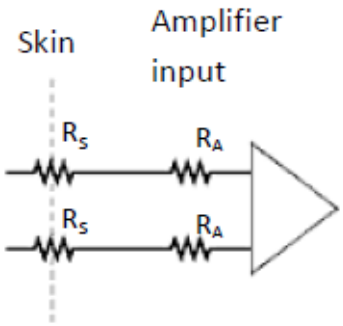

Figure 4.8: Interface of the skin impedance and the impedance of the sEMG amplifier input

The input signal of the amplifier is then amplified. For each muscle, the input signal is the result of the signals of three electrodes: the bipolar pair of electrodes placed over that muscle and the reference electrode making good contact in a neutral location (we choosed he knee for this work). The energy reaching both bipolar electrodes is compared with the signal of the reference electrode and the result is the input signal. The amplifier gain is defined as the ratio between the output and the input signal. For example, for an input of 2 mV and a gain of 1000, the output will be 2V. The range of gain is usually between 1 and 10000. The gains of all amplifiers constituting the Pocket EMG are referred in the Appendix A.

Another important feature of an amplifier is the frequency response. The firing rate of the muscle fibers is usually in the range of 8 to 50 Hz [17]. Therefore, the amplifier has to be capable of amplifying frequencies much higher than these. The bandwidth frequencies of an EMG amplifier are the range of EMG frequencies that can be amplified, without attenuation. The bandwidth of an amplifier is the difference between the higher cutoff frequency and the lower cutoff frequency. On these cutoff frequencies, the gain is 70.7% of the gain in the frequencies between those cutoff frequencies [98]. The amplifier gain is usually expressed in the logarithmic form and in decibels (dB):

Gain (dB) = 20 $\log_{10}$ (linear gain)

For a linear gain of 1000, the gain is 60 dB between the cutoff frequencies and the gain is 57 dB in the cutoff frequencies. The frequency responses for the amplifiers implemented in Pocket EMG are referred in the Appendix A.

Finally, another very important feature of the amplifiers used on sEMG is the CMRR (common mode rejection ratio). The Human body is like a good antenna that catches and

conducts the electromagnetic energy present in the near electric equipments. When someone works with a differential amplifier, those electromagnetic signals present the same magnitude in both inputs of the amplifier, generating in this way a common signal between them [16] [17].

A differential amplifier subtracts the signals in the input terminals, but it can't distinguish the common signal from the electromyographic signal, which is the one that really matters. It is hoped that the subtraction of two common signals results in a 0V and, thus, just the electromyographic signal will be present in the output. However, once these electromagnetic interferences usually present a high magnitude, it does not occur a perfect subtraction of them. The measure of that subtraction success is given by the CMRR factor, which represents the capacity to eliminate signals with the same polarity present in electric interferences. That capacity is expressed in dB. For differential amplifiers used in sEMG, the CMRR factor is very important and should be higher than 80-100 dB. The CMRR factor of the instrumentation amplifier implemented in Pocket EMG is 110 dB (see Appendix A).

4.3 Muscle activity during human gait

Human walking can be divided in typical phases. Several muscles are involved in the walking and seven of them were analyzed on this work.

4.3.1 The human gait. Definitions

A simplified diagram of the human gait during normal walking is represented in the figure 4.9. The gait can be defined as the way of moving the body from one place to another, by moving on feet in a synchronized order or rhythm [4]. There are many types of human gait, like walking, skipping, running and many others. In this dissertation, human walking is the type of gait being studied.

The gait cycle is the average interval of time between the occurrences of two similar locomotion movements. Each one of these intervals of time is a stride cycle. The gait cycle begins with the initial contact of one of the feet with the ground and ends with the next contact of that same foot with the ground. The gait cycle can be divided in two global periods: stance and swing. Stance is the period in which the foot referred above is in contact with the ground. Swing is the period in which that foot is in the air [4].

The gait can be divided in eight phases, each one presenting a typical pattern and a

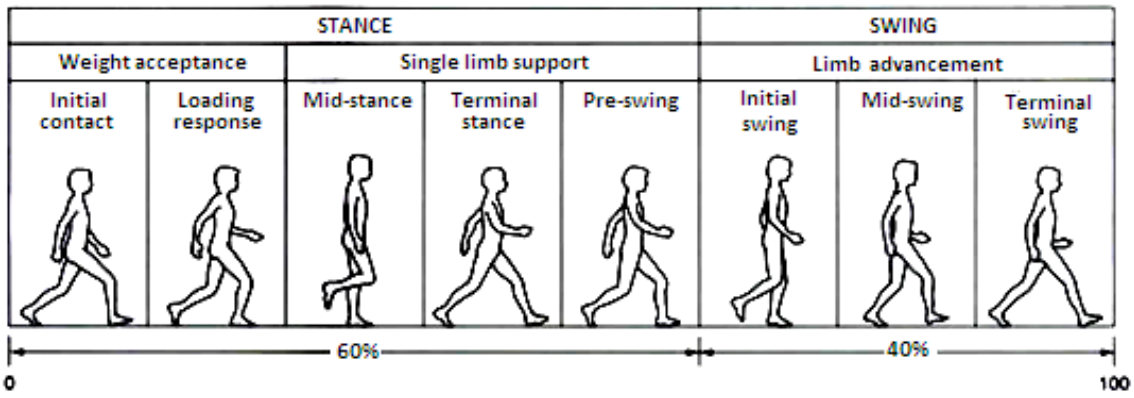

Figure 4.9: Human gait cycle. Used with permission from [33]

functional objective [73]. Those phases, illustrated in figure 4.9, are:

Phase 1 - **Initial contact**, which involves 0-2% interval of the gait cycle. In this phase, it is done the initial contact of the ipsilateral (on the same side of the body, *i.e.*, the reference of the analysis) foot with the ground. The objective of this phase is to obtain the correct alignment of the lower limb in order to begin the stance.

Phase 2 - **Loading response**, which involves 2-10% interval of the gait cycle. The aim of this phase is the shock absorption of the ipsilateral heel striking the ground and also to progress the walking. This phase ends when the contralateral (on the opposite side) foot leaves the ground and starts its swing movement.

Phase 3 - **Mid-stance**, which involves 10-30% interval of the gait cycle. The aim of this phase is the progression of the foot in the ground as well as to keep the stability of the limb and the trunk. This phases ends when the ipsilateral heel begins to lift off the ground. Weight has been transferred to the contralateral limb.

Phase 4 - **Terminal stance**, which involves 30-50% interval of the gait cycle. The support of the limb ends in this phase. The objective of this phase is the progression of the body in addition to the ipsilateral foot support. This phase ends when the contralateral foot strikes the ground.

Phase 5 - **Pre-swing**, which involves 50-60% interval of the gait cycle. The aim of this phase is to prepare the lower limb for the swing phase. This is the final phase of stance: it ends when the ipsilateral foot leaves the floor.

Phase 6 - **Initial swing**, which involves 60-73% interval of the gait cycle. The aim of this phase is to lift the ipsilateral foot from the ground and move the lower limb. This phase ends when the ipsilateral foot is opposite to the other.

Phase 7 - **Mid-swing**, which involves 73-87% interval of gait. This second phase of the swing has the aim of moving the limb and free the foot from the ground. This phase ends when the tibia of the ipsilateral limb is in a vertical position (the moment when the knee and hip flexion are similar).

Phase 8 - **Terminal swing**, which involves 87-100% interval of gait cycle. This phase ends when the ipsilateral foot strikes the ground again.

Figure 4.10-(A) represents the human planes of reference. There are three planes of reference in the human movement: sagittal, coronal and transversal.

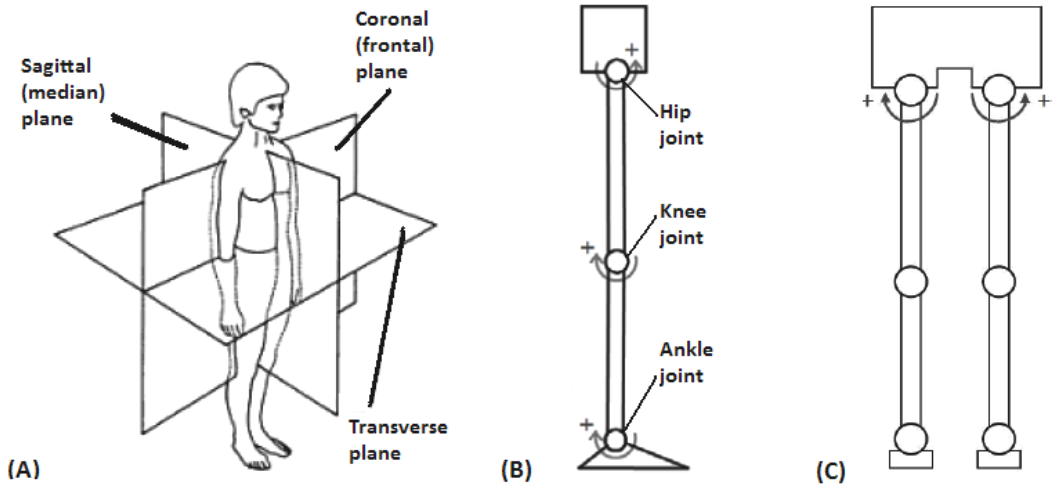

Figure 4.10: (A) Human body planes of reference. Adapted, with permission, from [97]. Image already reprinted from [94]; (B) Diagram of the leg (lateral vision) shown in the rest position (0 degrees at all joints) with the positive direction of movement indicated. Adapted, with permission, from [22]; (C) Diagram of both legs (frontal vision) shown in the rest position (0 degrees at all joints) with the positive direction of movement indicated

The movements made in the articulations can be classified in different types, from which the most important are:

- Flexion and extension. In these movements, there is, respectively, a decrease (positive direction in figure 4.10-(B)) or increase (negative direction in figure 4.10-(B)) of the angle between the limb's segment that moves and the limb's segment that stays fixed, in the sagittal plane. In relation to the ankle joint, the decrease (negative direction in figure 4.10-(B)) of the angle between the segments is called dorsiflexion and the increase (positive direction in figure 4.10-(B)) of the angle is called plantar flexion.

- Adduction and abduction, which are movements of the hip in the coronal plane. Abduction (positive direction in figure 4.10-(C)) is the motion of the hip away from the center of the body and adduction (negative direction in figure 4.10-(B)) is the motion of the hip in direction to the center of the body.

4.3.2 Muscles involved in walking

Part of the analysis of the normal walking consists in studying the muscular activation sequence, as well as the effect of each muscle on the body's dynamic. There are 28 major muscles involved in the human gait [7]. The muscles are the effectors that allow the movement. If some muscle of the lower limb is damaged, the gait will be modified. For this thesis, it was decided to focus on one joint, in order to study its activity during the walking in more detail. Therefore, seven muscles actuating in the knee joint were chosen to be studied in detail. Furthermore, these muscles are linked to the ankle or hip joint, which is also important to have a general idea about the activity of those joints during walking. These muscles are rectus femoris, vastus lateralis, semitendinosus, biceps femoris, gastrocnemius medialis, gastrocnemius lateralis and tibialis anterior. The general functions of the seven muscles are referred on table 4.1. All of them are represented in figure 4.11. By choosing these seven muscles, it is thus possible to study four major muscle groups: quadriceps (consists in the rectus femoris, vastus lateralis, vastus medialis and vastus intermedius muscles), hamstrings (consists in biceps femoris, semitendinosus and semimembranosus muscles), gastrocnemius (consists in gastrocnemius medialis and gastrocnemius lateralis) and tibialis anterior.

4.3.3 Electrodes location in the lower limbs. Techniques and standards

It was referred in section 4.2. that it is extremely important to determine the correct electrode location in sEMG. SENIAM recommendations for electrodes location on the seven muscles to be studied are detailed in the Appendix B. For each muscle, the location of the pair of electrodes is described as a specific point in a line between two anatomical landmarks.

Table 4.1: General functions of the seven muscles studied in this work

Muscle	Function
Rectus femoris	- Flexion of hip joint - Extension of knee joint
Vastus lateralis	- Extension of knee joint
Semitendinosus	- Extension of hip joint - Stabilization of pelvis in the saggital plane - Flexion and internal rotation of the knee joint
Biceps femoris	- Extension of the hip joint - Stabilization of pelvis in the saggital plane - Flexion and external rotation of the knee joint
Gastrocnemius medialis	- Plantar flexion of the ankle joint - Flexion of the knee joint
Gastrocnemius lateralis	- Plantar flexion of the ankle joint - Flexion of the knee joint
Tibialis anterior	- Dorsiflexion of the ankle joint

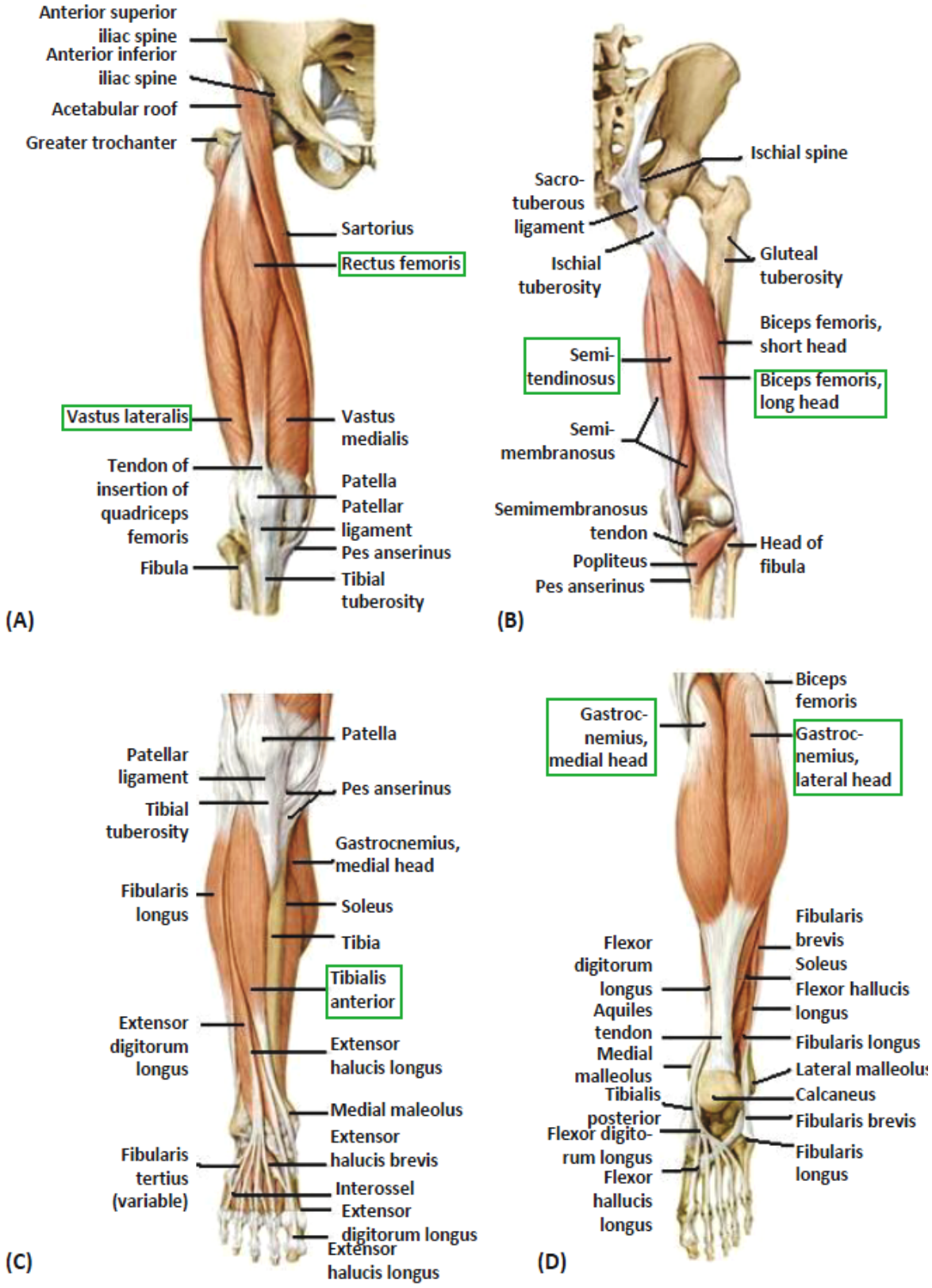

Figure 4.11: (A) Anterior thigh muscles of the right side; (B) Posterior thigh muscles of the right side; (C) Muscles of the leg: anterior view of the right side; (D) Muscles of the leg: posterior view of the right side. Adapted from [27]

Chapter 5

EMG and kinematics during human gait

Human walking is a very complex activity that results on the integrated action of the brain, nerves and muscles. Electromyographic recordings enable researchers to obtain very valuable information about neuromuscular activity during walking. Kinematics can also be recorded during walking. This chapter compares the EMG and kinematic patters during normal walking and walking with assistive/rehabilitation devices.

5.1 EMG Signal Processing

As referred in Chapter 4, the output of a general EMG system is usually the raw EMG signal. Raw EMG is the pure electromyographic signal, which can present artifacts (DC offset and motion artifacts) and high frequency noise. Therefore, raw EMG should be filtered because of the artifacts it contains and it also should be processed to be used in areas like the neuromuscular coordination and the gait analysis. The output of most recent EMG devices, including Pocket EMG, is the raw EMG already filtered.

5.1.1 Raw EMG

Raw EMG is composed by thousands of individual MUAPs that make up a series of spikes, which makes it difficult to analyze the muscle activity as a whole. Because of these constraints, Raw EMG is usually processed to represent the muscular activity [98]. The typical signal processing order followed by many laboratories around the world dedicated to the motion analysis is represented in figure 5.1.

The output signal of the gastrocnemius medialis activity during 10 seconds of walking is represented in Figure 5.2-(A). This signal is the raw EMG already filtered by the Pocket

Figure 5.1: Typical EMG signal processing order

EMG and it was acquired in a representative healthy subject of our study.

In order to determine the relationship between the EMG and the gait cycle, it is necessary to detect the initial heel contact with the ground and the toe-off. Some laboratories have equipment of 3D motion analysis that allows measuring the moments of heel strike and toe-off. But it is very difficult to integrate EMG data with biomechanical data. To solve this problem, instead they can use small footswitches (see Figure 5.3-(A)), an alternative that can be integrated with the Pocket EMG equipment. Footswitches are force sensitive resistors placed on the foot. They usually work in a binary manner, with only an on (when the force exceed the threshold) or off (when the force is lower than the threshold) signal. They can be placed on the heel, on the toe or on the metatarsal region. For this work, three footswitches were placed on heel, metatarsal 1 and metatarsal 5 (see Figure 5.3-(B)). Double-sided tape was placed on the back of the footswitches in order to hold them correctly. The footswitch signal represented in figure 5.2-(C) shows the three levels of activation of the three footswitches. This signal seems like a stair and the activation begins with the heel strike and ends with the toe off. Each footswitch presents different levels of activation.

5.1.2 Filtering

The power spectrum of sEMG describes the distribution of signal power as a function of the frequency of the harmonics of the signal. Usually, almost 95% of such power can be accounted by harmonics until 400 Hz. The other 5% is electrode and equipment noise. These components can be electronically attenuated using a low pass filter. SENIAM recommends a cutoff frequency of almost 500 Hz and sampling frequency of 1000 Hz. But spike-like artifacts, such as artifacts generated by electrical stimulation, are attenuated but not eliminated by a low pass filter with a cutoff frequency of 500 Hz. Pocket EMG has a low pass filter implemented with a cutoff frequency of 450 Hz in order to prevent any aliasing, once the sampling frequency is 1000 Hz. According to the Nyquist Theorem, the sampling frequency of an analogical signal should be equal or higher than twice the higher frequency of that signal's spectrum. Aliasing can occur if the signal has harmonics with frequency higher than half the sampling frequency [32].

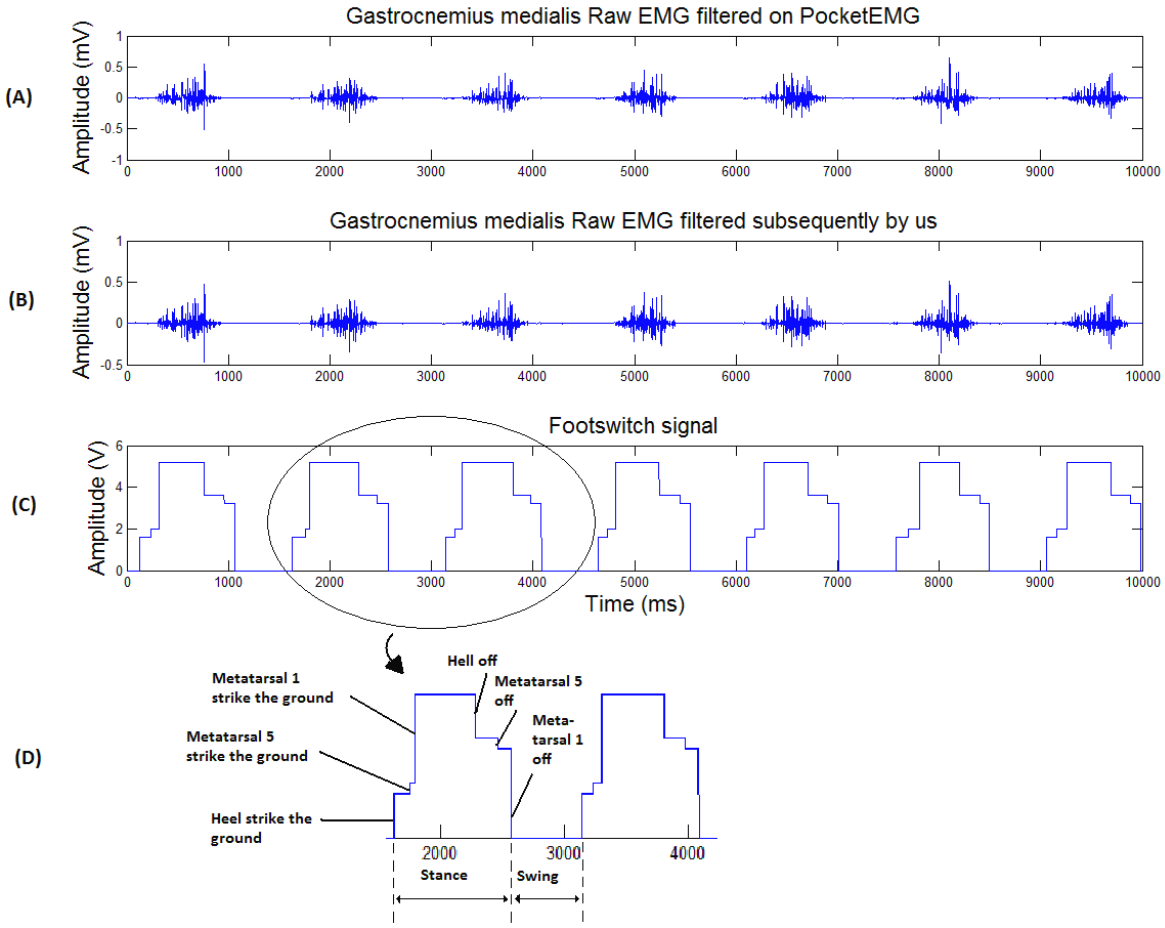

Figure 5.2: (A) Gastrocnemius medialis Raw EMG filtered in the Pocket EMG; (B) Gastrocnemius medialis EMG signal filtered by us; (C) Footswitch signal; (D) Explanation of each activation step in the footswitch signal

Due to movement artifacts and instability of the electrode-skin interface, raw EMG often shows slow variations of signal representing these artifacts. This happens due to changes in the small direct current offset voltage on each electrode [46]. The harmonics of these unwanted signals are usually in the frequency range of 0-20 Hz. In some EMG analysis, this range of frequency also contains harmonics of wanted signals representing some MUAPs. It is often used a high pass filter with a cutoff frequency between 10-20 Hz. Pocket EMG has already implemented an high pass filter with cutoff frequency of 15.7 Hz.

After all the practice acquired before the experiments, we decided to digitally implement a bandwidth filter of 20-400 Hz, independently of the used EMG equipment, to all output data of the experiences involving human walking. Thus, we implemented a digital first order Butterworth filter on Matlab to the signal already filtered by Pocket EMG.

An output signal of the Pocket EMG (Raw EMG filtered by the device) is presented in figure Figure 5.2-(A). The same signal, but filtered digitally by us, is presented in Figure 5.2-

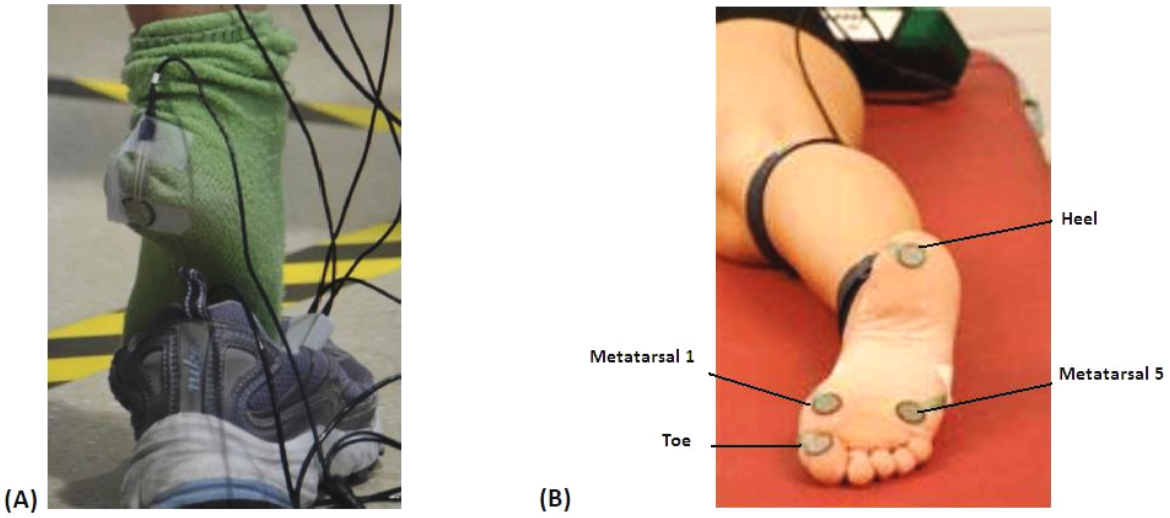

Figure 5.3: (A) Footswitch placed on the heel during one trial; (B) Four possible attachment sites on the bottom of the foot. Adapted, with permission, from [15]. Courtesy of ©NORAXON

(B). Once the bandwidth implemented on Matlab is very similar with the frequency response of the Pocket EMG system, our filtered EMG signal is very similar with the EMG signal filtered in the Pocket EMG. The power spectrum of these two signals is represented in figure 5.4.

In some cases, notch filters have been used to reduce the 50 Hz power line interference. But this is not a good practice, mainly because it removes power from a frequency band where EMG signals use to be high and near maximal power density (see figure 5.4). It was not used any notch filter on this work. However, as referred in section 4.2.2., Pocket EMG has a CMRR factor that eliminates this interference. Looking to figure 5.4-(B), we can notice that almost all the energy of the signal is in the 20-400 Hz range, with dominant energy in the 30-150 Hz range. If the CMRR factor was not sufficient, a great amount of energy would be concentrated in the 50 Hz of the power spectrum, which is not the case.

5.1.3 EMG envelope

In gait analysis, it is important to understand the level of activity of the muscles along the gait cycle. Therefore, there is an operation called enveloping that performs this requirement. The envelope can be computed by two different methods.

The first method involves two steps: rectify the filtered Raw EMG signal and then use a low pass filter to smooth the rectified signal. The smoothness of the envelope depends on the cutoff frequency of the low pass filter, and it is recommended to use a range from 3 to 15

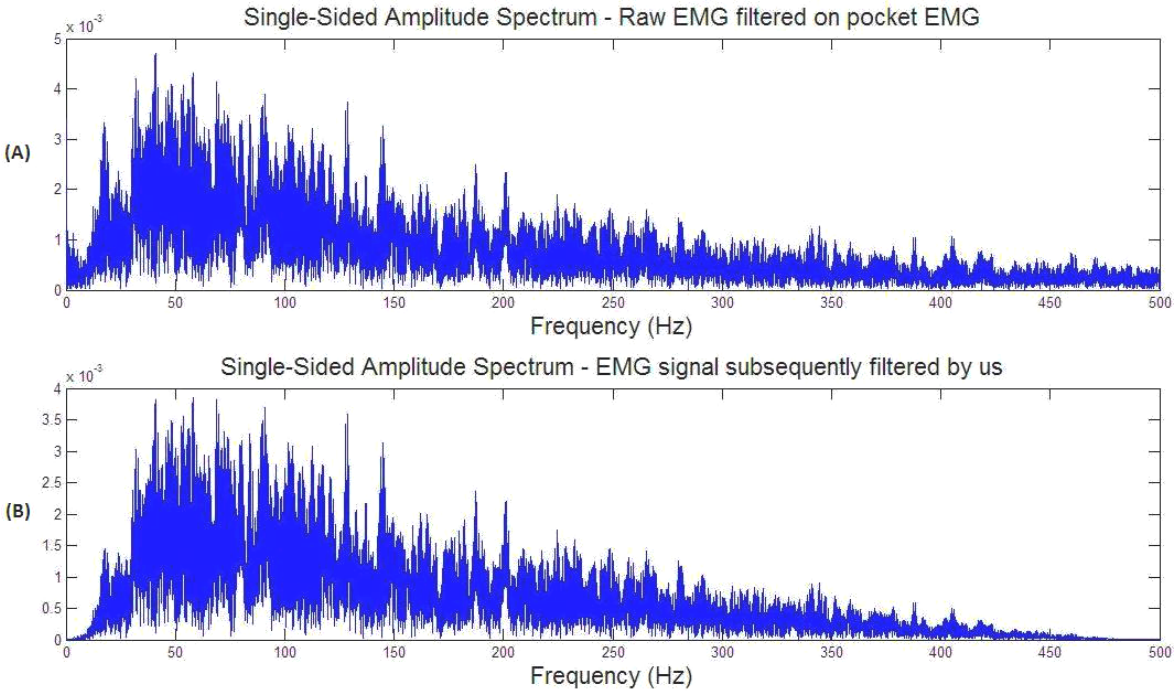

Figure 5.4: (A) Power spectrum of the Raw EMG filtered in the Pocket EMG; (B) Power spectrum of the Raw EMG filtered by us

Hz, depending on the desired smoothness.

The second method is similar with the first, but instead of rectifying the Raw EMG, it is computed its RMS (root mean squared), according to the formula 5.1:

$$RMS = \sqrt{\frac{\sum_{i=a-n/2}^{i=a+n/2} e_i^2}{n+1}} \tag{5.1}$$

where e is the EMG filtered signal, a is the central position of the window and n is the number of samples. This second method allows the researcher to create the RMS moving window, in which a time interval around each point of the filtered EMG signal is used to apply the RMS technique. Due to all the trials our group had performed before this study, it was decided to apply the second method of enveloping instead of the first one, mainly because the resulting envelopes are more fine and perceptible. In this work, it was applied a 50-point RMS algorithm for all filtered Raw EMG signals (see figure 5.5).

5.1.4 Amplitude normalization

EMG amplitude changes from person to person and also in the same person across different trials. Also, factors like the skin impedance and subcutaneous fatness may also affect EMG

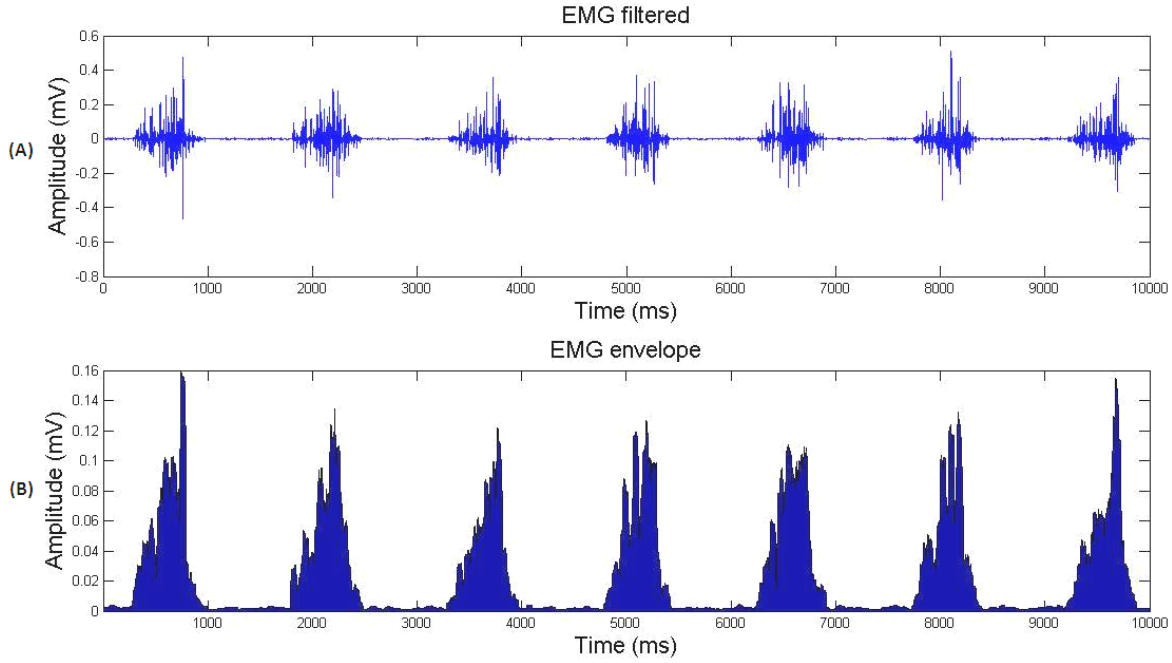

Figure 5.5: (A) EMG filtered; (B) EMG envelope was obtained after applying the 50-point RMS algorithm

amplitude. For these reasons, it is desirable to perform some form of EMG normalization in order to compare activation values between different muscles, between the same muscles in both legs of a person and to compare activation values between different studies or different persons in the same study [24].

There are many studies that explain the best way to normalize EMG signals [8] [66] [67] [53] [24]. However, a consensus about the the best method of normalization has yet to be reached. Normalization is often done by asking the person to perform a maximal isometric force[1]. Therefore, the maximum value (or the average of some maximum values) recorded during the task is used as a reference to normalize the EMG values of that person and for a specific muscle. Nevertheless, to generate a maximal force is subjective and requires a comprehensive anatomical knowledge and an appropriated device to ensure that the muscle being tested is the main one being activated [24]. Other methods to normalize EMG data are: to perform a sub-maximal isometric contraction [8] [24]; and to use the mean or the maximum value of the EMG envelope of at least six strides [8].

[1]Maximal isometric force is an exercise performed through the exertion of effort against a resistance, obtaining the maximum strength without change the muscle length

5.1.5 Time normalization

It is also important to time normalize EMG values in relation to the heel strike moments during the gait. Different tasks and trials may have different durations. Therefore, EMGs must be time normalized to compare results between them. For each trial, the moment of heel strike corresponds to 0% of the stride cycle and the next moment of heel strike corresponds to 100% of stride cycle. On the other hand, this second heel strike moment will correspond to 0% of the second stride cycle and the next heel strike will correspond to 100% of the second stride cycle and so on. Then, it is performed an interpolation of a fixed number of points for all gait cycles, for example between each 1% of each gait stride. So that, all gait strides will begin in 0%, end in 100% and have the same number of points. Finally, it is done the average of the EMG values from all gait strides and it is obtained a final time normalized gait cycle.

After time normalizing the EMGs from all the trials, we amplitude normalized them in relation to their maximum value. Figure 5.6-(A) presents an example of an EMG time normalized from 0-100% of gait cycle and amplitude normalized to its maximum value. After normalize each EMG, we smoothed them (see figure 5.6-(B)) to get more soft signals and valuable for the extraction of motor modules and activation signals (task explained in Chapter 6).

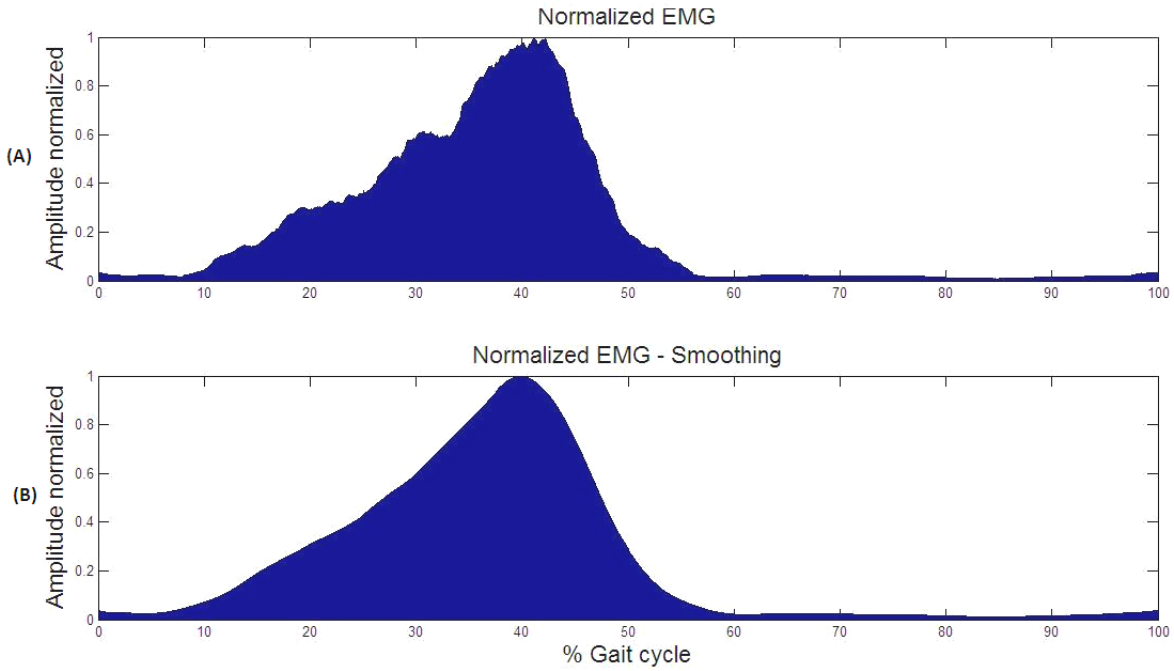

Figure 5.6: (A) Normalized EMG; (B) Smoothed normalized EMG

5.2 Kinematics Signal Processing

Like the EMG signals, kinematic information (in this case, angles of the joints) can also be processed. Kinematic data is usually low pass filtered using a cutoff frequency of 20 Hz [61] [35] [62]. After filtered, kinematic data is time normalized in the same way EMG signals are. Once the joint angles obtained for all the trials presented a very good smoothness, we decided not to filtered those signals. We just time normalized kinematic data.

5.3 EMG and kinematics patterns during treadmill gait

The major goal of motor rehabilitation is the recovery of optimum walking function [68]. Electromyographic and kinematic patterns of healthy people walking on treadmill are the reference to achieve this goal.

5.3.1 Activation patterns during normal gait

Muscular activation varies among young and old people, according the walking speed and depending if the person walks on a treadmill or overground. For example, older people present a strategy of stiffening the limb during single support phase (when only one foot is on the floor) and this can be the reason why they present reduced push off power at higher walking speeds [82]. Some studies have been focused on EMG patterns during different speeds of walking [82] [37]. In a general way, muscular activation increases with the increase of walking speed. Finally, there are also minimal activation differences depending on wether a person walks on a treadmill or overground [68]. The majority of the EMG studies were done on a treadmill mainly because it is much simpler to choose and control the gait speed.

For our study, only healthy young people performed the trials. The treadmill speed was changed across the trials and the tests were performed on the Lokomat treadmill.

Examples of typical Tibialis anterior and Rectus femoris EMG envelopes captured by us during treadmill gait are represented in figure 5.7. There are many studies about electromiographic signals in lower limbs muscles and there exist a great consensus among the studies and our results. For the same speed conditions, normalized EMG envelops of a given muscle present similar shape. Figure 5.8 represents the typical interval of activation of several muscles during the gait cycle.

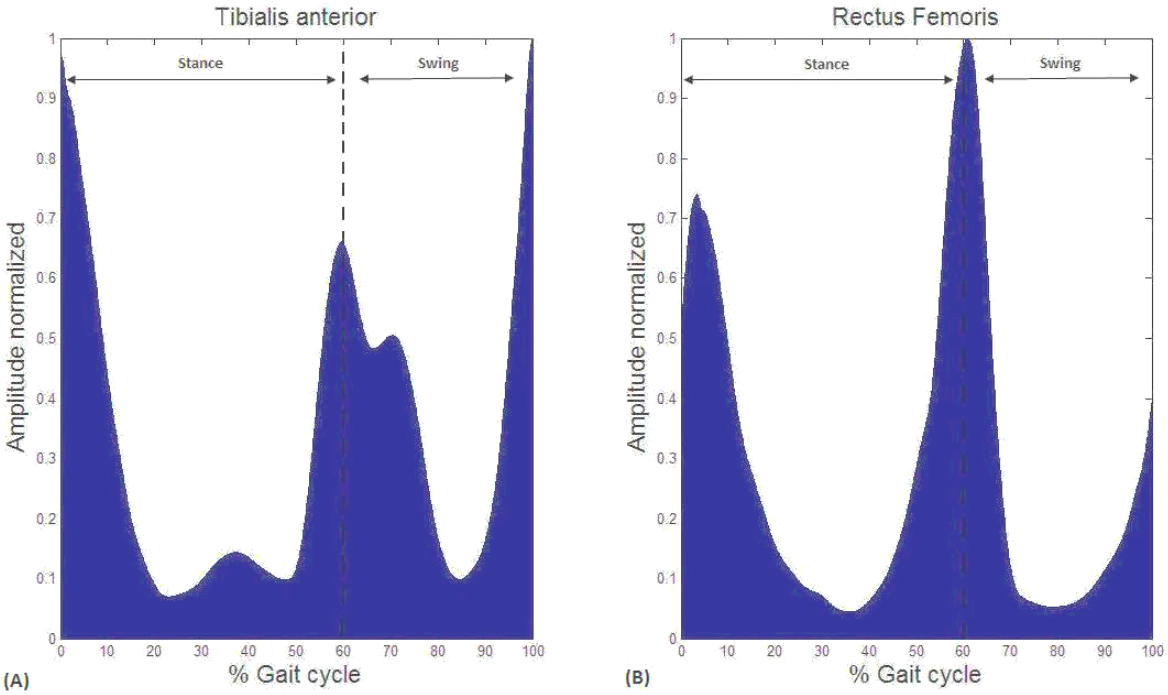

Figure 5.7: (A) Tibialis anterior EMG gait pattern; (B) Rectus femoris EMG gait pattern

5.3.2 Kinematics during normal gait

There are many studies detailing the kinematics patterns of normal gait. Typical kinematics during normal walking is represented in many books and scientific articles [73] [68] [35] [92]. Briefly, kinematics patterns of hip, knee and ankle joints have the general forms represented in figure 5.9 and the angles are obtained in relation to the joints references represented in figure 4.10-(B), in the sagittal plane.

About hip kinematics during normal gait, it starts the gait cycle in flexion. Then it extends until the end of terminal stance (50% of the gait cycle) and it finally flexes until the end of the gait cycle.

Knee angle curve presents two peaks of flexion: one in stance and the other in the swing phase, with the second one being much larger than the first. Knee is always in a positive position (angle higher than 0^0) in relation to the reference of the knee joint represented in figure 4.10-(B).

The ankle angle curve is usually in a neutral position (0^0) at the initial contact, after which it slightly dorsiflexes during loading response. Then, it plantarflexes again through the remaining stance. Almost in the transition from stance from swing, it dorsiflexes again. In mid-swing and terminal swing, the ankle angle returns to 0^0.

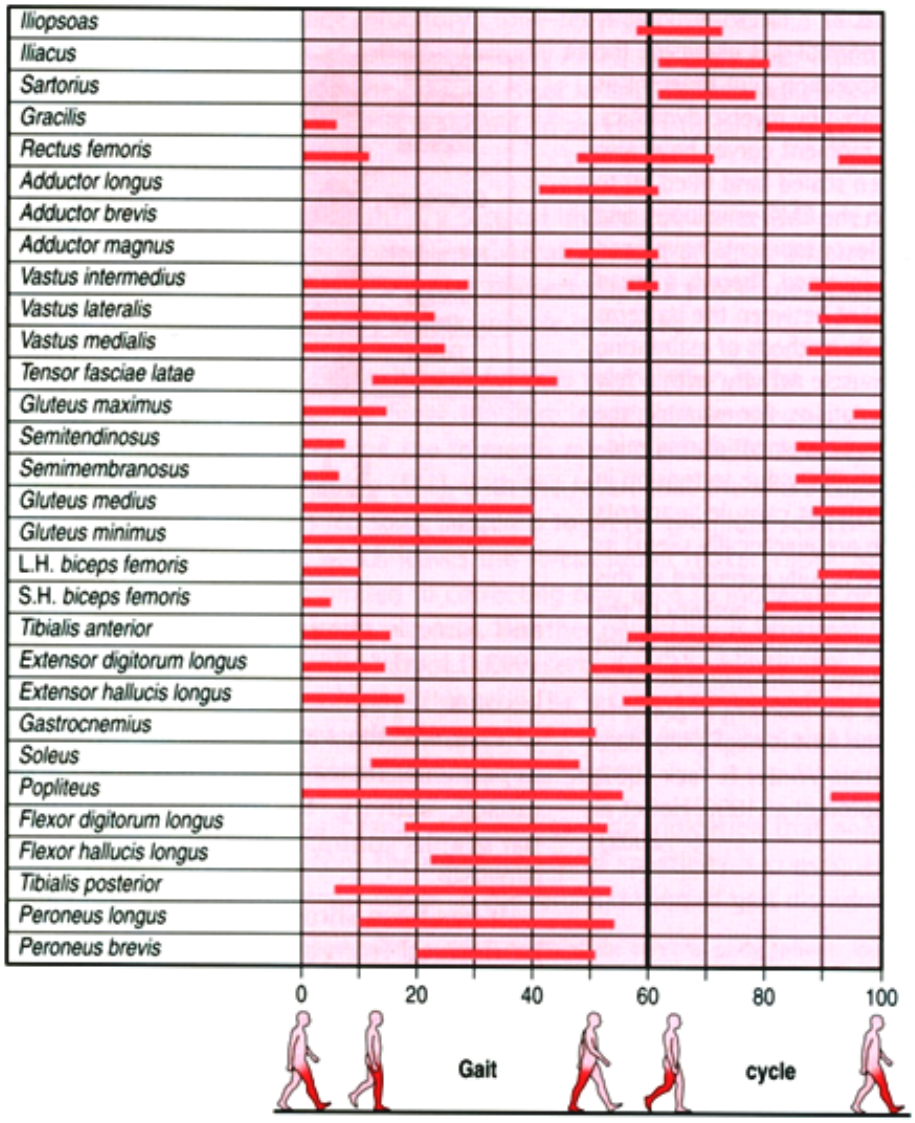

Figure 5.8: 'On/off' times of the muscles activity during gait in healthy people at a comfortable speed. Used with permission from [46]

5.4 EMG and kinematics during gait on assistive devices

It is clinically important to study how the walking assisted by robotic exoskeletons changes the muscular activation patterns, so that it is possible to compare activation patterns obtained in healthy people with the activation obtained in persons with disabilities. This is a step to establish new control strategies in training after neurologic injury [56].

More studies need to be done to completely clarify the influence of Lokomat in the electromyographic and kinematic patters. Our work addresses the muscular electric activation and kinematic patterns obtained during the walking in Lokomat, changing parameters like the guidance force and the speed.

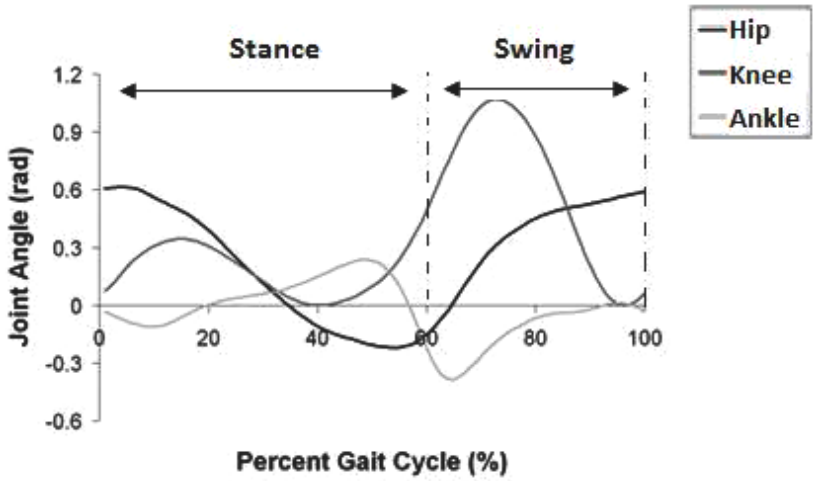

Figure 5.9: Kinematics during normal gait, in the sagittal plane. Adapted, with permission, from [22]

Hidler, J. et al [36] have been studying the differences of muscular activation in lower limb muscles during treadmill walking and Lokomat-assisted walking, using 100% of guidance force in Lokomat walking of healthy subjects. His group referred that there are differences of activation patterns between both types of walking, mainly because Lokomat limits the degrees of freedom of legs and pelvis. Among those differences, it can be mentioned, for example, that quadriceps (Rectus femoris and vastus lateralis) and hamstrings presented higher activity during the swing phase of Lokomat walking than treadmill walking, whereas tibialis anterior and gastrocnemius presented reduced activity along most of the gait cycle in Lokomat (see figure 5.10). In relation to the gastrocnemius and tibialis anterior activity during Lokomat walking, the authors reported that the drop in muscle activity can be related with the use of footlifters, which assist ankle dorsiflexion for toe clearance during swing phase [36]. In relation to the quadriceps, the explanation can be the fact that people usually rotate their hips and also abduct their legs to allow the toe to clear the floor, which are movements quite limited to perform in Lokomat. Therefore, people exert higher muscle activity in the quadriceps to help in the elevation of the feet and preventing toe from getting caught in the treadmill [36].

Klarner, T. et al [47] suggested that the body weight support (BWS) and the stride frequency used in Lokomat should be taken into account for optimization of motor output during locomotor training. In their study [47], muscular activity per stride tended to decrease when using increased BWS and faster stride frequency. Mazzoleni, S. et al [58] reported higher muscular activity when the subjects actively cooperated with the Lokomat than when they were passive.

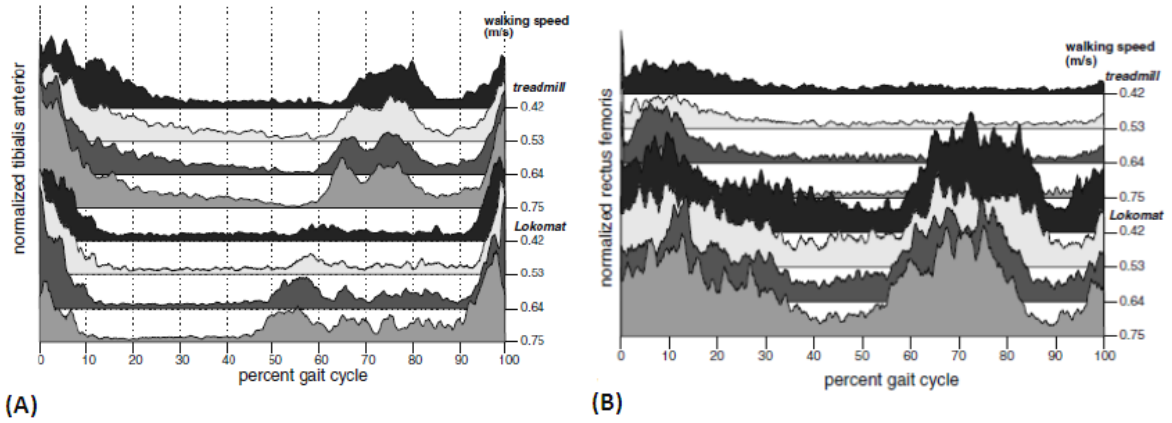

Figure 5.10: Average normalized Tibialis anterior (A) and Rectus femoris (B) activity for different speeds and for Lokomat and treadmill walking. Used with permission from [36]

van Asseldonk et al [92] studied the effects on muscle activity of walking in healthy young individuals using the gait trainer LOPES. During the trials, the ankle was free to move and LOPES was controlled providing minimal resistance during walking, an almost free walking mode. Rectus femoris presented higher activity in LOPES during the transition from stance to swing. During initial contact, the activity of rectus femoris and vastus lateralis was lower in LOPES. For the other gait phases, the overall activity of both muscles was similar between LOPES and treadmill walking. Biceps femoris presented higher activity in LOPES walking. Gastrocnemius presented smaller activity during terminal stance in LOPES walking, whereas tibialis anterior showed higher activity during pre-swing and initial swing in LOPES walking.

In relation to the portable exoskeletons, Ferris et al [25] [80] [9] [45] have built pneumatically - powered lower limb exoskeletons in order to retrain motor deficits. These exoskeletons work with proportional myoelectric control, by using the EMG signal of gastrocnemius or soleus. These studies reported that healthy individuals adapted very well to walking with these ankle exoskeletons, reducing their overall energy expenditure. Persons with incomplete spinal cord injury have showed modification of muscle activity patterns, as they practice walking with these exoskeletons.

Lewis and Ferris [51] suggested a relation between ankle and hip muscle activation during human walking. They hypothesized that changes in ankle kinematics could result in hip kinematic changes. They related that walking with increased ankle push off resulted in lower peak of hip moment, as well as lower peak of hip extension moment. They suggested that

increasing ankle push off during walking (by using exoskeletons, for example) may help to compensate hip muscles weakness or injury and to reduce hip joint forces.

Typical kinematic patterns in the knee joint during Lokomat walking are represented in figure 5.11-(A). Using 100% of guidance force in healthy subjects, Hidler [35] found no statistical differences in the knee range of motion and peak flexion angle between treadmill gait and Lokomat gait. However, his group found much more hip and ankle extension, and also greater hip and angle range of motion in Lokomat (figure 5.11-(B) and figure 5.11-(C)). The reduced degrees of freedom in Lokomat can be the reason for these kinematic differences. Despite being firmly attached to the device and forced to follow a pre-defined pattern when using 100% of guidance force, subjects can move in relation to the device, which in part explains these kinematics differences [35].

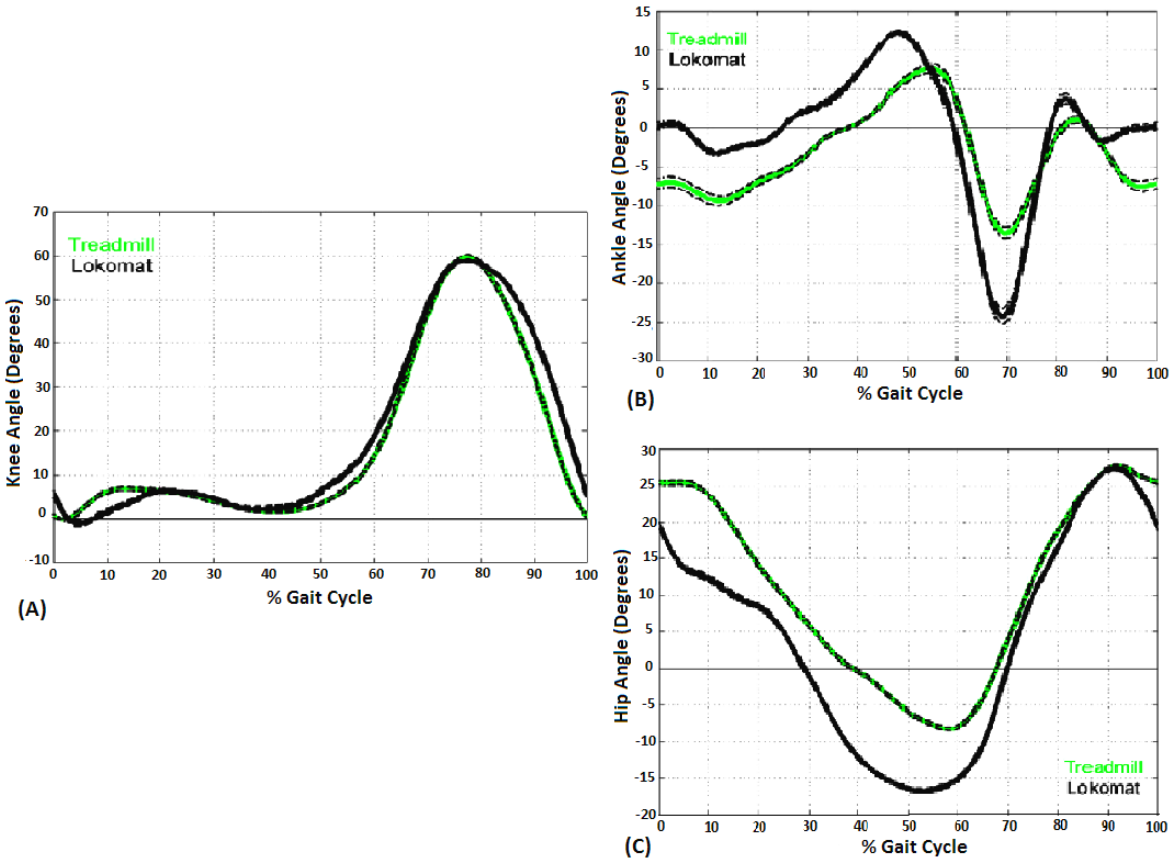

Figure 5.11: (A) Knee, (B) Ankle and (C) Hip joint angles during Lokomat and treadmill walking of a representative subject. Used with permission from [35]

Using the exoskeleton LOPES, van Asseldonk et al [92] obtained relevant decrease of the knee angle range. In relation to the hip, they obtained similar kinematic patterns. These

kinematics results are the opposite of the results obtained with Lokomat [35].

Using the same exoskeleton used by Ferris et al [25] [80] [9] [45], Kao et al [44] obtained large differences in ankle joint kinematics compared with normal walking without exoskeleton. There were no large differences in knee or hip joint kinematics during both types of walking. Hip, knee and ankle joint kinetic patterns were only slightly different comparing both types of walking. With these results, the authors suggested that humans aim for similar joint kinetic patterns when walking with robotic assistance rather than similar kinematic patterns. They also reported that greater robotic assistance provided during initial practice results in longer time for adaptation than use lesser robotic assistance.

Chapter 6

Modular organization of the nervous system

The correct operation and integration of information from different structures of the nervous system results in the voluntary movements of our daily life. In the first section of this chapter, some of the roles of three important brain structures involved in producing movements are explained. In the second section, we explain the recent theory about the existence of a low-dimension organizational structure of the nervous system, which may be the basis of the neuromechanical output during walking and some other different tasks. Our research analyzes the effects that robotic devices can have in such an organizational structure, especially to repair the damaged organizational structure presented in people with motor impairments.

6.1 Structures controlling movement

The correct execution of voluntary movements mainly depends on the integration of information and the correct operation of the different parts of the nervous system [11] [76]. Some brain structures decide the movements to be performed at each instant and send the neural signals corresponding to those actions to the motorneurons of the spinal cord. These signals result in the muscular activation and contraction responsible for the execution of those movements [11]. When some damage occurs in a structure integrating this circuit (for example, a stroke), it may affect the correct execution of the desired voluntary movements.

Figures 6.1 and 6.2 present the most important brain structures responsible for the movement control. Three structures present a major role in the coordination of the movement. These structures are: cerebral cortex, basal ganglia and cerebellum [70].

In order to decide which movements the body should perform at each moment, the motor cortex receives information from other brain structures. For example, it receives information

from the parietal lobe about the position of the body in space, information from the anterior frontal lobe about the goal to be achieved and the proposed strategy, information from the temporal lobe about strategies already performed in the past, and so on. If some damage occurs in some region of the motor cortex, the part of the body controlled by that region will become paralyzed. This happens because each part of the body is controlled by some region of the motor cortex.

Basal ganglia is a set of neural structures located deep inside the brain (see figure 6.2). Basal ganglia receives information from different regions of the cortex, processes that information and sends it to the motor cortex via thalamus. This sequence of sending information to and from the basal ganglia, which operates in conjunction with another involving the cerebellum, selects and triggers coordinated voluntary movements. The role of the basal ganglia in starting and regulating motor commands is visible in people with damages in the basal ganglia, as the people who suffer from Parkinson's disease. People who suffer from Parkinson's disease have difficult in starting the planned movements, tremble and perform those moments in a slow way once they can start them.

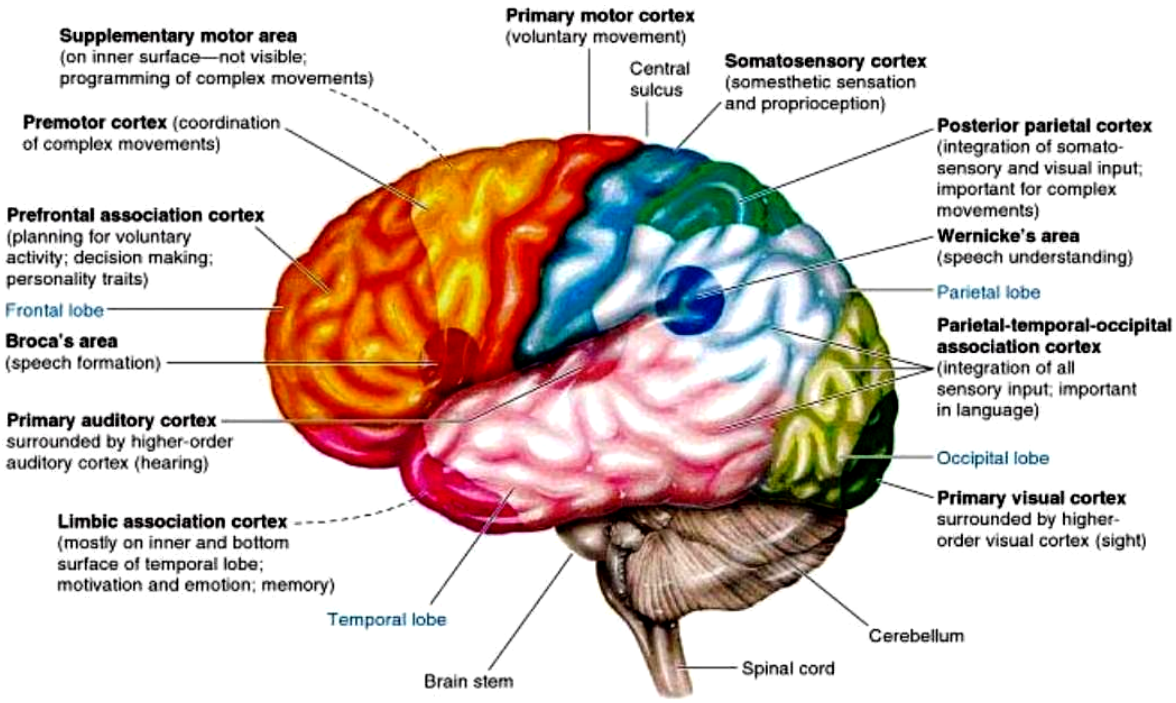

Figure 6.1: Regions of the cerebral cortex and their functions [84].
Reproduced by permission. www.cengage.com/permissions

The cerebellum receives information from different regions of the cortex. Then, it sends information to the motor cortex about the pretended direction, force and duration of the movement. This sequence of sending information to and from the cerebellum, acts in con-

junction with another sequence involving the basal ganglia to regulate the motor control. People with damages in the cerebellum presents difficulty grasping a target with their hands and display balancing problems [70].

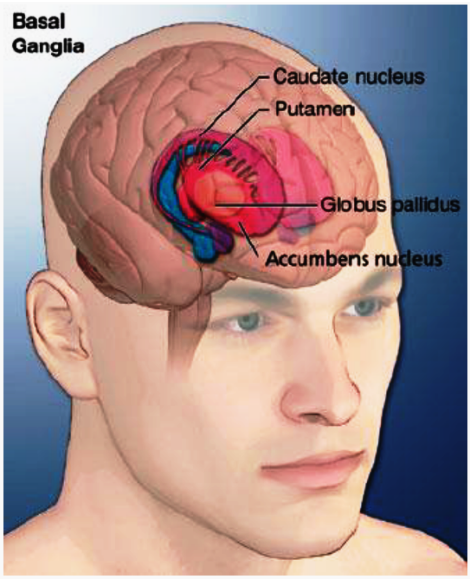

Figure 6.2: The main basal ganglia structures are the caudate nucleus, the putamen and the accumbens nucleus. Used with permission from [26]

Every brain structure is constituted by thousands of neurons. There are millions of neurons controlling the muscles involved in human movements. The human body has more muscles than degrees of freedom. In fact, some muscles cross multiple joints. Therefore, actual studies have been trying to understand how the central nervous system produce the neuronal responses corresponding to the planned movements, coordinating a large number of degrees of freedom of the musculoskeletal system [12] [87] [50] [64] [19] [40] [10] [41]. Actual evidences suggest that the nervous system controls motor tasks by using a low-dimensional modular organization of muscle activation constituted by motor modules and activation signals [12] [39]. Recent computer simulations [59] [63] [64] showed that some motor tasks (including the walking) can be produced through the coordinated activation of few modules, each one associated with specific biomechanical subtasks.

6.2 Motor modules and activation signals

There is growing evidence that muscle activity is controlled by a low dimensional modular organization. Recent studies have suggested that the coordinated activation of muscles during walking is controlled by the central nervous system through activation signals (also

referred in the literature as factors or control signals) and motor modules (also referred as loadings or synergies) [28]. This modular control is represented in figure 6.3.

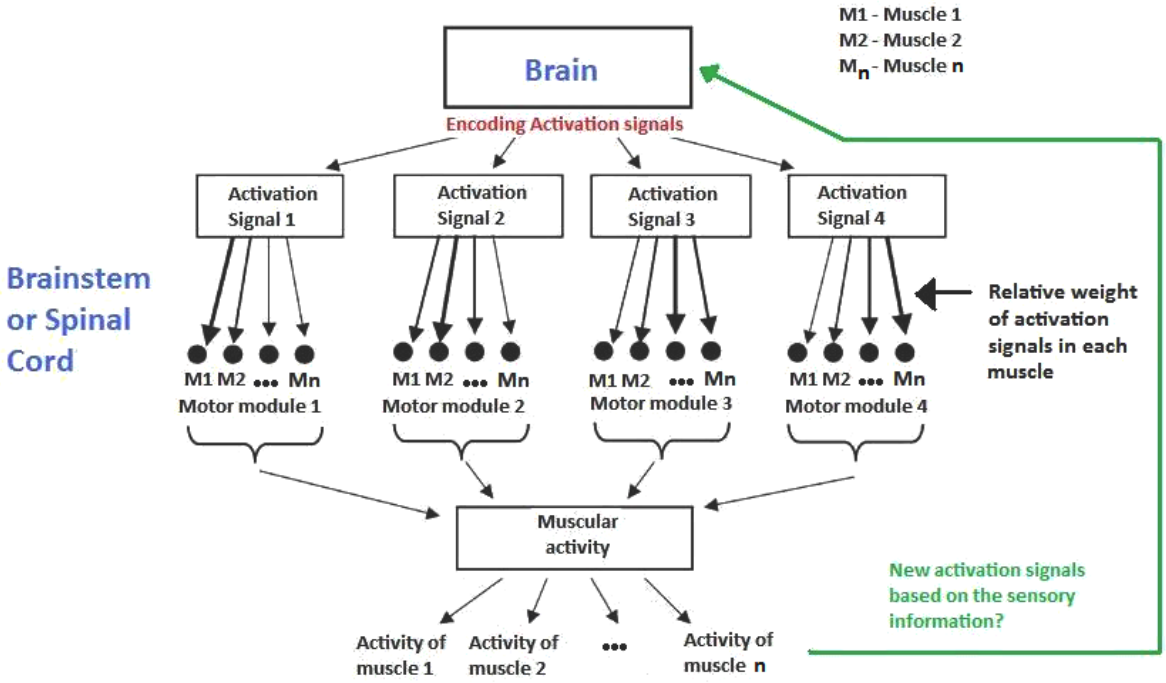

Figure 6.3: Theory of the modular control presented by nervous system to control movements

Taking into account the different names given to the same components of this control, we had to decide which names to use throughout this dissertation. Thus, this modular organization (represented in figure 6.3) can be thought as a neuronal network in which the activation signals are generated in some brain structures according to the sensory information received about the different tasks to be performed. Then, the activation signals are directed to the motorneurons via a premotor network (it can be located in the brain stem or in the spinal cord) that specifies the relative weight of each activation signal in each muscle. The relative weight of each activation signal is given by the respective motor module (that specifies the weight of the respective activation signal in the muscles). The set of an activation signal and the respective motor module is called module.

To better understand this concept of modular organization, a practical example is represented in figure 6.4. The average muscular activation of seven muscles (EMG envelopes in Figure 6.4-(A)), during Treadmill walking using 2.0 Km/h, can be achieved using four modules. Each module consists of an activation signal (Figure 6.4-(D)) and the respective motor module (Figure 6.4-(C)) that contains the relative weight of the activation signal for each of

the seven muscles. Thus, muscle activity (black lines in figure 6.4-(B)) is given by the sum of the contributions from all the activation signals (colored lines in figure 6.4-(B)) weighted by the motor modules acting on it. As can be seen, the reconstruction of muscular activity shown in Figure 6.4-(B) is very similar with the muscular activity represented in Figure 6.4-(A). Therefore, with few modules it is possible to control several muscles and with a high precision of movements.

The researcher's opinions about this modular control diverge in the following: some researchers report that the motor modules remain very similar for the different motor tasks performed; other researchers report that the activation signals remain approximately constant for the different activities performed. If researchers can identify all the modules, how they change according to the different motor tasks performed and according to the type of impairment of each person, it can be possible to develop focused therapy to train the damaged modules. The comprehension of this modular organization will be useful for movement restoration by using, for example, FES (functional electrical stimulation) if few modules can describe several functional tasks.

Clark et al [12] have been studying how this modular control works. Based on other works [50] [87] about the use of nonnegative matrix factorization (NNMF) algorithms, his team tested the hypothesis that muscular activation patterns during walking are produced through the variable activation of a small set of modules. They tested the hypothesis that subjects with post-stroke hemiparesis would have damaged modules, leading to the verified impaired walking performance. It was shown less complex coordination patterns in post-stroke patients, with less modules needed to account for muscle activation during walking at their preferred speed compared with healthy subjects. Their results showed a highly dependence on the neural control signals to perform a correct walking. They also suggested a common modular organization of muscle coordination underlying walking in both healthy and post-stroke subjects [12].

Ivanenko has been also researching the common modules in healthy subjects by applying different gravitational loads using a harness during walking [39] [41], performing voluntary tasks on overground walking [40] and comparing walking with running activation [10].

According to Neptune et al. [64] [63], Clark et al. [12] and McGowan et al. [59], four modules can be identified and are capable of producing different activities as normal

walking, walking with body weight support, walking with body mass increased/decreased, kicking and stepping. Each module was found to be associated with specific biomechanical tasks:

- Module 1 (higher activity in hip and knee extensors) provides body weight support in early stance [59];
- Module 2 (higher activity in ankle plantar flexors) provides body support as well as forward propulsion in late stance [59];
- Module 3 (higher activity in tibialis anterior and rectus femoris) contributes to decelerate the leg during early and late swing [59] and contributes to ground clearance of the foot [64];
- Module 4 (higher activity of the hamstrings) contributes to decelerate the leg in late swing and propel the body during early stance [59] [64].

Several control strategies have been proposed to control rehabilitation devices and most of them use more assistance as the patient really need. Provide more assistance than needed can have negative consequences for motor learning [56]. Recent studies have been focused on 'assist-as-needed' control algorithms for control robotic rehabilitation devices, which promotes muscular activity of patients during the robotic walking [92]. Robotic guidance force used in Lokomat is the amount of aid the patient receives during the walking.

Robotic assisted walking can be used to induce activation patterns during walking that might be beneficial for the recovery of patients with motor impairments.

One of the goals of our study is to analyze the effects of the robotic guidance force and gait speed on the modular organization of walking in healthy subjects during the use of a rehabilitation exoskeleton (Lokomat, in this case). Our hypothesis is that walking under variations of robotic guidance force and gait speed can be represented by a reduced number of motor modules and activation signals. If we confirm this fact, we should conclude what is the effect that the robotic therapy can have in such a modular control, especially in the reeducation of the damaged modules present in people with motor impairments.

Actual computational techniques allow researchers to extract motor modules and activation signals from the EMG envelopes of each muscle. The most used mathematical algorithms to do that are nonnegative methods and PCA (Principal Component Analysis).

Nonnegative methods are more successful for this purpose than orthogonal methods like PCA. In PCA algorithms, motor modules can have negative values and, therefore, many features of the activation signals cancel each other on data reconstruction, which means that their contribution to the final output patterns depends on the activity of other modules. On the other hand, nonnegative methods only allow the addition and never the subtraction of features. Therefore, each contribution of the activation signals can be analyzed independently [87]. For these reasons, we decided to use a NNMF (nonnegative matrix factorization) algorithm [52] to extract motor modules and activation signals from the EMG normalized envelopes from all the trials performed by individuals and by the average group.

Given an m x t data matrix V with $V_{ij} \geq 0$ and a pre-specified integer $n < \min(m,t)$, NNMF finds two non-negative matrices $W \in R^{m,xn}$ and $H \in R^{n,xt}$ such that $V \approx W.H$. For this study, the matrix V represents the EMG envelopes, the matrix W represents the motor modules and the matrix H represents the activation signals. A Matlab NNMF algorithm (Appendix C) adapted by Lin [52] was used to extract motor modules and activation signals.

Each normalized EMG envelope (with values from 0 to 1) from all the trials was combined into an m x t matrix (see figure 6.4-(A)), called EMG_0, where m indicates the number of muscles (seven muscles in this case) and t is the time base (101 values that represents the gait cycle from 0% until 100%).

The NNMF algorithm was applied to the EMG_0 matrix for extraction of motor modules from each subject and for each condition. A priori, the number of activation signals, n, was specified by us (two, three and four activation signals), and the NNMF algorithm found the properties of the modules by populating two matrices: an m x n matrix (with values from 0 to 1), which specifies the relative weighting (motor modules) of a muscle in each activation signal, and an n x t matrix (with values from 0 to 1), which specifies the activation timing of each activation signal. These two matrices were multiplied to produce an m x t matrix (see figure 6.4-(B)), called EMG_r, in an attempt to reconstruct the EMG signals.

For each iteractive optimization of the algorithm, EMG_r was compared to EMG_0 by calculating the sum of the squared errors $(EMG_0 - EMG_r)^2$ and the result was used until converge on the motor modules and the activation timings of the activation signals that minimized the error.

The results we obtained using two, three and four modules are presented in Chapter 8.

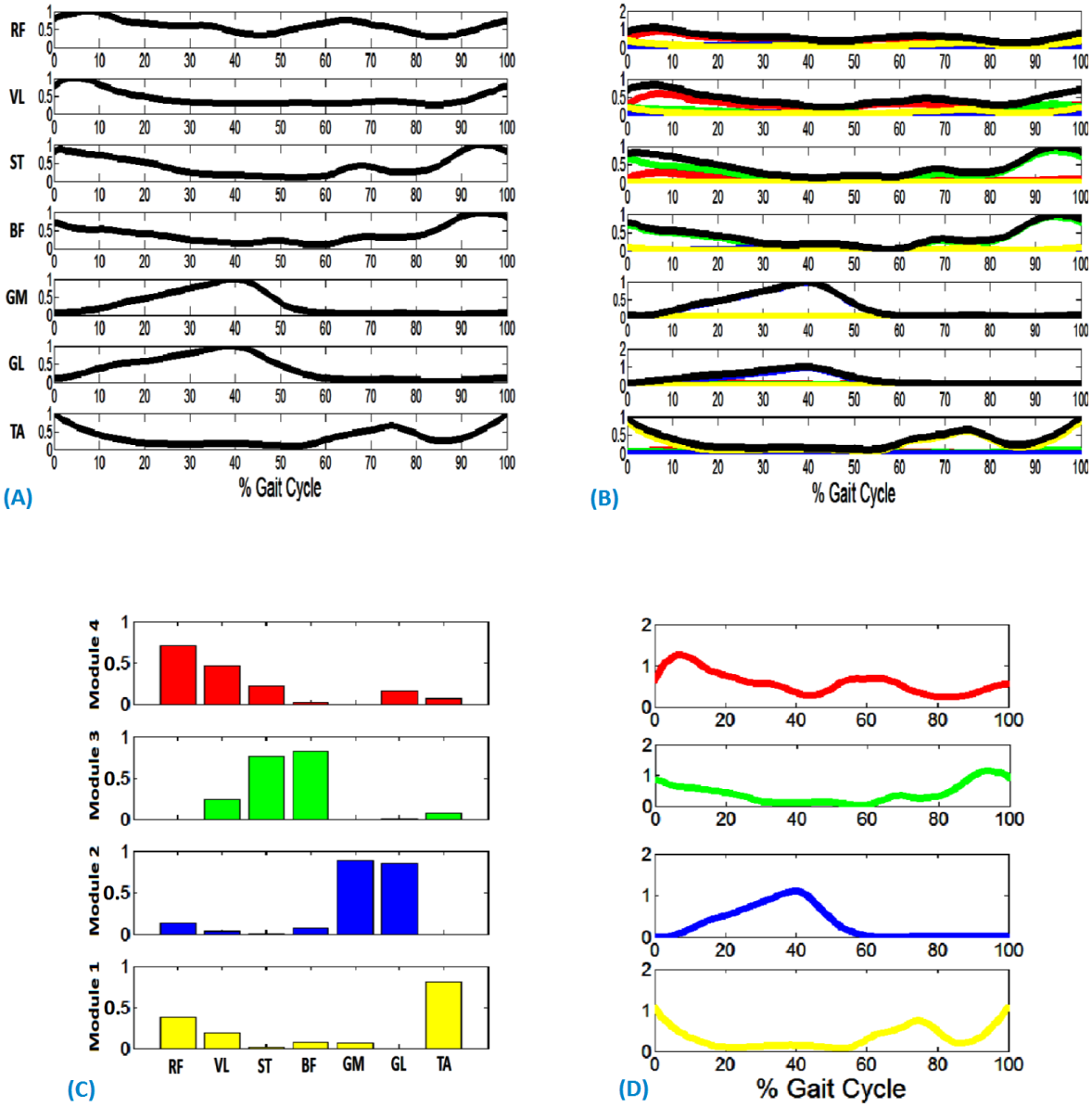

Figure 6.4: Reconstruction of the normalized and smoothed EMG envelopes using a nonnegative matrix factorization (NNMF) algorithm. (A) Normalized and smoothed EMG envelopes of the average group, at 2.0 km/h in Treadmill walking, for seven muscles of the lower limb. NNMF extracted 4 modules capable of reconstruct the EMG data. (B) Total muscle activity (black lines) is given by the sum of the contributions from all the activation signals weighting by the motor modules acting on it (colored lines). Each module include (C) one motor module (muscles weightings) and (D) one activation signal (activation timing profile) across the gait cycle.

Chapter 7

Experimental Protocol

The previous chapters have been useful to allow the reader to understand the procedures that we performed with the participants of this study, as well as the posterior data analysis. The same procedures were performed for all the participants included in the study. Thus, this chapter begins with a brief description of the participants. Then, it continues with a description of the Lokomat (the robotic device used in this study) and the procedures to record electromyographic and kinematic data on both treadmill and Lokomat walking. The chapter follows with the procedures that we implemented to process the data recorded during the trials. Finally, the chapter ends referring the Statistical Analysis we used to conclude about the results of the research.

7.1 Participants

Eight healthy participants (6 males and 2 females; age = 25,75 ± 4,37 years; body weight = 69,5 ± 9,84 Kg; height = 1,76 ± 0,08) with no neurological injuries or gait disorders participated in the study, performing the procedures reported in section 7.2. The characteristics of the individuals are listed in Table 7.1. The participants had no previous experience with the robotic-assisted walking. A local committee provided ethic approval for this study. Participants gave verbal consent to perform the experiments and to be recorded.

7.2 Procedures

Only the members of the research group that took the Lokomat® Certificate Course 'User for research purpose' given by Hocoma AG could coordinate the experiments performed on

Table 7.1: Description of the individuals

Individual	Sex	Age(years)	Weight(Kg)	Height(m)
I1	Male	21	66	1,82
I2	Male	22	75	1,68
I3	Male	33	75	1,85
I4	Female	21	55	1,68
I5	Male	26	85	1,87
I6	Female	29	58	1,71
I7	Male	25	68	1,72
I8	Male	29	74	1,74

this study.

Lokomat's features were already described in section 2.3.1. Briefly, Lokomat is a robotic orthoses composed of a treadmill and a body-weight support system, which controls the user's legs movements in the sagital plane [13]. Lokomat has four degrees of freedom, allowing the movement control of hip (one degree of freedom in the left hip and other in the right hip) and knees (one degree of freedom in the left knee and other in the right knee) in the sagittal plane [13]. During the trainings, the feet stay in neutral position because of the footlifters the patient need to put on (see figure 2.3). The trajectory, the speed and the guidance force (the amount of aid the patient receives during the walking) used in Lokomat is totally programmable. A value of 100% of guidance force corresponds to a strict guiding (position control with stiff Lokomat joints) of the exoskeleton. A value of 0% corresponds to free run mode (easily moveable Lokomat joints).

Each trial lasted from 100 to 120 minutes. This time period included the person's preparation which entailed their skin preparation, electrodes placement, as well as the goniometer and the footswitches accommodation. Hocoma suggests to wear appropriate clothing (long pants or tracksuit pants made of soft cotton fabrics), in order to reduce the patient's risk of skin irritation and lesions. But these are the recommendations for the type of clothing during normal training, *i.e.*, without electrodes placed on the legs. Thus, each participant had to use sneakers, thick and comfortable shorts and a thick shirt.

The protocol followed by each participant is then described:

- With the participant standing, we measured the length of his/her upper leg (from the femur's greater trochanter to its epicondyle) in centimeters and lower leg (from the knee joint cavity to the sole of the foot, including the sneakers). These two values were inserted in Lokomat software in order to adapt the walking to the patient.

- Then, with the participant sitting on a chair, we verified the cuffs that better suited him/her.

- We marked the regions where the cuffs would be fitted.

- If the subject had hair in the area where the electrodes would be placed, we would do all the SENIAM recommendations before putting the electrodes (see section 4.2.). After that, we fastened the bipolar electrodes (Ag-AgCl, Fiab S.p.A.) to specific locations of the subject's dominant leg, according to the recommended sensor placement procedure described in Appendix B, for the seven muscles studied (Rectus femoris, Vastus lateralis, Semitendinosus, Biceps femoris, Gastrocnemius medialis, Gastrocnemius lateralis and Tibialis anterior) and also taking into account the regions where the cuffs would be fitted. Then, we wrapped the electrodes with bandages to ensure that the wires did not impede the subject's walking. The EMG data were recorded using an EMG acquisition system (BTS Pocket EMG, Myolab) handled by the participant during the trials. The data was wirelessly streamed to a laptop.

- We put the goniometer in the knee joint (in the sagittal plane), the footswitches on the foot of the dominant leg (we knew which was the dominant leg by asking the participant) and the reference electrode in the knee of the dominant leg.

- When the subject was fully instrumented, he/she was asked to walk at a self-selected speed on the treadmill for approximately 4 minutes in order to get used to the treadmill. After this adaptation period, the subject walked at three different walking speeds (1.5, 2.0 and 2.5 Km/h). The order was randomly selected to eliminate any bias associated with the order in which speeds were tested. With each change in treadmill speed, the subject walked for one minute adaptation phase, after which EMG and kinematic data was collected for another one minute. At the end of this treadmill session and since

Lokomat has implemented a system to measure joints kinematics, the gonimeter was removed from the participant.

- After that, we put a harness on the participant (see figure 7.1). We lifted the participant so that he/she was no longer touching the treadmill. Finally, we set the BWS (Body Weight Support) to 30% of his/her weight.

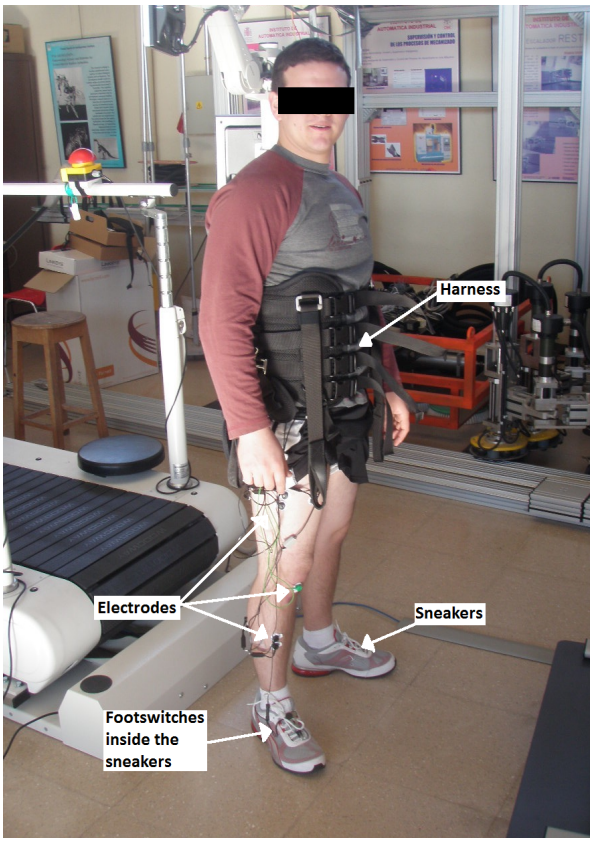

Figure 7.1: Participant before being lifted by the Body Weight Support system

- We attached the Lokomat to the participant using special hooks to the harness. Then, the participant was fitted to Lokomat, according to the features of the device that better suited the participant (see figure 7.2): pelvic depth; Lokomat upper leg length; and Lokomat lower leg length. After this, we fitted the cuffs.

- The final step before starting Lokomat walking was to put the footlifters on the participant. During the Lokomat walking, we had to confirm constantly if the footlifters pulled the feet up sufficiently in the swing phase so that they do not touch the treadmill. If not, we would have to adjust them correctly during the walking.

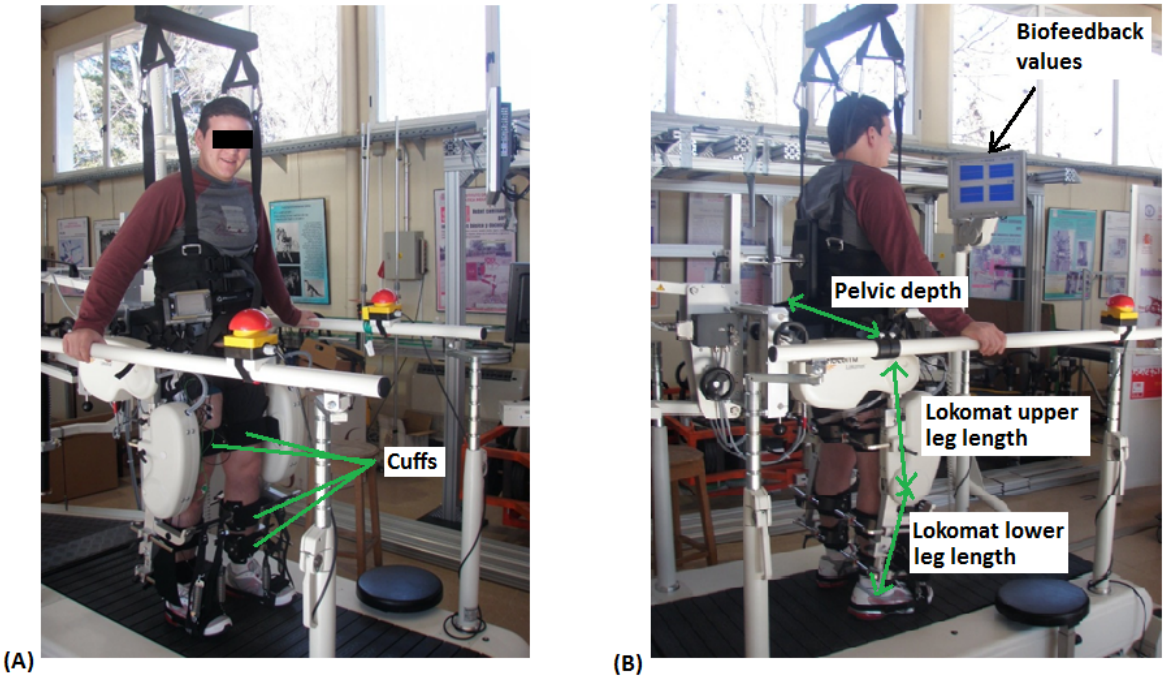

Figure 7.2: (A) Cuffs used to attach the participant's legs to the Lokomat; (B) Some Lokomat's features include the pelvic depth, the upper and the lower leg length. The participant follows his performance watching the visual representation of biofeedback in a special screen.

- When the subject was correctly fitted on Lokomat, Lokomat initiated stepping with the participant still in the air and using 100% of guidance force. The participant was allowed to walk in the Lokomat for 4 minutes at 1.5 Km/h in order to get used to the device.

- At the end this period, we lowered the participant, constantly verifying if the feet correctly touched the treadmill. This transition was extremely important, so that the participant could correctly walk.

- After this adaptation period, Lokomat's walking speed was then randomly set to one of the three speeds (1.5, 2.0 and 2.5 Km/h) used during treadmill ambulation, and after one minute of adaptation, EMG data was collected for another one minute sequence. This same procedure was repeated for all the three speeds. At the end of this sequence, we repeated the same procedure for the four different guidance forces (100%, 70%, 40% and 20%) studied, in a randomly order and a resting time of 4 minutes between each different guidance force. During all the trials on Lokomat, the body weigh support was always 30% of the participant weight. The participants were asked to actively

follow the robotic guidance aided by the Lokomat's visual representation of biofeedback[1] values (see figure 7.2-(B)). The visual biofeedback values, designed to motivate the patient to improving the walking performance [54] [55] [78], were displayed step-by-step in line graphs representing the walking performance over the last steps. In particular, the participants were instructed to follow the robotic movements in order to maintain a constant biofeedback value during each trial.

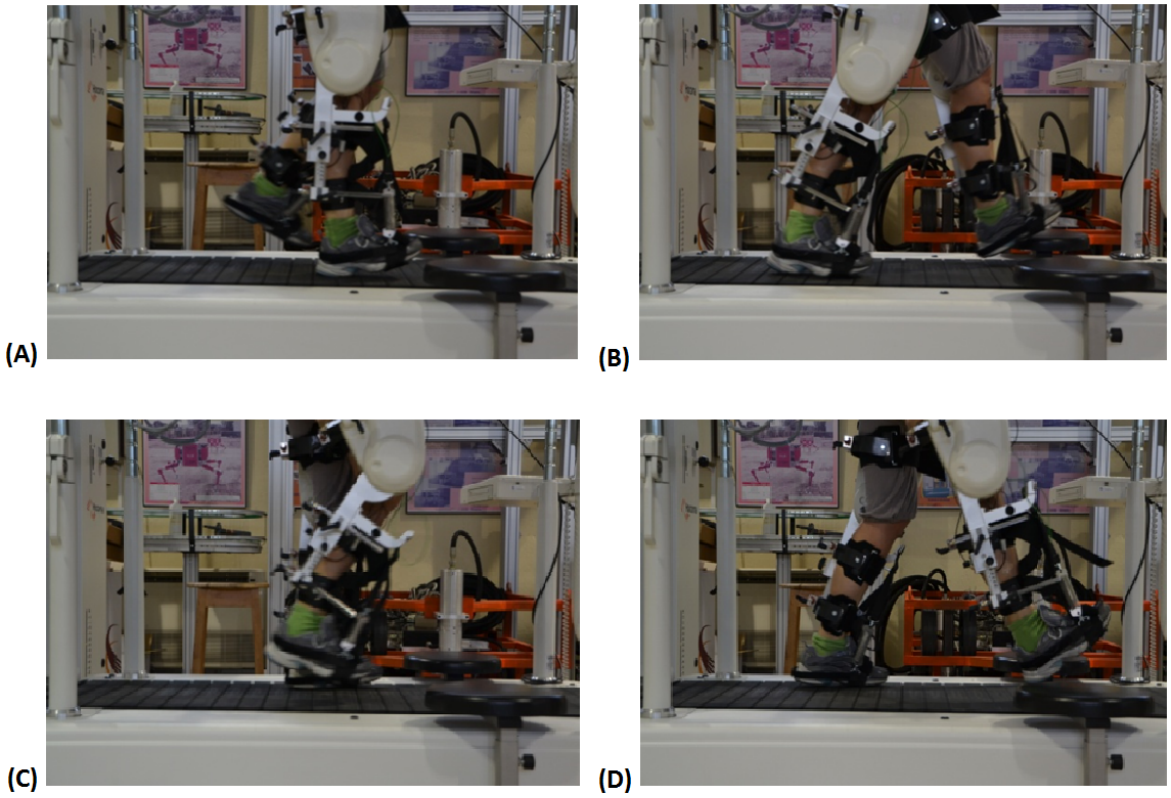

Figure 7.3: Lokomat implements gait trajectories very similar with the normal walking. (A) - (D) sequence represents one stride cycle

- At the end of Lokomat walking, we stopped the exoskeleton and removed the participant inside it. After removed all the electrodes from the body, the participant cleaned his/her skin with alcohol.

[1]The biofeedback system displays the patient's activity in real time during the walking. The displayed values are average values of the forces measured within the Lokomat drives, weighted according to the gait cycle phase. The biofeedback values are strongly correlated with the force or torque values. However, they are not displayed in Newtons or Newton meters, but in biofeedback units.

7.3 EMG signal analysis

The ten central stride cycles of each recorded trial were selected for analysis. Data was analyzed using Matlab 7.0 (The Mathworks, Natick, MA) and SPSS statistical software (v. 18.0 IBM).

The EMG signals were processed as described in section 5.1. Raw EMG data (output signals of the Pocket EMG) was band-passed filtered (first order zero-lag Butterworth digital, pass-band 20-400 Hz) to attenuate DC offset, motion artifacts and high frequency noise. EMG signals were smoothed using a 50-point root mean squared (RMS) algorithm. The smoothed EMG signals were interpolated per each stride cycle in order to obtain average stride cycles with 101 points. Stride cycles were then averaged to obtain a time-normalized gait cycles with 101 points. For each muscle and participant, each time-normalized EMG signal was amplitude-normalized by its maximal value obtained in all the conditions of speed and guidance force. These normalized EMG signals were computed to obtain the average of the group, for each muscle and condition of speed and guidance force.

For each subject and for the average of the group, the normalized EMG signals of each condition were combined into an m x t matrix (EMG_0), where m indicates the number of muscles (seven muscles in this case) and t is the time base (101 values that represent the gait cycle from 0% until 100%) (see section 6.2. for details).

An NNMF (nonnegative matrix factorization) algorithm was applied to the m x t matrix for extraction of motor modules and activation signals from each subject and for each condition. A priori, the number of activation signals, n, was specified (two, three and four activation signals), and the NNMF algorithm found the properties of the modules by populating two matrices: an m x n matrix, which specifies the relative weighting (motor modules) of a muscle in each activation signal, and an n x t matrix, which specifies the activation timing of each activation signal. These two matrices were multiplied to produce an m x t matrix (EMG_r) in an attempt to reconstruct the EMG signals. EMG_r was compared to EMG_0 (original EMG signals) by calculating the sum of the squared errors $(EMG_0 - EMG_r)^2$ and the result was used for iterative optimization until it converged on the motor modules and the activation timings of the activation signals that minimized the error.

The variability accounted for (VAF) was calculated to determine the minimum number of activation signals needed to adequately reconstruct the EMG_0 of each subject and of the average of the group. The VAF was calculated as the ratio of the sum of the squared error values to the sum of the squared EMG_0 values, according to the equation 7.1:

$$VAF = 1 - \frac{\sum_a^b (EMG_0 - EMG_r)^2}{\sum_a^b EMG_0^2} \tag{7.1}$$

where a and b denote the beggining and the end of the interval of analysis.

VAF was calculated for each muscle and for each condition of guidance force and speed. In order to ensure the quality of reconstructed signals within each region of the gait cycle, VAF was also calculated within seven phases of the gait cycle: 1) *Initial double support* (corresponding to *Initial contact* plus *Loading response*), 2) *Mid-stance*, 3) *Terminal stance*, 4) *Pre-swing*, 5) *Initial swing*, 6) *Mid-swing* and 7) *Terminal swing* (see table 7.2). We analyzed seven gait phases instead of eight (such as those presented in subsection 4.3.1.), because *Initial contact* phase only occupies 2% of the gait cycle. For VAF analysis, it is wise to analyze longer intervals. Thus, we combined *Initial contact* plus *Loading response*, obtaining the *Initial double support* phase [2].

Table 7.2: Segmentation of the gait cycle into seven phases for the calculation of the VAF (variability accounted for) of each phase

Initial double support	Mid-stance	Terminal stance	Pre-swing	Initial swing	Mid-swing	Terminal swing
0-10% Gait Cycle	10-30% Gait Cycle	30-50% Gait Cycle	50-60% Gait Cycle	60-73% Gait Cycle	73-87% Gait Cycle	87-100% Gait Cycle
Stance				Swing		

We analyzed VAF results from the computed activation signals from the average EMG of the group. A minimal VAF value of 80% was required to consider the reconstruction quality satisfactory, as referred by Clark et al. [12] and Gizzi et al. [28].

[2] Some authors denominate the 0-10% interval of gait cycle as *Initial Double Support* [1] [2] [48]. For that reason and since we combined two gait phases to form one with this same duration, we decided to denominate this gait phase with the same name referred by these authors. These authors denominated the 50-60% interval of gait cycle as *Terminal Double Support*.

In order to analyze if the motor modules can be similar for all the conditions of speed and guidance force, the activation signals were also computed using the same motor modules (the modules obtained previously in Treadmill using 2.5 Km/h, 2.0 Km/h and 1.5 Km/h speed) for all conditions.

The percentage contribution of the different gait phases to the total muscle activity (EMG envelopes) and activation signals during stance and swing was calculated for all conditions of force and speed.

7.4 Kinematic and kinetic values

Kinematic (joint angles during both types of walking) and kinetic (interaction forces between each participant and Lokomat in the hip and knee joints) data was averaged per each stride in order to obtain an average cycle with 101 points. Finally, these kinematic and kinetic data was time normalized, expressed as a percentage of the total gait cycle, *i.e.*, 0-100%.

The angular Range Of Motion (ROM) in the sagittal plane for hip and knee was found by subtracting the minimum joint angle from the maximum joint angle for Lokomat trials for each condition of Guidance Force (GF) and speed. The ROM in the sagittal plane for knee during the Treadmill walking was also calculated, for each condition of speed. The time (% of gait cycle) at which the minimum and maximum angles were obtained, for all conditions, were also determined.

The kinetic Range Of Forces (ROF) in the hip and knee joints of Lokomat was found by subtracting the minimum joint force from the maximum joint force for Lokomat trials for each condition of Guidance Force (GF) and speed and also for each gait phase.

For both types of walking (treadmill and robotic-aided) and for all the conditions of speed and guidance force, we calculated the time duration of the gait cycle (mean ± standard deviation) for the group average, as well as the stance and swing ratio. All the gait parameters were calculated based on footswitch data.

7.5 Statistical analysis

To perform the statistical analysis, each activation signal and EMG envelope was characterized by seven values - the seven integral values of each gait phase.

Motor modules and activation signals differences across subjects in treadmill gait, for each condition, were assessed using a three -factor (name of the participant, speed; and muscle) ANOVA and Tukey's post hoc analysis.

Motor modules and activation signals differences across subjects in robotic-assisted walking, for each condition, were assessed using a four -factor (name of the participant, % GF; speed; and muscle) ANOVA and Tukey's post hoc analysis. Motor modules differences for each subject in robotic-assisted walking, for each condition, were assessed using a three -factor (% GF; speed; and muscle) ANOVA and Tukey's post hoc analysis. The association between subjects and their activation signals was assessed using a Spearman's correlation.

Activation signals and motor modules average group differences between Treadmill and Lokomat walking were assessed using a Spearman's correlation.

In order to analyze the possible existence of the same motor modules for all conditions of walking, the activation signals were computed using the same motor modules (the motor modules obtained in Treadmill using 2.5 Km/h, 2.0 Km/h and 1.5 Km/h speed) for all conditions. A Spearman's correlation was used to analyze the differences between these activation signals.

A correlation between the percentage contribution of different periods (gait phases) to total muscle activity (EMG envelopes) and activation signals during stance and swing, for all conditions of force and speed, was assessed using a Spearman's correlation.

For all these statistical tests, the level of significance was defined as 0,05.

Chapter 8

Experimental Results and Discussion

Four modules were required to reconstruct the EMG envelops with VAF (variability accounted for) superior than 80% for all muscles and gait phases (see Table 8.3). This result supports previous studies reporting the same number of modules [12] [64] [63] [59] [28]. Ivanenko et al. [39] identified 5 modules, but the extra module was highly related with erector spinae and iliopsas muscles, which are muscles that we did not record their activity.
With only two (Table 8.1) or three (Table 8.2) modules, several VAF values of our work were lower than 80%. Therefore, the results presented on this chapter are related with the analysis performed with four modules.

The computed motor modules, activation signals and EMG envelopes for all conditions of guidance force and speed are represented on figures 8.1, 8.2 and 8.3.

The extracted motor modules and activation signals revealed that the activity of each muscle consisted in contributions from each module, but it is usually dominated by a single module (except Rectus femoris and Vastus lateralis), as represented on figures 8.1, 8.2 and 8.3.

For all the conditions of speed and guidance force, the modular control presented the following characteristics:

- Module 1 consisted mainly of flexor activity from the Rectus femoris (hip flexor) and activity of the Vastus lateralis (knee extensor). This module was mainly active during the early stance phase.

- Module 2 mostly consisted of activity of the Semitendinosus (knee flexor) and Biceps femoris (hip extensor) muscles at late swing and early stance.

- Module 3 consisted mainly of activity of the Gastrocnemius medialis and Gastrocnemius lateralis (ankle plantarflexors) and this module was primarily active during late stance.
- Module 4 consisted mainly of activity of the Tibialis anterior (ankle dorsiflexor). This module was mainly active during early stance and early swing.

8.1 Modular organization during treadmill walking

The calculated motor modules on treadmill gait are very similar among subjects (p-values very high - Table 8.4-(A)). The motor modules are also very similar across speeds.

In relation to the activation signals, they are relatively similar among subjects (p=0.621). Activation signals vary slightly with the speed, but the differences are not so much significant (p=0.301 - Table 8.4-(B)).

Our computed activations signals and motor modules extracted during treadmill walking were very similar with the ones obtained by Clark et al. [12].

8.2 Modular organization during Lokomat walking

The calculated motor modules during robot-aided walking were similar among subjects (p=0,985 - Table 8.5) and among the group average (see table 8.7 and figure 8.5).

The results showed that activation signals during Lokomat walking are quite different among subjects (see Figure 8.6), for the same conditions (p=0.03 - Table 8.6). These activation signals also changed with the speed (see Figure 8.4), for the same guidance force conditions (p=0.014 - Table 8.6).

8.3 Modular organization comparing Treadmill with Lokomat walking

Analyzing the correlations of activation signals (tables 8.8-(A), 8.9-(A), 8.10-(A) and 8.11-(A)) for all conditions of Guidance force and speed, we can refer that:

- The correlations between robotic-guided walking using 20% GF and 1.5 Km/h speed with the other conditions presented the lowest values. This result was expected, since the participants related discomfort during this condition.

- Robotic-guided walking with 100% GF presented the lowest correlations with the treadmill walking condition.

- Robotic-guided conditions with 40% and 20% of guidance force presented the higher similarities with respect to treadmill walking, except for the combination of 20% of guidance force and 1.5 Km/h speed.

Analyzing the correlations of motor modules (tables 8.8-(B), 8.9-(B), 8.10-(B) and 8.11-(B)) for all conditions of Guidance force and speed, we can refer that:

- The robotic-aided condition of 20% GF and 1.5 Km/h speed, presents the lowest correlation values in relation to the other conditions.

- The other combinations present high correlation values among themselves.

Therefore, we can refer that the motor modules values are significantly similar both on treadmill and Lokomat, whereas the activation signals vary much more. From all conditions analyzed in this study, the activation signals and the correspondent motor modules in Lokomat walking at 1.5 Km/h and with 20% GF presented lower correlation values in relation to the other conditions. This result was expected, because it was a very 'robotized gait' (see kinematic pattern in figure 8.10) and also because individuals mentioned discomfort while walking with this combination of force and speed. In relation to the other conditions, we can observe that the computed motor modules and activation signals of the trials using 40% and 20% of GF presented higher correlation values with the results from treadmill, more than the results from 100% and 70% of GF compared with treadmill. This fact supports the idea that walking with less GF would conduct to similar activation signals and motor modules to the obtained in treadmill, for healthy subjects.

We tested the computation of activation signals with fixed motor modules (Figure 8.7), using the computed motor modules of Treadmill walking with 2.5 Km/h, 2.0 Km/h and 1.5 Km/h speeds (represented in figures 8.3, 8.2 and 8.1, respectively). This analysis revealed the following characteristics:

- Activation signal 1 was similar across all combinations.

- Activation signal 2 was similar for treadmill walking and Lokomat walking using 20% and 40% GF at low speeds.

- All the correlations were similar for activation signal 3. The correlations between treadmill and Lokomat walking with 20% GF were the best, with all values higher than 0,90.

- High similarity of activation signal 4 between treadmill and Lokomat walking was observed with 20% of guidance force (at low speeds).

The result of this analysis with fixed motor modules also showed good accuracy in the reconstruction of the EMG envelopes. This result confirms that motor modules are similar across variations of guidance force and speed, whereas the activation signals vary much more, depending on the speed and the amount of aiding given by the orthoses.

Using the fixed motor modules obtained in Treadmill using 1.5 Km/h speed, the VAF was 91,85 ± 30,88%; using the fixed motor modules obtained in Treadmill using 2.0 Km/h speed, the VAF was 95,15 ± 12%; using the fixed motor modules obtained in Treadmill using 2.5 Km/h speed, the VAF was 92,98 ± 19,48%. Thus, the quality of reconstruction using the fixed motor modules obtained in Treadmill using 2.0 Km/h was better than the reconstruction using the fixed motor modules obtained in Treadmill using 2.5 Km/h and 1.5 Km/h. We believe that this result support the idea that Rectus femoris activity depend on the same activation of two specific modules (our modules 1 and 4, which are the same modules referred by McGowan et al. [59]), as the motor modules obtained in Treadmill using 2.0 Km/h, in opposition to the motor modules obtained in Treadmill using 2.5 Km/h and 1.5 Km/h, where only one module and three modules contribute, respectively, to the total activity of Rectus femoris.

8.4 Muscular activation

The average EMG envelopes recorded from the seven muscles, for both types of walking and for all conditions of guidance force and speed, are illustrated in Figure 8.8. Different muscular activation patterns were obtained according to the demand.

In general, muscular activation increased with the increase of speed, for all conditions of guidance force used in Lokomat and for treadmill walking. Generally, there was also higher muscular activation for 20% and 40% GF in respect to the other guidance forces, for all conditions with the same speed.

We found that the activation patterns of Rectus femoris and Vastus lateralis presented higher activity during robotic-guided walking than treadmill walking, for all the variations of

guidance force and speed. There was significantly less contribution of Gastrocnemius medialis, Gastrocnemius lateralis and Tibialis anterior to the mechanical demand imposed during robotic-guided walking than treadmill walking. In general, the hamstrings (Semitendinosus and Biceps femoris) presented similar activation patterns for both types of walking. Nevertheless, the activity of the hamstrings during Lokomat walking was typically lower than the obtained on Treadmill walking in the transition from swing to stance and the initial 30% of gait cycle.

In relation to gastrocnemius medialis, gastrocnemius lateralis and tibialis anterior activity during Lokomat walking, Hidler [36] reported that the drop in muscle activity (he only used 100% of guidance force) could be related with the use of footlifters, which assist ankle dorsiflexion for toe clearance during swing phase. Interestingly, we obtained less muscular activity not only using 100% of guidance force, but also for the other guidance forces. In relation to the quadriceps (Rectus femoris and Vastus lateralis), Hidler explained that people usually rotate their hips and also abduct their legs to allow the toe to clear the floor, which are movements quite limited to perform in Lokomat. Therefore, participants of his study (just using 100% of guidance force) exerted higher muscle activity in the quadriceps to help in the elevation of the feet and preventing toe from getting caught in the treadmill. Interestingly, we obtained higher activity for all the guidance forces.

Partial contributions of each gait phase to the total muscular activity per stride revealed higher correlation values for Vastus lateralis, Semitendinosus and Biceps femoris, when comparing both types of walking.

8.5 Gait parameters

The analyzed gait parameters showed some differences between Treadmill walking and robotic-aided walking. The gait cycle time was much shorter during Treadmill walking (See Table 8.12). The fact that the average group took much more time to complete a step cycle during Lokomat walking than Treadmill walking may influence muscular activation.

The percentage of stance phase was longer in Lokomat walking using 100% and 70% of guidance force. When walking with 40% and 20% of guidance force, the average group presented similar percentages of stance phase compared with walking in treadmill.

For both types of walking and for all the conditions of guidance force, the gait cycle time

increased with the decrease in speed.

8.6 Kinematics

In order to analyze if the participants would change joint trajectories as a response to the altered mechanical demand, we examined the average knee and hip joints trajectories and the correspondent ROM (range of motion) in the sagittal plane.

Knee joint angular patterns for all the conditions, according to the speed are represented in Figure 8.9. It can be observed that the range of motion in the knee while walking on treadmill is slightly higher than the obtained during robotic-guided walking. Normal physiological and symmetrical gait patterns were obtained for each condition.

Figure 8.10 represents the average knee and hip angular trajectories, for all the conditions of robotic-aided walking.

Angular patterns and the correspondent ROM were very similar for all conditions, except for the condition of 20% GF. Nevertheless, despite being firmly strapped into the Lokomat, a small amount of variance was found. This happened, because each participant can produce relative movement in relation to the Lokomat, although Lokomat guides the limbs of all subjects through pre-programmed trajectories. In general, the ROM decreased with the decreasing amount of guidance force (Table 8.13).

The ROM of the hip joint, using 20% GF, was smaller when compared with the other conditions of guidance force, for the same walking speed. The ROM of the knee joint using 20% GF and 1.5 Km/h was smaller when compared with the other conditions. In general, it was found that the ROM of both knee and hip joints increased with the speed and the % GF, except for the condition of 20% GF, where the hip ROM decreased with the increase of speed.

The time at which occurred the minimum angle of hip joint was similar for all conditions, taking place at the transition from terminal stance to pre-swing (in the region of 50% of gait cycle), except for 20% GF and 1.5 Km/h, where the minimum angle was obtained in the middle of terminal stance (in the region of 40% of gait cycle). The time at which occurred the maximum angle of hip joint was similar for all conditions, taking place at mid-swing (in the region of 73-87% of gait cycle).

The time at which occurred the minimum angle of knee joint was similar for all conditions, taking place at transition from swing to stance (in the region of 100% of gait cycle). The time at which occurred the maximum angle of knee joint was similar for all conditions, taking place at the final of initial swing (in the region of 73% of gait cycle).

8.7 Force (Kinetics)

In order to determine if subjects would modify the patterns of interaction forces during the gait cycle, we examined the average knee and hip exoskeleton joint forces. We observed that in general, subjects were able to walk with a similar kinematic pattern imposed by the robot. But changes in the mechanical pattern, related with the changes in modular control and induced by altered demand, were observed (Figure 8.11). In general, the ROF (Range Of Forces) decreased with the decrease of GF and the increase of speed.

Main deviations across combinations in the interactions forces were found in the transition from stance to swing (in the region of 60% of gait cycle).

8.7.1 Hip Kinetics (joint forces)

For the hip joint, we observed that with 20% and 40% GF, as the leg moved to prepare the swing motion and initiate it, relative hip extension and flexion torques were small. Nevertheless, for higher GF (70% and 100%), the hip torque patterns required a more complex strategy as subjects exerted significantly higher hip flexion torques at mid-swing (in the region of 73-87% of gait cycle). This reveals a strategy that is adopted to pull the leg towards swing that is accentuated with augmented mechanical demand. This behavior correlates with the increased RF (hip flexor) activity and decreased activity of the hamstrings (hip extensor).

8.7.2 Knee Kinetics (joint forces)

For the knee joint, the ROF (Table 8.14-(B)) decreased with the decrease of GF and the increase of speed. The ROF using 20% and 40% GF is reduced when compared to higher levels of GF. The main differences in forces across combinations for this joint were observed in the transition from stance to swing (in the region of 60% of gait cycle). For 20% and 40% GF, the limb produced reduced extension torques during pre-swing (in the region of 50-60% of gait cycle), followed by reduced flexion torques at initial swing (in the region of 60-73%

of gait cycle). In turn, using 70% and 100% GF resulted in increased knee extension torques at pre-swing followed by increased knee flexion torques at initial swing. This behavior correlates with the increased RF (knee extensor) and VL (knee extensor) activity during the stance phase.

Table 8.1: Evaluation of the quality of reconstruction (VAF) per gait phase, using only two modules. VAF values equal or higher than 80% are colored in green. VAF values equal or higher than 70% are colored in yellow. VAF values lower than 70% are colored in red.

				Phase of Gait Cycle							
				Phase 1 Initial double support (0-10% GC)	Phase 2 Mid stance (10-30% GC)	Phase 3 Terminal stance (30-50% GC)	Phase 4 Preswing (50-60% GC)	Phase 5 Initial swing (60-73% GC)	Phase 6 Mid swing (73-87% GC)	Phase 7 Terminal swing(87-100% GC)	Gait Cycle (GC) (0-100%)
Treadmill		1.5 Km/h	RF	0,99	0,99	1,00	0,99	0,99	0,94	0,98	0,99944
			VL	1,00	1,00	1,00	0,92	1,00	0,97	1,00	0,99993
			ST	0,99	0,96	0,97	-0,22	0,68	0,56	0,99	0,99737
			BF	1,00	0,99	0,99	1,00	0,68	1,00	0,99	0,99979
			GM	0,99	0,99	1,00	0,94	0,57	1,00	0,25	0,99965
			GL	0,99	0,99	1,00	1,00	0,71	0,53	0,98	0,99973
			TA	1,00	0,91	0,84	0,62	0,96	0,95	0,99	0,99968
		2.0 Km/h	RF	1,00	1,00	0,98	0,85	0,90	1,00	0,84	0,99924
			VL	0,96	1,00	1,00	0,99	0,91	0,97	0,94	0,99926
			ST	1,00	0,99	1,00	-0,01	0,92	0,95	0,98	0,99913
			BF	0,92	1,00	0,96	0,58	0,70	0,99	0,93	1,00000
			GM	0,78	0,99	1,00	0,54	0,47	0,76	0,03	0,99857
			GL	1,00	1,00	1,00	1,00	0,71	1,00	0,97	0,99994
			TA	1,00	0,72	0,78	0,90	0,94	0,94	0,99	0,99948
		2.5 Km/h	RF	1,00	1,00	0,98	0,75	0,83	0,99	0,75	0,99784
			VL	0,98	0,99	0,99	1,00	0,98	0,98	0,99	0,99977
			ST	1,00	0,99	1,00	-0,17	0,91	0,97	0,98	0,99888
			BF	0,89	1,00	0,94	0,01	0,32	0,96	0,95	0,99994
			GM	0,84	1,00	1,00	0,02	-2,13	0,87	0,14	0,99749
			GL	1,00	1,00	1,00	0,90	-0,61	0,99	0,81	0,99966
			TA	1,00	0,79	0,90	0,94	0,96	0,98	0,99	0,99988
Lokomat	100% GF	1.5 Km/h	RF	0,99	0,97	1,00	1,00	0,98	0,78	0,75	0,99966
			VL	0,99	0,93	0,99	1,00	0,95	-0,82	0,52	0,99733
			ST	0,91	0,88	1,00	1,00	0,97	0,93	0,88	0,99766
			BF	0,97	0,97	0,98	0,85	1,00	0,89	0,98	0,99913
			GM	0,96	0,91	1,00	1,00	0,98	0,82	0,89	0,99915
			GL	1,00	0,98	1,00	1,00	0,95	0,95	0,94	0,99998
			TA	0,88	1,00	0,97	0,86	0,73	-12,14	0,52	0,99524
		2.0 Km/h	RF	1,00	1,00	1,00	0,93	0,99	0,83	0,97	1,00000
			VL	0,99	0,97	1,00	0,96	0,99	-0,08	0,94	0,99949
			ST	0,87	0,85	1,00	0,08	0,99	0,88	0,86	0,99929
			BF	0,82	0,99	1,00	-0,05	0,98	0,78	1,00	0,99870
			GM	0,86	0,99	1,00	0,63	0,97	0,82	0,97	0,99977
			GL	1,00	0,99	1,00	1,00	0,88	1,00	0,99	0,99997
			TA	0,92	1,00	0,95	0,99	0,92	0,44	0,86	0,99798
		2.5 Km/h	RF	0,98	0,95	0,97	0,96	0,97	0,86	0,82	0,99989
			VL	0,94	0,98	0,94	0,93	0,94	0,63	0,94	0,99951
			ST	0,84	1,00	0,84	0,74	1,00	1,00	0,95	0,99991
			BF	0,90	0,96	0,70	1,00	0,95	0,95	0,98	0,99865
			GM	0,82	0,94	0,98	0,67	0,98	0,85	0,96	0,99967
			GL	0,84	0,96	0,99	0,98	0,99	0,87	0,95	0,99968
			TA	0,82	1,00	0,78	1,00	1,00	0,00	0,96	0,99613
	70% GF	1.5 Km/h	RF	0,99	0,99	1,00	1,00	0,91	0,99	0,74	0,99963
			VL	0,99	0,96	1,00	0,99	0,94	0,75	0,03	0,99825
			ST	0,99	0,62	0,98	0,98	0,95	0,94	0,76	0,99932
			BF	0,68	0,73	0,99	0,98	0,98	0,80	0,75	0,99713
			GM	1,00	0,98	1,00	0,91	1,00	0,99	0,94	0,99998
			GL	1,00	1,00	1,00	0,97	0,99	0,95	0,97	0,99999
			TA	0,98	1,00	0,98	0,98	0,94	0,16	0,84	0,99844
		2.0 Km/h	RF	1,00	0,97	0,99	0,97	0,94	0,93	0,65	0,99999
			VL	1,00	0,94	1,00	1,00	1,00	0,28	-0,02	0,99908
			ST	0,99	0,42	0,99	0,92	0,92	0,92	0,79	0,99902
			BF	0,49	0,59	0,86	0,82	0,78	0,69	0,80	0,99279
			GM	1,00	0,57	1,00	0,85	1,00	0,80	0,87	0,99991
			GL	1,00	1,00	1,00	0,99	0,95	0,99	0,97	0,99999
			TA	0,90	1,00	0,98	0,98	0,93	0,54	0,47	0,99414
		2.5 Km/h	RF	0,99	0,98	0,99	1,00	1,00	0,91	1,00	0,99998
			VL	0,98	1,00	0,77	0,95	0,99	0,98	0,98	1,00000
			ST	0,90	1,00	-0,77	0,98	0,99	1,00	0,98	0,99967
			BF	0,99	0,91	0,05	0,92	0,98	0,97	0,99	0,99992
			GM	0,63	0,95	0,78	0,79	0,97	0,94	0,99	0,99988
			GL	0,41	0,97	0,77	1,00	0,94	0,59	1,00	0,99961
			TA	0,83	0,98	-1,91	0,47	1,00	0,99	0,98	0,99590
	40% GF	1.5 Km/h	RF	0,99	1,00	1,00	0,95	0,97	0,92	0,91	0,99984
			VL	0,98	0,93	0,99	0,67	0,45	0,96	0,87	0,99837
			ST	1,00	0,96	0,99	0,92	0,80	0,42	0,91	0,99979
			BF	0,97	1,00	0,99	1,00	0,79	0,96	0,89	0,99999
			GM	1,00	0,83	1,00	0,97	0,97	0,90	0,82	0,99989
			GL	0,99	1,00	1,00	0,97	0,93	0,21	0,96	0,99994
			TA	0,99	0,89	1,00	0,93	0,89	1,00	0,90	0,99965
		2.0 Km/h	RF	0,99	0,90	1,00	0,99	0,98	0,92	0,04	0,99991
			VL	1,00	0,93	0,98	1,00	0,97	0,27	0,09	0,99960
			ST	1,00	0,29	0,85	0,98	0,98	1,00	0,75	0,99980
			BF	0,98	0,96	0,98	1,00	1,00	0,91	0,95	0,99957
			GM	0,98	0,60	1,00	0,97	0,99	0,96	0,92	0,99997
			GL	1,00	1,00	1,00	0,99	1,00	0,94	0,96	0,99999
			TA	0,97	0,95	0,91	1,00	1,00	0,99	0,96	0,99979
		2.5 Km/h	RF	1,00	0,97	0,98	0,98	0,98	0,87	1,00	0,99999
			VL	0,96	1,00	0,84	0,95	0,99	1,00	1,00	0,99996
			ST	0,98	0,97	0,66	0,97	0,94	0,99	0,99	0,99980
			BF	1,00	0,93	0,84	0,97	1,00	0,97	0,92	0,99974
			GM	0,82	0,95	0,90	0,86	0,97	0,98	1,00	0,99997
			GL	0,08	0,83	0,83	0,99	0,97	1,00	0,98	0,99944
			TA	0,75	0,99	-1,24	0,81	0,99	0,66	0,99	0,99565
	20% GF	1.5 Km/h	RF	0,84	0,97	0,95	0,29	0,99	0,78	0,74	0,99891
			VL	0,89	0,99	1,00	0,06	0,41	1,00	1,00	0,99970
			ST	0,98	1,00	0,93	0,94	0,95	0,62	0,98	0,99969
			BF	0,99	1,00	0,99	1,00	0,99	0,99	0,98	0,99996
			GM	0,83	1,00	1,00	0,99	0,90	1,00	1,00	0,99997
			GL	1,00	0,99	1,00	0,98	0,97	0,96	0,99	0,99998
			TA	0,90	0,84	0,97	0,91	0,91	1,00	0,98	0,99974
		2.0 Km/h	RF	0,99	0,97	0,96	0,92	1,00	0,97	0,89	1,00000
			VL	0,94	0,91	0,87	0,70	0,97	0,99	0,79	0,99973
			ST	0,98	0,94	0,88	0,96	0,77	0,92	0,97	0,99962
			BF	0,89	1,00	0,91	0,98	0,92	0,98	0,99	0,99966
			GM	0,94	0,89	0,99	0,96	1,00	0,98	0,95	1,00000
			GL	0,92	0,97	0,99	0,98	0,98	1,00	0,89	0,99998
			TA	0,97	0,59	1,00	1,00	0,85	1,00	0,93	0,99980
		2.5 Km/h	RF	1,00	0,96	0,95	1,00	0,99	0,98	0,99	0,99994
			VL	0,95	0,92	0,94	0,66	0,79	0,33	0,93	0,99775
			ST	0,95	0,80	0,90	0,96	1,00	1,00	0,96	0,99993
			BF	0,58	0,95	0,79	0,99	1,00	0,83	0,99	0,99587
			GM	1,00	0,82	0,98	0,97	0,99	0,91	0,98	0,99983
			GL	0,81	0,98	0,99	0,98	1,00	0,91	0,95	0,99955
			TA	0,88	0,95	0,96	0,96	0,87	0,15	0,75	0,99973

Table 8.2: Evaluation of the quality of reconstruction (VAF) per gait phase, using only three modules. VAF values equal or higher than 80% are colored in green. VAF values equal or higher than 70% are colored in yellow. VAF values lower than 70% are colored in red.

				Phase of Gait Cycle							
				Phase 1 Initial double support (0-10% GC)	Phase 2 Mid stance (10-30% GC)	Phase 3 Terminal stance (30-50% GC)	Phase 4 Preswing (50-60% GC)	Phase 5 Initial swing (60-73% GC)	Phase 6 Mid swing (73-87% GC)	Phase 7 Terminal swing(87-100% GC)	Gait Cycle (GC) (0-100%)
Treadmill		1.5 Km/h	RF	1,00	1,00	1,00	1,00	1,00	1,00	1,00	1,00000
			VL	1,00	1,00	1,00	0,91	0,99	0,98	1,00	0,99986
			ST	1,00	1,00	1,00	0,37	1,00	0,99	1,00	0,99986
			BF	0,98	1,00	1,00	0,98	0,95	0,97	1,00	0,99996
			GM	1,00	0,98	1,00	0,95	0,93	0,84	0,48	0,99992
			GL	1,00	1,00	1,00	1,00	1,00	0,99	0,76	0,99998
			TA	1,00	1,00	0,96	0,38	1,00	1,00	1,00	0,99986
		2.0 Km/h	RF	0,99	1,00	1,00	0,98	0,99	1,00	1,00	0,99982
			VL	0,97	1,00	1,00	1,00	0,78	0,97	0,99	0,99883
			ST	1,00	0,99	0,98	0,95	1,00	0,96	1,00	0,99975
			BF	0,99	1,00	1,00	0,83	1,00	0,98	1,00	0,99946
			GM	1,00	0,99	1,00	0,89	0,64	0,52	0,92	1,00000
			GL	1,00	1,00	1,00	1,00	0,94	0,99	1,00	0,99999
			TA	1,00	0,75	0,72	0,47	0,98	0,94	1,00	0,99987
		2.5 Km/h	RF	0,99	1,00	1,00	0,99	1,00	1,00	1,00	0,99985
			VL	0,98	0,99	1,00	0,99	0,96	0,98	1,00	0,99961
			ST	1,00	1,00	0,99	0,98	1,00	0,95	1,00	0,99983
			BF	0,95	1,00	1,00	0,58	0,99	0,98	1,00	0,99922
			GM	0,99	1,00	1,00	0,95	0,54	0,75	0,99	0,99999
			GL	0,99	1,00	1,00	1,00	0,90	0,95	0,99	0,99997
			TA	1,00	0,81	0,86	0,64	0,99	0,97	1,00	0,99999
Lokomat	100% GF	1.5 Km/h	RF	0,99	1,00	1,00	1,00	0,97	0,99	0,99	0,99992
			VL	0,99	0,99	1,00	0,97	0,99	1,00	1,00	0,99993
			ST	1,00	1,00	0,99	0,97	1,00	0,99	0,99	0,99999
			BF	1,00	1,00	0,99	0,95	0,99	0,99	0,99	0,99999
			GM	0,97	0,99	1,00	1,00	0,99	1,00	1,00	0,99999
			GL	0,99	0,99	1,00	1,00	0,94	1,00	0,99	0,99996
			TA	0,98	0,90	0,88	0,95	0,93	0,76	0,98	1,00000
		2.0 Km/h	RF	1,00	1,00	1,00	0,98	0,98	1,00	1,00	0,99987
			VL	1,00	0,99	1,00	1,00	1,00	1,00	1,00	0,99999
			ST	1,00	0,99	1,00	0,99	0,96	0,98	0,97	0,99994
			BF	1,00	0,99	1,00	1,00	1,00	0,99	0,94	0,99997
			GM	0,99	1,00	1,00	0,93	0,98	1,00	1,00	1,00000
			GL	1,00	0,99	1,00	1,00	0,88	1,00	0,99	0,99995
			TA	0,98	0,98	0,96	0,90	0,98	1,00	1,00	0,99982
		2.5 Km/h	RF	0,99	0,99	1,00	1,00	1,00	0,98	0,97	0,99993
			VL	1,00	1,00	1,00	0,99	0,99	1,00	1,00	0,99999
			ST	1,00	0,99	0,97	0,99	0,97	0,99	0,98	0,99990
			BF	1,00	1,00	0,98	0,94	0,99	0,99	0,94	0,99967
			GM	0,98	1,00	1,00	0,95	1,00	1,00	1,00	0,99996
			GL	1,00	0,99	1,00	1,00	1,00	1,00	1,00	1,00000
			TA	0,98	0,93	1,00	0,88	0,96	0,97	0,98	0,99957
	70% GF	1.5 Km/h	RF	0,97	1,00	1,00	1,00	0,92	0,94	0,99	0,99909
			VL	1,00	1,00	1,00	0,96	0,90	0,99	1,00	0,99961
			ST	0,99	1,00	1,00	1,00	0,99	0,98	1,00	0,99988
			BF	0,95	0,99	1,00	1,00	1,00	0,99	1,00	0,99991
			GM	0,97	1,00	1,00	0,92	1,00	0,99	1,00	0,99985
			GL	1,00	1,00	1,00	0,98	0,99	0,99	1,00	1,00000
			TA	0,97	0,98	0,98	0,98	0,92	0,68	0,98	0,99944
		2.0 Km/h	RF	0,98	1,00	1,00	0,99	0,97	0,98	1,00	0,99949
			VL	1,00	1,00	1,00	1,00	1,00	1,00	1,00	1,00000
			ST	0,99	0,99	0,99	1,00	1,00	0,97	0,99	0,99979
			BF	0,92	0,96	0,99	1,00	1,00	0,98	0,99	0,99950
			GM	0,94	0,93	1,00	0,91	0,99	1,00	1,00	0,99988
			GL	1,00	1,00	1,00	0,99	0,96	0,99	1,00	0,99999
			TA	0,95	0,95	0,95	0,91	0,81	0,86	1,00	0,99783
		2.5 Km/h	RF	0,97	0,98	1,00	0,99	1,00	0,95	0,99	0,99993
			VL	1,00	0,99	1,00	0,96	1,00	0,98	1,00	0,99992
			ST	1,00	0,98	0,99	1,00	1,00	0,99	0,99	0,99994
			BF	0,93	0,96	0,99	0,97	1,00	0,99	0,98	0,99964
			GM	0,97	1,00	1,00	0,94	1,00	1,00	1,00	0,99993
			GL	1,00	1,00	1,00	0,99	1,00	0,98	1,00	1,00000
			TA	0,94	0,94	0,93	0,25	0,97	0,96	1,00	0,99768
	40% GF	1.5 Km/h	RF	0,98	1,00	1,00	1,00	1,00	0,98	0,98	0,99987
			VL	0,98	0,96	1,00	0,86	0,18	0,86	1,00	0,99829
			ST	1,00	1,00	1,00	1,00	0,98	0,99	1,00	0,99986
			BF	0,98	0,98	1,00	0,95	0,95	0,98	0,99	0,99998
			GM	1,00	0,93	1,00	1,00	0,88	0,96	1,00	0,99986
			GL	0,99	1,00	1,00	0,99	0,98	0,72	0,97	0,99995
			TA	1,00	0,85	0,99	0,90	0,92	1,00	0,97	0,99968
		2.0 Km/h	RF	0,98	1,00	1,00	1,00	0,99	0,99	1,00	0,99991
			VL	1,00	1,00	1,00	1,00	0,95	0,91	1,00	0,99972
			ST	1,00	0,98	0,98	1,00	0,99	0,86	0,99	0,99965
			BF	0,98	1,00	1,00	0,99	0,99	0,97	1,00	0,99963
			GM	0,99	0,99	1,00	0,99	1,00	1,00	1,00	0,99988
			GL	1,00	1,00	1,00	0,99	1,00	0,98	1,00	1,00000
			TA	0,97	0,95	0,95	1,00	1,00	0,99	0,95	0,99952
		2.5 Km/h	RF	0,98	0,98	1,00	0,98	0,99	0,89	1,00	0,99995
			VL	1,00	0,99	1,00	0,96	1,00	0,98	1,00	0,99998
			ST	1,00	1,00	1,00	0,99	0,97	0,99	0,99	0,99996
			BF	0,98	0,98	1,00	0,98	0,99	0,97	0,92	0,99944
			GM	0,99	1,00	1,00	0,93	1,00	0,99	1,00	0,99991
			GL	0,99	0,98	1,00	0,97	1,00	1,00	0,99	1,00000
			TA	0,96	0,88	0,94	0,66	0,97	0,51	1,00	0,99835
	20% GF	1.5 Km/h	RF	0,97	1,00	1,00	0,93	0,96	1,00	1,00	0,99999
			VL	0,92	0,99	1,00	-0,17	0,58	0,98	1,00	0,99990
			ST	1,00	1,00	1,00	0,99	1,00	1,00	1,00	0,99999
			BF	0,98	1,00	1,00	1,00	1,00	1,00	0,99	1,00000
			GM	0,88	1,00	1,00	0,99	0,92	0,97	1,00	0,99999
			GL	1,00	0,99	1,00	0,98	0,97	0,93	0,99	0,99999
			TA	0,95	0,90	1,00	0,89	0,93	0,97	1,00	0,99991
		2.0 Km/h	RF	1,00	1,00	1,00	1,00	1,00	0,99	1,00	0,99998
			VL	1,00	1,00	1,00	1,00	0,97	0,96	1,00	0,99990
			ST	1,00	0,96	1,00	1,00	0,77	0,94	0,99	0,99946
			BF	0,95	0,96	0,99	1,00	0,92	0,97	1,00	0,99974
			GM	1,00	1,00	1,00	1,00	1,00	0,99	1,00	0,99999
			GL	1,00	1,00	1,00	1,00	0,98	1,00	1,00	1,00000
			TA	0,97	0,58	1,00	1,00	0,85	1,00	0,94	0,99980
		2.5 Km/h	RF	0,98	0,99	0,98	0,99	1,00	0,99	1,00	0,99998
			VL	1,00	0,99	1,00	0,82	0,86	1,00	1,00	0,99987
			ST	1,00	0,99	1,00	0,98	0,99	0,94	0,99	0,99973
			BF	0,99	0,89	0,98	0,99	1,00	0,97	0,98	0,99959
			GM	0,97	0,95	1,00	0,95	1,00	1,00	1,00	0,99996
			GL	1,00	1,00	1,00	0,99	1,00	0,98	1,00	0,99999
			TA	0,98	0,64	0,97	0,91	0,83	0,99	0,97	0,99961

Table 8.3: Evaluation of the quality of reconstruction (VAF) per gait phase, using only four modules. All the VAF values are equal or higher than 80%. Therefore, all of them are colored in green.

				Phase of Gait Cycle							
				Phase 1 Initial double support (0-10% GC)	Phase 2 Mid stance (10-30% GC)	Phase 3 Terminal stance (30-50% GC)	Phase 4 Preswing (50-60% GC)	Phase 5 Initial swing (60-73% GC)	Phase 6 Mid swing (73-87% GC)	Phase 7 Terminal swing(87-100% GC)	Gait Cycle (GC) (0-100%)
Treadmill	1.5 Km/h	RF		1,00	1,00	1,00	0,99	1,00	1,00	1,00	0,99998
		VL		1,00	1,00	1,00	1,00	1,00	1,00	1,00	0,99999
		ST		1,00	1,00	1,00	0,81	0,99	0,99	1,00	0,99993
		BF		0,99	1,00	1,00	0,98	0,95	0,98	1,00	0,99995
		GM		1,00	0,98	1,00	1,00	1,00	0,96	0,82	0,99999
		GL		1,00	1,00	1,00	1,00	1,00	0,98	0,81	0,99998
		TA		1,00	1,00	1,00	0,97	1,00	1,00	1,00	0,99999
	2.0 Km/h	RF		0,99	1,00	1,00	0,99	0,99	1,00	1,00	0,99970
		VL		0,98	1,00	1,00	0,97	0,84	1,00	1,00	0,99915
		ST		1,00	1,00	1,00	0,82	0,99	0,99	1,00	0,99986
		BF		0,99	1,00	1,00	0,83	1,00	0,99	1,00	0,99953
		GM		0,99	1,00	1,00	0,98	0,98	1,00	0,99	0,99995
		GL		1,00	1,00	1,00	1,00	0,88	0,99	1,00	0,99998
		TA		1,00	1,00	1,00	0,99	1,00	1,00	1,00	0,99995
	2.5 Km/h	RF		1,00	1,00	1,00	1,00	1,00	1,00	1,00	0,99998
		VL		0,99	0,99	0,99	1,00	0,96	0,98	1,00	0,99982
		ST		1,00	1,00	1,00	0,88	1,00	0,96	1,00	0,99970
		BF		0,99	0,99	0,99	0,92	1,00	0,97	1,00	0,99956
		GM		0,97	1,00	1,00	0,99	0,83	0,79	0,95	0,99997
		GL		1,00	1,00	1,00	1,00	0,92	0,94	1,00	0,99999
		TA		0,99	0,95	0,97	1,00	0,99	0,98	1,00	0,99967
Lokomat	100% GF	1.5 Km/h	RF	1,00	1,00	1,00	1,00	0,98	1,00	1,00	0,99992
			VL	1,00	1,00	1,00	1,00	0,97	0,98	0,99	0,99993
			ST	1,00	1,00	0,98	0,98	0,99	0,99	0,99	0,99999
			BF	1,00	1,00	0,99	0,98	0,98	0,99	0,99	0,99999
			GM	1,00	1,00	1,00	1,00	0,99	1,00	1,00	0,99999
			GL	1,00	1,00	1,00	1,00	0,95	1,00	1,00	0,99996
			TA	1,00	1,00	1,00	1,00	1,00	0,98	1,00	1,00000
		2.0 Km/h	RF	1,00	1,00	1,00	0,98	0,99	1,00	1,00	0,99993
			VL	1,00	1,00	1,00	1,00	0,99	0,99	1,00	0,99997
			ST	1,00	1,00	0,98	0,97	0,99	1,00	1,00	1,00000
			BF	1,00	1,00	0,97	0,92	0,98	1,00	0,99	0,99996
			GM	0,98	1,00	1,00	0,91	0,99	1,00	1,00	0,99997
			GL	1,00	1,00	1,00	1,00	0,95	0,98	0,99	1,00000
			TA	1,00	1,00	0,99	0,93	1,00	0,98	0,97	0,99888
		2.5 Km/h	RF	1,00	1,00	1,00	1,00	1,00	1,00	1,00	0,99999
			VL	1,00	1,00	1,00	1,00	0,99	1,00	1,00	0,99999
			ST	0,99	0,98	0,97	1,00	0,96	0,99	0,99	0,99994
			BF	0,99	0,97	0,98	1,00	0,98	0,99	0,97	0,99991
			GM	1,00	1,00	1,00	0,98	1,00	1,00	1,00	1,00000
			GL	1,00	1,00	1,00	0,99	1,00	1,00	1,00	0,99999
			TA	1,00	1,00	1,00	1,00	0,99	0,99	0,99	1,00000
	70% GF	1.5 Km/h	RF	1,00	1,00	1,00	1,00	0,99	1,00	1,00	0,99992
			VL	1,00	1,00	1,00	0,96	0,91	1,00	1,00	0,99965
			ST	1,00	1,00	1,00	1,00	0,99	1,00	1,00	0,99998
			BF	1,00	1,00	1,00	1,00	0,95	1,00	1,00	0,99993
			GM	1,00	1,00	1,00	0,92	1,00	1,00	1,00	0,99996
			GL	1,00	1,00	1,00	0,98	1,00	1,00	1,00	0,99998
			TA	1,00	1,00	1,00	0,99	0,99	1,00	1,00	0,99992
		2.0 Km/h	RF	1,00	1,00	1,00	1,00	0,99	1,00	1,00	0,99996
			VL	1,00	1,00	1,00	0,99	0,99	1,00	1,00	0,99996
			ST	1,00	1,00	0,98	0,98	0,99	0,99	1,00	1,00000
			BF	1,00	1,00	0,96	0,96	0,94	0,99	0,99	0,99999
			GM	1,00	0,99	1,00	0,96	0,97	0,98	0,99	0,99999
			GL	1,00	1,00	1,00	0,99	0,96	0,99	1,00	0,99997
			TA	1,00	1,00	0,99	1,00	0,99	0,95	0,98	1,00000
		2.5 Km/h	RF	1,00	1,00	1,00	0,97	1,00	1,00	1,00	0,99995
			VL	1,00	0,99	1,00	0,96	1,00	0,99	1,00	0,99984
			ST	1,00	1,00	0,99	0,98	1,00	0,99	0,99	1,00000
			BF	1,00	1,00	0,99	1,00	1,00	1,00	0,99	1,00000
			GM	1,00	1,00	1,00	0,97	1,00	1,00	1,00	1,00000
			GL	1,00	1,00	1,00	0,99	1,00	0,99	1,00	0,99999
			TA	1,00	1,00	1,00	0,81	0,99	0,97	0,98	0,99984
	40% GF	1.5 Km/h	RF	0,98	1,00	1,00	0,99	1,00	0,99	0,98	0,99992
			VL	0,99	1,00	1,00	1,00	1,00	0,96	0,98	0,99985
			ST	1,00	1,00	1,00	1,00	1,00	1,00	1,00	0,99995
			BF	0,97	1,00	1,00	0,99	1,00	0,96	0,99	0,99975
			GM	1,00	1,00	1,00	0,99	1,00	1,00	1,00	0,99998
			GL	0,99	1,00	1,00	0,98	1,00	0,81	0,96	0,99999
			TA	0,99	1,00	1,00	0,99	1,00	0,98	0,99	0,99991
		2.0 Km/h	RF	1,00	1,00	1,00	1,00	1,00	1,00	1,00	1,00000
			VL	1,00	1,00	1,00	1,00	0,97	0,96	0,98	0,99991
			ST	1,00	0,99	0,99	1,00	0,99	0,83	0,99	0,99948
			BF	1,00	1,00	1,00	1,00	1,00	0,99	1,00	0,99993
			GM	1,00	1,00	1,00	0,99	1,00	1,00	1,00	1,00000
			GL	1,00	1,00	1,00	0,99	1,00	0,99	1,00	0,99999
			TA	1,00	1,00	1,00	1,00	0,98	0,98	0,99	0,99987
		2.5 Km/h	RF	1,00	1,00	1,00	0,96	1,00	0,99	0,98	0,99995
			VL	1,00	1,00	1,00	0,96	1,00	1,00	1,00	0,99993
			ST	0,99	0,99	0,99	0,98	0,97	1,00	0,99	0,99999
			BF	0,99	0,98	0,99	1,00	0,98	1,00	0,96	0,99997
			GM	1,00	0,99	1,00	0,94	1,00	1,00	1,00	0,99999
			GL	1,00	0,99	1,00	0,97	1,00	0,99	0,98	0,99997
			TA	1,00	1,00	1,00	0,82	0,99	0,97	0,97	0,99996
	20% GF	1.5 Km/h	RF	1,00	1,00	1,00	0,98	1,00	1,00	1,00	1,00000
			VL	1,00	1,00	1,00	0,99	0,98	1,00	1,00	1,00000
			ST	1,00	1,00	1,00	0,99	1,00	1,00	1,00	1,00000
			BF	0,98	1,00	1,00	1,00	1,00	1,00	0,99	1,00000
			GM	0,99	1,00	1,00	1,00	1,00	1,00	1,00	1,00000
			GL	0,99	1,00	1,00	1,00	1,00	1,00	0,99	1,00000
			TA	0,99	1,00	1,00	1,00	1,00	1,00	1,00	1,00000
		2.0 Km/h	RF	1,00	1,00	1,00	1,00	1,00	0,99	1,00	0,99997
			VL	1,00	1,00	1,00	1,00	0,99	0,96	1,00	0,99990
			ST	1,00	0,99	1,00	1,00	0,92	0,94	1,00	0,99951
			BF	1,00	0,99	1,00	1,00	0,95	0,98	1,00	0,99962
			GM	1,00	1,00	1,00	1,00	1,00	1,00	1,00	0,99999
			GL	0,99	1,00	1,00	1,00	1,00	1,00	0,99	1,00000
			TA	1,00	0,99	1,00	1,00	1,00	0,99	1,00	0,99991
		2.5 Km/h	RF	1,00	1,00	0,99	0,98	0,99	1,00	1,00	0,99997
			VL	1,00	1,00	0,99	0,85	0,95	1,00	1,00	0,99988
			ST	1,00	1,00	1,00	0,99	0,98	0,94	0,99	0,99972
			BF	1,00	1,00	1,00	1,00	0,96	0,98	0,98	0,99956
			GM	1,00	1,00	1,00	0,93	1,00	0,99	1,00	0,99995
			GL	1,00	1,00	1,00	0,99	1,00	0,99	1,00	0,99999
			TA	1,00	1,00	0,99	0,96	0,99	0,96	0,98	0,99969

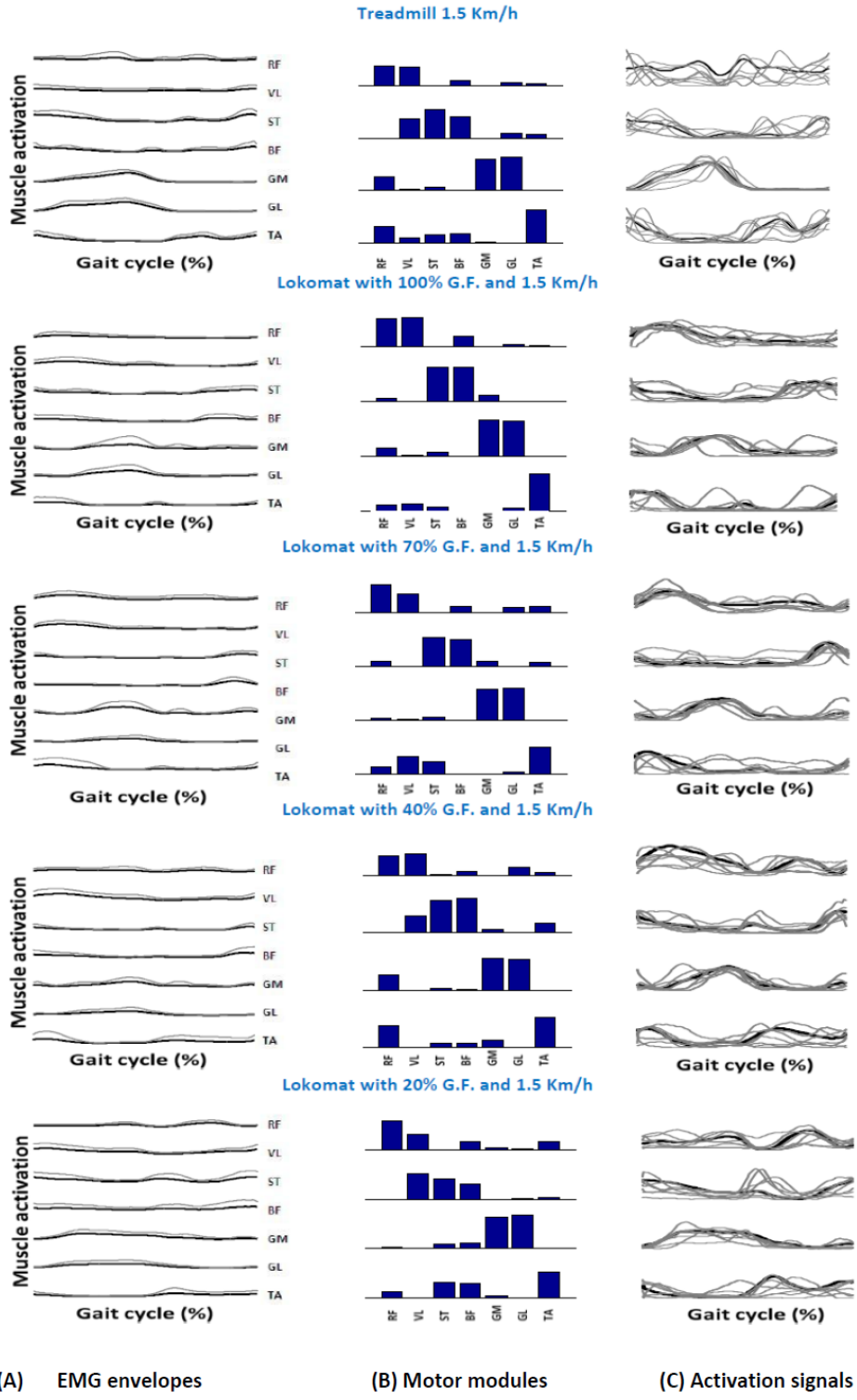

Figure 8.1: Modules obtained for all the conditions of Treadmill and Lokomat walking using 1.5 Km/h. (A) Average (black lines) and standard deviation (gray lines) of the EMG envelopes of the seven muscles for all the conditions using 1.5 Km/k. (B) Average motor modules and (C) the correspondent activation signals. Thin gray lines represent the results of each individual of the study, whereas the thick black lines represent the group average.

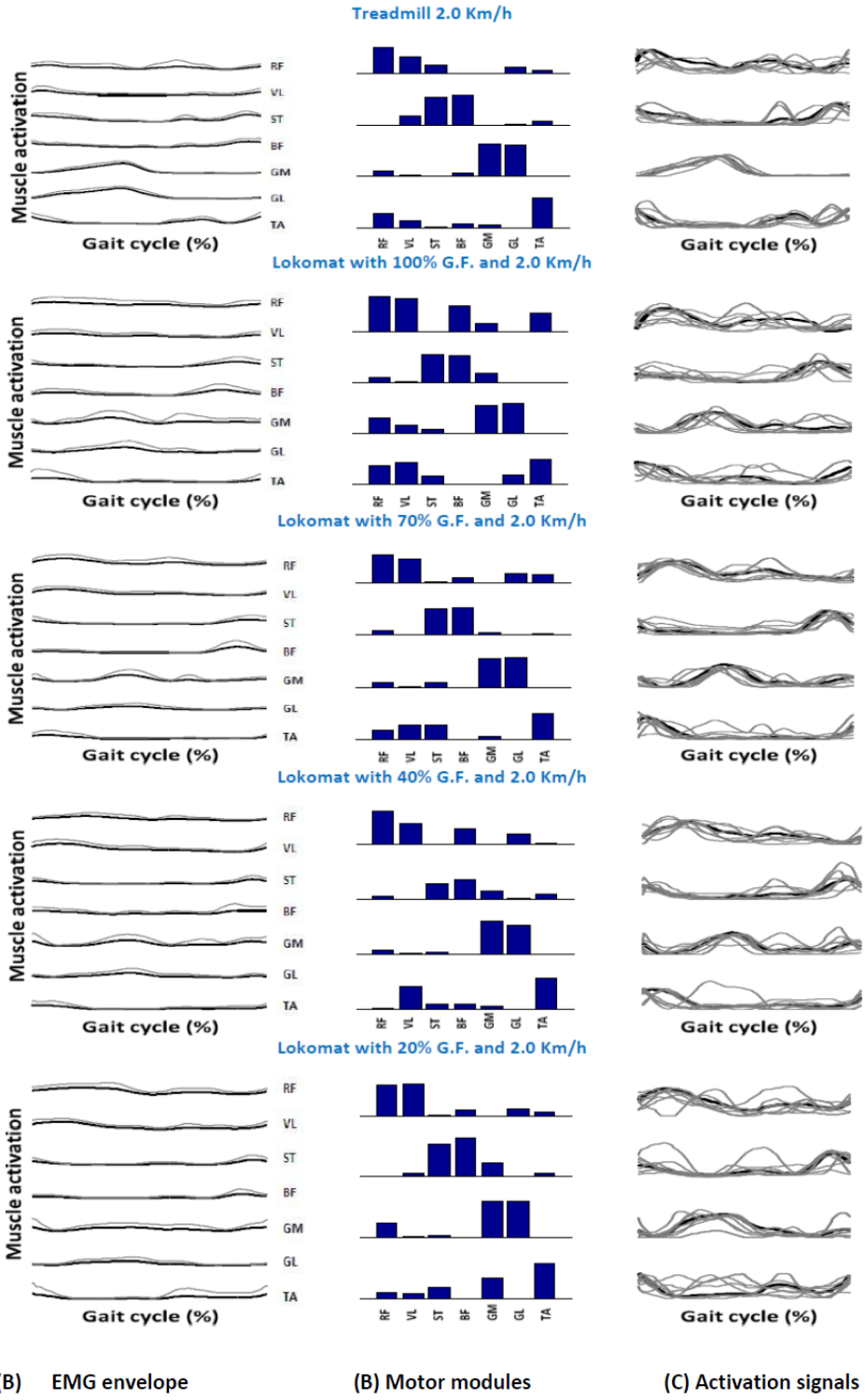

Figure 8.2: Modules obtained for all the conditions of Treadmill and Lokomat walking using 2.0 Km/h. (A) Average (black lines) and standard deviation (gray lines) of the EMG envelopes of the seven muscles for all the conditions using 2.0 Km/k. (B) Average motor modules and (C) the correspondent activation signals. Thin gray lines represent the results of each individual of the study, whereas the thick black lines represent the group average.

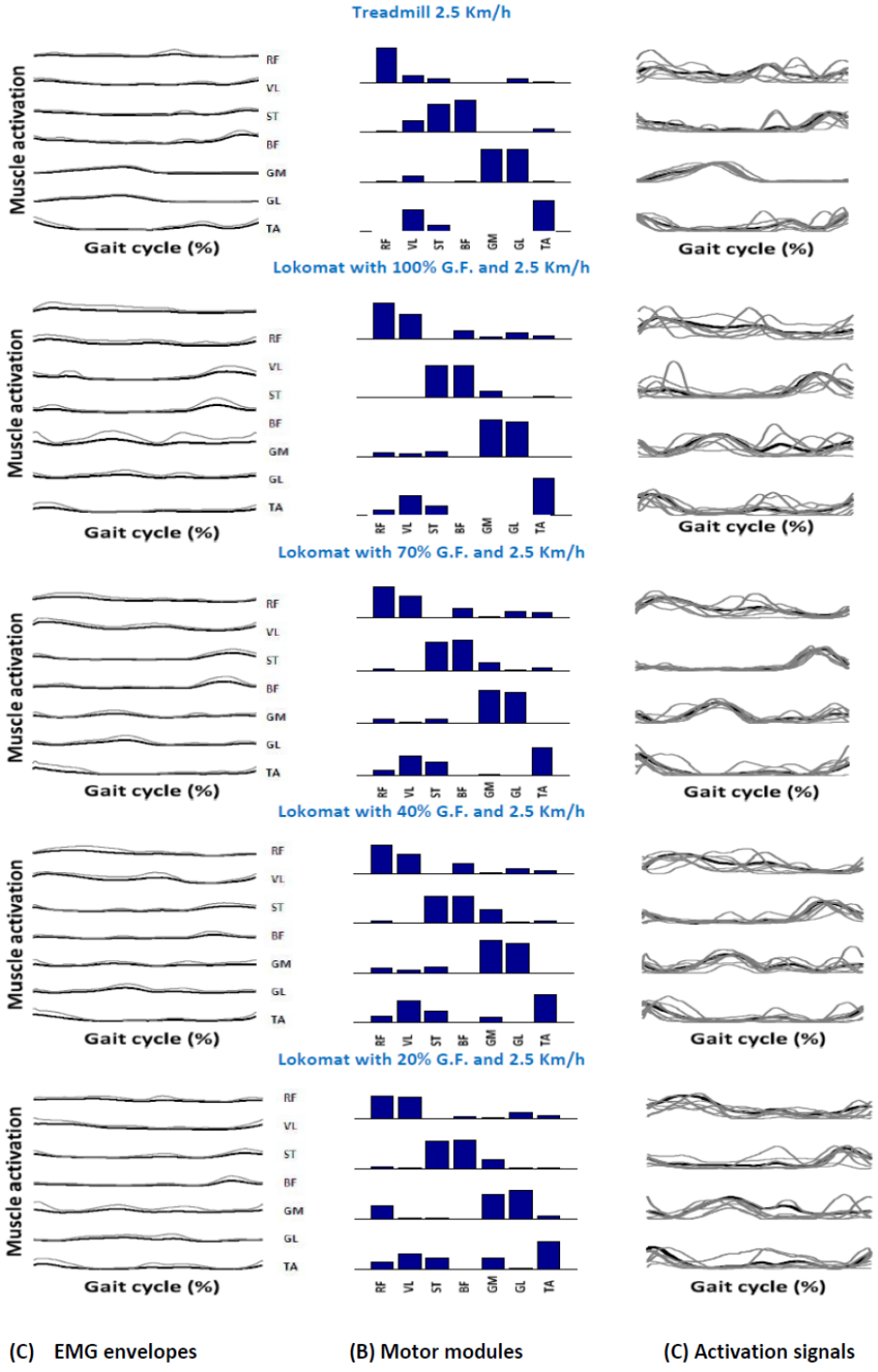

Figure 8.3: Modules obtained for all the conditions of Treadmill and Lokomat walking using 2.5 Km/h. (A) Average (black lines) and standard deviation (gray lines) of the EMG envelopes of the seven muscles for all the conditions using 2.5 Km/k. (B) Average motor modules and (C) the correspondent activation signals. Thin gray lines represent the results of each individual of the study, whereas the thick black lines represent the group average.

Table 8.4: Similarity tests of the (A) motor modules and (B) activation signals actuating on Treadmill walking, across participants.

(A) Similarity of the motor modules extracted on Treadmill, among subjects

Tests of Between-Subjects Effects

Dependent Variable: Motor modules values

Source	Type III Sum of Squares	df	Mean Square	F	Sig.
Corrected Model	1,456[a]	167	,009	,071	1,000
Intercept	46,287	1	46,287	375,082	,000
Subject	,073	7	,010	,084	,999
Speed	,006	2	,003	,025	,975
Muscle	,474	6	,079	,641	,698
Subject * Speed	,046	14	,003	,027	1,000
Subject * Muscle	,482	42	,011	,093	1,000
Speed * Muscle	,037	12	,003	,025	1,000
Subject * Speed * Muscle	,338	84	,004	,033	1,000
Error	62,196	504	,123		
Total	109,938	672			
Corrected Total	63,652	671			

a. R Squared = ,023 (Adjusted R Squared = -,301)

(B) Similarity of the activation signals extracted on Treadmill, among subjects

Tests of Between-Subjects Effects

Dependent Variable: Activation signals values

Source	Type III Sum of Squares	df	Mean Square	F	Sig.
Corrected Model	953,150[a]	95	10,033	,383	1,000
Intercept	17433,624	1	17433,624	665,722	,000
Subject	139,451	7	19,922	,761	,621
Speed	62,956	2	31,478	1,202	,301
Activation_signal_number	221,367	3	73,789	2,818	,038
Subject * Speed	21,720	14	1,551	,059	1,000
Subject *	297,463	21	14,165	,541	,954
Activation_signal_number					
Speed *	38,484	6	6,414	,245	,961
Activation_signal_number					
Subject * Speed*	171,709	42	4,088	,156	1,000
Activation_signal_number					
Error	15084,029	576	26,188		
Total	33470,803	672			
Corrected Total	16037,178	671			

a. R Squared = ,059 (Adjusted R Squared = -,096)

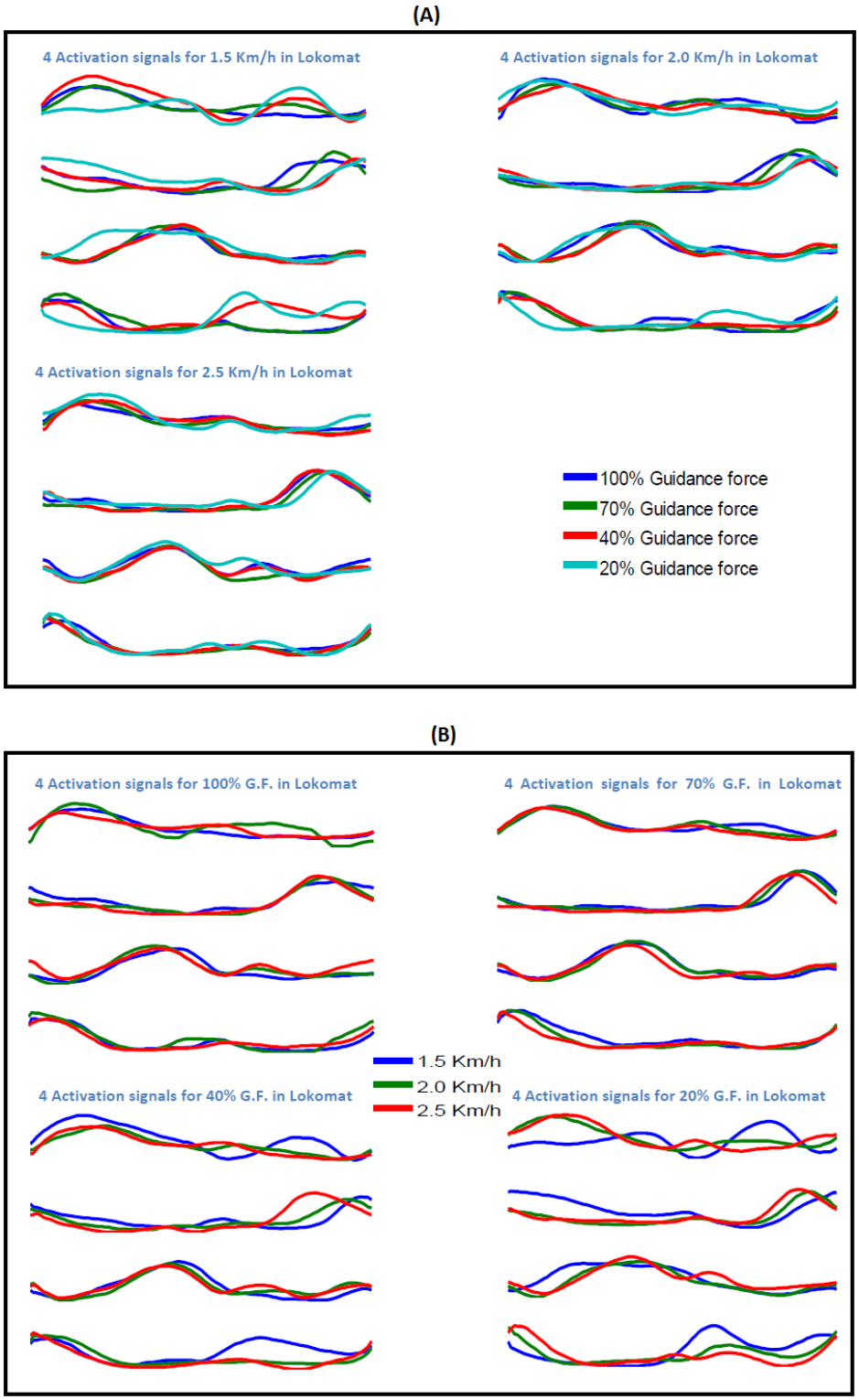

Figure 8.4: Activation signals (A) per gait speed and (B) per guidance force in the robotic condition

Table 8.5: Similarity tests of the motor modules actuating on robotic-guided walking, across participants

Similarity of the motor modules extracted on Lokomat walking, among subjects

Tests of Between-Subjects Effects

Dependent Variable: Motor modules values

Source	Type III Sum of Squares	df	Mean Square	F	Sig.
Corrected Model	6,623[a]	671	,010	,076	1,000
Intercept	193,480	1	193,480	1492,884	,000
Subject	,184	7	,026	,203	,985
Force	,018	3	,006	,045	,987
Speed	,035	2	,017	,134	,874
Muscle	,592	6	,099	,761	,601
Subject * Force	,171	21	,008	,063	1,000
Subject * Speed	,050	14	,004	,028	1,000
Subject * Muscle	1,670	42	,040	,307	1,000
Force * Speed	,086	6	,014	,110	,995
Force * Muscle	,302	18	,017	,129	1,000
Speed * Muscle	,132	12	,011	,085	1,000
Subject * Force * Speed	,215	42	,005	,039	1,000
Subject * Force * Muscle	,859	126	,007	,053	1,000
Subject * Speed * Muscle	,462	84	,006	,042	1,000
Force * Speed * Muscle	,343	36	,010	,073	1,000
Subject * Force * Speed * Muscle	1,506	252	,006	,046	1,000
Error	261,277	2016	,130		
Total	461,380	2688			
Corrected Total	267,900	2687			

a. R Squared = ,025 (Adjusted R Squared = -,300)

Table 8.6: Similarity tests of the activation signals actuating during robotic-guided walking, across participants

Similarity of the activation signals extracted on Lokomat, among subjects

Tests of Between-Subjects Effects

Dependent Variable: Activation signals values

Source	Type III Sum of Squares	df	Mean Square	F	Sig.
Corrected Model	8525,608[a]	383	22,260	,858	,971
Intercept	84188,594	1	84188,594	3246,218	,000
Subject	569,402	7	81,343	3,136	,003
Force	64,141	3	21,380	,824	,480
Speed	221,406	2	110,703	4,269	,014
Activation_signal_number	1857,774	3	619,258	23,878	,000
Subject * Force	419,269	21	19,965	,770	,760
Subject * Speed	181,003	14	12,929	,499	,935
Subject * Activation_signal_number	1285,211	21	61,201	2,360	,000
Force * Speed	64,854	6	10,809	,417	,868
Force * Activation_signal_number	194,886	9	21,654	,835	,584
Speed * Activation_signal_number	122,360	6	20,393	,786	,581
Subject * Force * Speed	362,664	42	8,635	,333	1,000
Subject * Force * Activation_signal_number	1044,595	63	16,581	,639	,988
Subject * Speed * Activation_signal_number	480,084	42	11,431	,441	,999
Force * Speed * Activation_signal_number	329,933	18	18,330	,707	,807
Subject * Force * Speed * Activation_signal_number	1328,026	126	10,540	,406	1,000
Error	59752,767	2304	25,934		
Total	152466,968	2688			
Corrected Total	68278,375	2687			

a. R Squared = ,125 (Adjusted R Squared = -,021)

Table 8.7: Similarity tests of the motor modules actuating on robotic-guided walking, in relation to the group average

Similarity of the motor modules extracted on Lokomat, among the group average

Tests of Between-Subjects Effects

Dependent Variable: Motor modules values

Source	Type III Sum of Squares	df	Mean Square	F	Sig.
Corrected Model	,432[a]	83	,005	,041	1,000
Intercept	24,402	1	24,402	193,547	,000
Force	,016	3	,005	,041	,989
Speed	,007	2	,003	,026	,974
Músculo	,106	6	,018	,140	,991
Force * Speed	,018	6	,003	,023	1,000
Force * Músculo	,083	18	,005	,037	1,000
Speed * Músculo	,050	12	,004	,033	1,000
Force * Speed * Músculo	,153	36	,004	,034	1,000
Error	31,771	252	,126		
Total	56,605	336			
Corrected Total	32,203	335			

a. R Squared = ,013 (Adjusted R Squared = -,312)

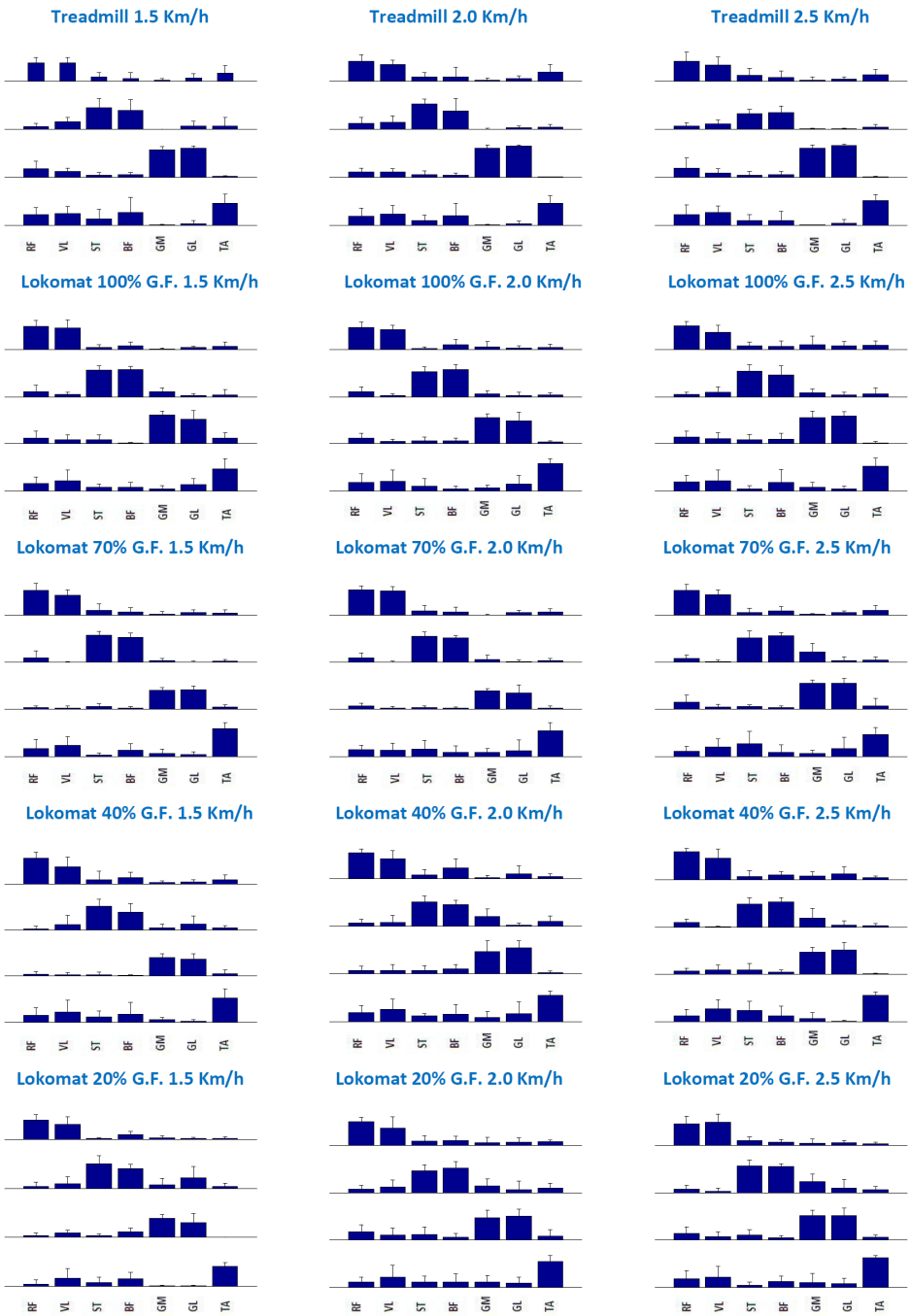

Figure 8.5: Representation of average motor modules for all the conditions of walking (mean and standard deviation among participants)

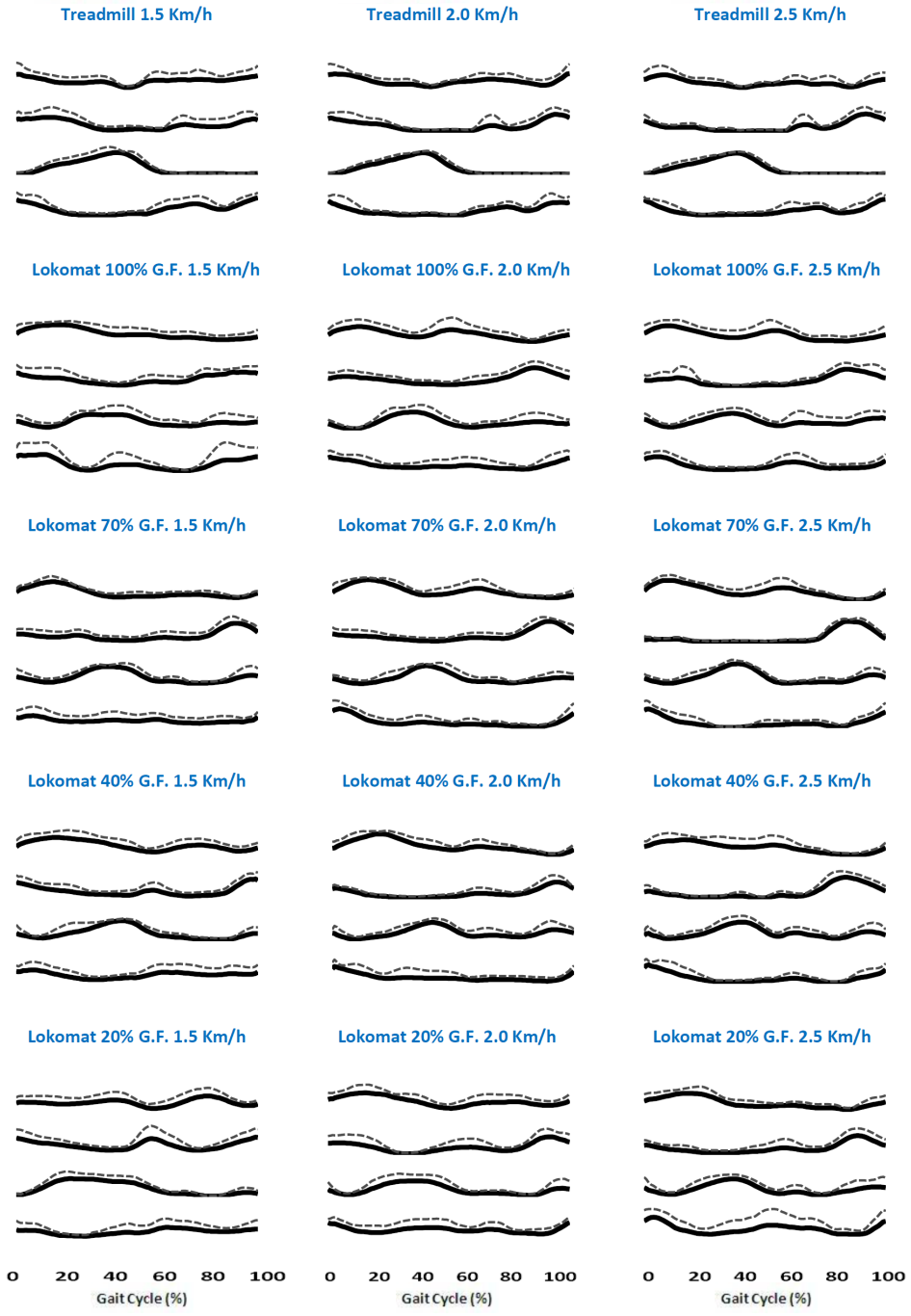

Figure 8.6: Representation of average activation signals for all the conditions of walking (mean and standard deviation among participants)

Table 8.8: Evaluation of Module 1. 'Tr.' represents Treadmill and 'Lo.' represents Lokomat. (A) Correlation of activation signal 1 among all the conditions of guidance force and speed in the average group. (B) Correlation of motor module 1 among all the conditions of guidance force and speed in the average group.

A) Activation signal 1

Tr. 1.5 Km/h	1														
Tr. 2.0 Km/h	,494	1													
Tr. 2.5 Km/h	,733	,850*	1												
Lo. 1.5 Km/h 20% GF	,550	-,034	,030	1											
Lo. 2.0 Km/h 20% GF	,636	,886**	,730	,364	1										
Lo. 2.5 Km/h 20% GF	,571	,872*	,685	,161	,949**	1									
Lo. 1.5 Km/h 40% GF	,762*	,764*	,656	,571	,957**	,879**	1								
Lo. 2.0 Km/h 40% GF	,857*	,834*	,849*	,361	,922**	,892**	,934**	1							
Lo. 2.5 Km/h 40% GF	,818*	,861*	,845*	,247	,900**	,906**	,901**	,988**	1						
Lo. 1.5 Km/h 70% GF	,752	,800*	,756*	,447	,959**	,895**	,956**	,958**	,921**	1					
Lo. 2.0 Km/h 70% GF	,758*	,869*	,848*	,247	,928**	,913**	,900**	,979**	,974**	,967**	1				
Lo. 2.5 Km/h 70% GF	,727	,920**	,846*	,197	,944**	,942**	,905**	,974**	,985**	,942**	,987**	1			
Lo. 1.5 Km/h 100% GF	,723	,897**	,779*	,290	,971**	,965**	,948**	,967**	,971**	,941**	,958**	,984**	1		
Lo. 2.0 Km/h 100% GF	,682	,835*	,812*	,278	,897**	,828*	,866*	,920**	,902**	,957**	,968**	,935**	,887**	1	
Lo. 2.5 Km/h 100% GF	,797*	,869*	,807*	,264	,899**	,902**	,908**	,965**	,985**	,882**	,932**	,966**	,974**	,842*	1
Condition	**Tr. 1.5 Km/h**	**Tr. 2.0 Km/h**	**Tr. 2.5 Km/h**	**Lo. 1.5 Km/h 20% GF**	**Lo. 2.0 Km/h 20% GF**	**Lo. 2.5 Km/h 20% GF**	**Lo. 1.5 Km/h 40% GF**	**Lo. 2.0 Km/h 40% GF**	**Lo. 2.5 Km/h 40% GF**	**Lo. 1.5 Km/h 70% GF**	**Lo. 2.0 Km/h 70% GF**	**Lo. 2.5 Km/h 70% GF**	**Lo. 1.5 Km/h 100% GF**	**Lo. 2.0 Km/h 100% GF**	**Lo. 2.5 Km/h 100% GF**

* Correlation is significant at the 0.05 level (2-tailed).
** Correlation is significant at the 0.01 level (2-tailed).

B) Motor module 1

Tr. 1.5 Km/h	1														
Tr. 2.0 Km/h	,889**	1													
Tr. 2.5 Km/h	,759*	,902**	1												
Lo. 1.5 Km/h 20% GF	,899**	,827*	,873*	1											
Lo. 2.0 Km/h 20% GF	,993**	,895**	,738	,865*	1										
Lo. 2.5 Km/h 20% GF	,980**	,916**	,765*	,854*	,995**	1									
Lo. 1.5 Km/h 40% GF	,974**	,872*	,699	,818*	,991**	,991**	1								
Lo. 2.0 Km/h 40% GF	,909**	,818*	,820*	,895**	,883**	,871*	,878**	1							
Lo. 2.5 Km/h 40% GF	,972**	,876**	,838*	,953**	,950**	,937**	,928**	,972**	1						
Lo. 1.5 Km/h 70% GF	,957**	,898**	,873*	,969**	,946**	,945**	,925**	,941**	,986**	1					
Lo. 2.0 Km/h 70% GF	,967**	,895**	,783*	,896**	,979**	,984**	,978**	,893**	,951**	,972**	1				
Lo. 2.5 Km/h 70% GF	,973**	,895**	,852*	,955**	,961**	,956**	,943**	,958**	,995**	,996**	,973**	1			
Lo. 1.5 Km/h 100% GF	,992**	,847*	,710	,875**	,977**	,953**	,955**	,909**	,963**	,929**	,933**	,953**	1		
Lo. 2.0 Km/h 100% GF	,854*	,599	,578	,896**	,808*	,758*	,760*	,798*	,872*	,846*	,795*	,852*	,871*	1	
Lo. 2.5 Km/h 100% GF	,972**	,915**	,875**	,948**	,959**	,957**	,938**	,956**	,992**	,990**	,963**	,996**	,953**	,825*	1
Condition	**Tr. 1.5 Km/h**	**Tr. 2.0 Km/h**	**Tr. 2.5 Km/h**	**Lo. 1.5 Km/h 20% GF**	**Lo. 2.0 Km/h 20% GF**	**Lo. 2.5 Km/h 20% GF**	**Lo. 1.5 Km/h 40% GF**	**Lo. 2.0 Km/h 40% GF**	**Lo. 2.5 Km/h 40% GF**	**Lo. 1.5 Km/h 70% GF**	**Lo. 2.0 Km/h 70% GF**	**Lo. 2.5 Km/h 70% GF**	**Lo. 1.5 Km/h 100% GF**	**Lo. 2.0 Km/h 100% GF**	**Lo. 2.5 Km/h 100% GF**

* Correlation is significant at the 0.05 level (2-tailed).
** Correlation is significant at the 0.01 level (2-tailed).

Table 8.9: Evaluation of Module 2. 'Tr.' represents Treadmill and 'Lo.' represents Lokomat. (A) Correlation of activation signal 2 among all the conditions of guidance force and speed in the average group. (B) Correlation of motor module 2 among all the conditions of guidance force and speed in the average group.

A) Activation signal 2

Tr. 1.5 Km/h	1														
Tr. 2.0 Km/h	,851*	1													
Tr. 2.5 Km/h	,804*	,994**	1												
Lo. 1.5 Km/h 20% GF	,905**	,622	,575	1											
Lo. 2.0 Km/h 20% GF	,584	,888**	,922**	,339	1										
Lo. 2.5 Km/h 20% GF	,416	,786*	,844*	,187	,924**	1									
Lo. 1.5 Km/h 40% GF	,901**	,895**	,876**	,783*	,804*	0,586	1								
Lo. 2.0 Km/h 40% GF	,536	,883**	,912**	,255	,976**	,920**	,73	1							
Lo. 2.5 Km/h 40% GF	,047	,492	,553	-,233	,659	,851*	,146	,744	1						
Lo. 1.5 Km/h 70% GF	,41	,808*	,863*	,157	,960**	,974**	,633	,955**	,792*	1					
Lo. 2.0 Km/h 70% GF	,357	,757*	,814*	,076	,899**	,987**	,515	,913**	,901**	,966**	1				
Lo. 2.5 Km/h 70% GF	,128	,567	,637	-,136	,743	,925**	,254	,789*	,979**	,872*	,957**	1			
Lo. 1.5 Km/h 100% GF	,571	,821*	,847*	,301	,786*	,893**	,549	,818*	,828*	,818*	,907**	,863*	1		
Lo. 2.0 Km/h 100% GF	,318	,684	,734	,06	,733	,914**	,345	,788*	,938**	,843*	,938**	,961**	,950**	1	
Lo. 2.5 Km/h 100% GF	,209	,579	,63	-,079	,65	,855*	,22	,715	,958**	,775*	,906**	,961**	,921**	,981**	1
Condition	**Tr. 1.5 Km/h**	**Tr. 2.0 Km/h**	**Tr. 2.5 Km/h**	**Lo. 1.5 Km/h 20% GF**	**Lo. 2.0 Km/h 20% GF**	**Lo. 2.5 Km/h 20% GF**	**Lo. 1.5 Km/h 40% GF**	**Lo. 2.0 Km/h 40% GF**	**Lo. 2.5 Km/h 40% GF**	**Lo. 1.5 Km/h 70% GF**	**Lo. 2.0 Km/h 70% GF**	**Lo. 2.5 Km/h 70% GF**	**Lo. 1.5 Km/h 100% GF**	**Lo. 2.0 Km/h 100% GF**	**Lo. 2.5 Km/h 100% GF**

* Correlation is significant at the 0.05 level (2-tailed).
** Correlation is significant at the 0.01 level (2-tailed).

B) Motor module 2

Tr. 1.5 Km/h	1														
Tr. 2.0 Km/h	,902**	1													
Tr. 2.5 Km/h	,907**	,997**	1												
Lo. 1.5 Km/h 20% GF	,917**	,710	,739	1											
Lo. 2.0 Km/h 20% GF	,713	,919**	,903**	,474	1										
Lo. 2.5 Km/h 20% GF	,712	,918**	,896**	,449	,994**	1									
Lo. 1.5 Km/h 40% GF	,931**	,983**	,986**	,791*	,875*	,860*	1								
Lo. 2.0 Km/h 40% GF	,591	,863*	,842*	,328	,980**	,976**	,809*	1							
Lo. 2.5 Km/h 40% GF	,643	,860*	,832*	,373	,983**	,990**	,799*	,974**	1						
Lo. 1.5 Km/h 70% GF	,727	,928**	,900**	,444	,948**	,972**	,868*	,945**	,950**	1					
Lo. 2.0 Km/h 70% GF	,764*	,954**	,935**	,495	,952**	,971**	,892**	,935**	,936**	,991**	1				
Lo. 2.5 Km/h 70% GF	,733	,939**	,917**	,462	,987**	,995**	,885**	,973**	,976**	,985**	,985**	1			
Lo. 1.5 Km/h 100% GF	,752	,942**	,920**	,484	,974**	,991**	,881**	,953**	,969**	,990**	,993**	,995**	1		
Lo. 2.0 Km/h 100% GF	,716	,912**	,889**	,458	,981**	,995**	,849*	,961**	,986**	,976**	,975**	,988**	,993**	1	
Lo. 2.5 Km/h 100% GF	,770*	,947**	,924**	,500	,980**	,992**	,893**	,953**	,972**	,984**	,986**	,996**	,997**	,988**	1
Condition	**Tr. 1.5 Km/h**	**Tr. 2.0 Km/h**	**Tr. 2.5 Km/h**	**Lo. 1.5 Km/h 20% GF**	**Lo. 2.0 Km/h 20% GF**	**Lo. 2.5 Km/h 20% GF**	**Lo. 1.5 Km/h 40% GF**	**Lo. 2.0 Km/h 40% GF**	**Lo. 2.5 Km/h 40% GF**	**Lo. 1.5 Km/h 70% GF**	**Lo. 2.0 Km/h 70% GF**	**Lo. 2.5 Km/h 70% GF**	**Lo. 1.5 Km/h 100% GF**	**Lo. 2.0 Km/h 100% GF**	**Lo. 2.5 Km/h 100% GF**

* Correlation is significant at the 0.05 level (2-tailed).
** Correlation is significant at the 0.01 level (2-tailed).

Table 8.10: Evaluation of Module 3. 'Tr.' represents Treadmill and 'Lo.' represents Lokomat. (A) Correlation of activation signal 3 among all the conditions of guidance force and speed in the average group. (B) Correlation of motor module 3 among all the conditions of guidance force and speed in the average group.

A) Activation signal 3

Condition	Tr. 1.5 Km/h	Tr. 2.0 Km/h	Tr. 2.5 Km/h	Lo. 1.5 Km/h 20% GF	Lo. 2.0 Km/h 20% GF	Lo. 2.5 Km/h 20% GF	Lo. 1.5 Km/h 40% GF	Lo. 2.0 Km/h 40% GF	Lo. 2.5 Km/h 40% GF	Lo. 1.5 Km/h 70% GF	Lo. 2.0 Km/h 70% GF	Lo. 2.5 Km/h 70% GF	Lo. 1.5 Km/h 100% GF	Lo. 2.0 Km/h 100% GF	Lo. 2.5 Km/h 100% GF
Tr. 1.5 Km/h	1														
Tr. 2.0 Km/h	,997**	1													
Tr. 2.5 Km/h	,993**	,997**	1												
Lo. 1.5 Km/h 20% GF	,963**	,953**	,960**	1											
Lo. 2.0 Km/h 20% GF	,977**	,977**	,961**	,928**	1										
Lo. 2.5 Km/h 20% GF	,943**	,946**	,921**	,861*	,984**	1									
Lo. 1.5 Km/h 40% GF	,945**	,944**	,921**	,847*	,976**	,979**	1								
Lo. 2.0 Km/h 40% GF	,834*	,851*	,821*	,681	,896**	,932**	,951**	1							
Lo. 2.5 Km/h 40% GF	,894**	,908**	,886**	,784*	,950**	,978**	,964**	,972**	1						
Lo. 1.5 Km/h 70% GF	,935**	,940**	,919**	,825*	,968**	,978**	,996**	,971**	,979**	1					
Lo. 2.0 Km/h 70% GF	,849*	,860*	,831*	,697	,904**	,940**	,966**	,995**	,971**	,980**	1				
Lo. 2.5 Km/h 70% GF	,888**	,909**	,892**	,759*	,921**	,933**	,951**	,981**	,972**	,974**	,973**	1			
Lo. 1.5 Km/h 100% GF	,935**	,942**	,917**	,821*	,968**	,985**	,990**	,970**	,979**	,995**	,975**	,971**	1		
Lo. 2.0 Km/h 100% GF	,940**	,950**	,928**	,860*	,976**	,990**	,956**	,927**	,975**	,963**	,923**	,943**	,978**	1	
Lo. 2.5 Km/h 100% GF	,890**	,913**	,901**	,797*	,935**	,948**	,928**	,946**	,985**	,952**	,934**	,974**	,951**	,964**	1

* Correlation is significant at the 0.05 level (2-tailed).
** Correlation is significant at the 0.01 level (2-tailed).

B) Motor module 3

Condition	Tr. 1.5 Km/h	Tr. 2.0 Km/h	Tr. 2.5 Km/h	Lo. 1.5 Km/h 20% GF	Lo. 2.0 Km/h 20% GF	Lo. 2.5 Km/h 20% GF	Lo. 1.5 Km/h 40% GF	Lo. 2.0 Km/h 40% GF	Lo. 2.5 Km/h 40% GF	Lo. 1.5 Km/h 70% GF	Lo. 2.0 Km/h 70% GF	Lo. 2.5 Km/h 70% GF	Lo. 1.5 Km/h 100% GF	Lo. 2.0 Km/h 100% GF	Lo. 2.5 Km/h 100% GF
Tr. 1.5 Km/h	1														
Tr. 2.0 Km/h	,970**	1													
Tr. 2.5 Km/h	,931**	,984**	1												
Lo. 1.5 Km/h 20% GF	,929**	,980**	,972**	1											
Lo. 2.0 Km/h 20% GF	,999**	,977**	,939**	,935**	1										
Lo. 2.5 Km/h 20% GF	,990**	,952**	,906**	,906**	,988**	1									
Lo. 1.5 Km/h 40% GF	,996**	,962**	,911**	,913**	,997**	,984**	1								
Lo. 2.0 Km/h 40% GF	,965**	,993**	,982**	,974**	,973**	,938**	,957**	1							
Lo. 2.5 Km/h 40% GF	,963**	,984**	,979**	,973**	,968**	,930**	,951**	,996**	1						
Lo. 1.5 Km/h 70% GF	,960**	,991**	,988**	,988**	,965**	,939**	,943**	,993**	,993**	1					
Lo. 2.0 Km/h 70% GF	,970**	,986**	,976**	,983**	,973**	,947**	,955**	,992**	,995**	,997**	1				
Lo. 2.5 Km/h 70% GF	,965**	,990**	,982**	,983**	,971**	,939**	,952**	,997**	,998**	,998**	,998**	1			
Lo. 1.5 Km/h 100% GF	,984**	,990**	,970**	,972**	,988**	,963**	,975**	,994**	,994**	,992**	,997**	,996**	1		
Lo. 2.0 Km/h 100% GF	,980**	,935**	,912**	,873*	,974**	,966**	,971**	,928**	,931**	,923**	,934**	,926**	,951**	1	
Lo. 2.5 Km/h 100% GF	,960**	,989**	,988**	,981**	,965**	,931**	,944**	,996**	,998**	,998**	,997**	,999**	,993**	,928**	1

* Correlation is significant at the 0.05 level (2-tailed).
** Correlation is significant at the 0.01 level (2-tailed).

Table 8.11: Evaluation of Module 4. 'Tr.' represents Treadmill and 'Lo.' represents Lokomat. (A) Correlation of activation signal 4 among all the conditions of guidance force and speed in the average group. (B) Correlation of motor module 4 among all the conditions of guidance force and speed in the average group.

A) Activation signal 4

Tr. 1.5 Km/h	1														
Tr. 2.0 Km/h	,941**	1													
Tr. 2.5 Km/h	,846*	,881**	1												
Lo. 1.5 Km/h 20% GF	,413	,557	,310	1											
Lo. 2.0 Km/h 20% GF	,741	,914**	,869*	,555	1										
Lo. 2.5 Km/h 20% GF	,306	,418	,734	-,125	,633	1									
Lo. 1.5 Km/h 40% GF	,784*	,797*	,631	,526	,714	,289	1								
Lo. 2.0 Km/h 40% GF	,233	,133	,543	-,509	,186	,792*	,112	1							
Lo. 2.5 Km/h 40% GF	,285	,331	,725	-,182	,493	,948**	,132	,867*	1						
Lo. 1.5 Km/h 70% GF	,061	-,049	,401	-,569	,021	,715	-,063	,977**	,830*	1					
Lo. 2.0 Km/h 70% GF	,286	,263	,668	-,351	,374	,912**	,157	,964**	,966**	,924**	1				
Lo. 2.5 Km/h 70% GF	,359	,385	,755*	-,206	,519	,957**	,238	,897**	,987**	,836*	,981**	1			
Lo. 1.5 Km/h 100% GF	,068	-,006	,450	-,515	,095	,784*	-,055	,971**	,892**	,985**	,957**	,895**	1		
Lo. 2.0 Km/h 100% GF	,108	,088	,533	-,432	,206	,788*	-,200	,869*	,921**	,887**	,913**	,882**	,919**	1	
Lo. 2.5 Km/h 100% GF	,397	,362	,750	-,240	,429	,879**	,192	,927**	,968**	,880**	,981**	,978**	,923**	,912**	1
Condition	**Tr. 1.5 Km/h**	**Tr. 2.0 Km/h**	**Tr. 2.5 Km/h**	**Lo. 1.5 Km/h 20% GF**	**Lo. 2.0 Km/h 20% GF**	**Lo. 2.5 Km/h 20% GF**	**Lo. 1.5 Km/h 40% GF**	**Lo. 2.0 Km/h 40% GF**	**Lo. 2.5 Km/h 40% GF**	**Lo. 1.5 Km/h 70% GF**	**Lo. 2.0 Km/h 70% GF**	**Lo. 2.5 Km/h 70% GF**	**Lo. 1.5 Km/h 100% GF**	**Lo. 2.0 Km/h 100% GF**	**Lo. 2.5 Km/h 100% GF**

* Correlation is significant at the 0.05 level (2-tailed).
** Correlation is significant at the 0.01 level (2-tailed).

B) Motor module 4

Tr. 1.5 Km/h	1														
Tr. 2.0 Km/h	,941**	1													
Tr. 2.5 Km/h	,620	,726	1												
Lo. 1.5 Km/h 20% GF	,831*	,635	,463	1											
Lo. 2.0 Km/h 20% GF	,673	,723	,623	,616	1										
Lo. 2.5 Km/h 20% GF	,683	,771*	,889**	,537	,874*	1									
Lo. 1.5 Km/h 40% GF	,920**	,915**	,430	,649	,719	,623	1								
Lo. 2.0 Km/h 40% GF	,625	,726	,989**	,491	,624	,873*	,425	1							
Lo. 2.5 Km/h 40% GF	,622	,724	,969**	,437	,673	,945**	,483	,948**	1						
Lo. 1.5 Km/h 70% GF	,705	,754	,949**	,529	,609	,891**	,530	,907**	,965**	1					
Lo. 2.0 Km/h 70% GF	,778*	,786*	,873*	,623	,702	,918**	,648	,831*	,932**	,970**	1				
Lo. 2.5 Km/h 70% GF	,661	,714	,962**	,519	,626	,912**	,478	,930**	,983**	,992**	,962**	1			
Lo. 1.5 Km/h 100% GF	,882**	,934**	,849*	,692	,792*	,852*	,784*	,832*	,812*	,853*	,852*	,823*	1		
Lo. 2.0 Km/h 100% GF	,635	,757*	,769*	,220	,345	,661	,562	,705	,790*	,854*	,800*	,803*	,733	1	
Lo. 2.5 Km/h 100% GF	,754	,828*	,979**	,580	,703	,921**	,589	,961**	,964**	,972**	,933**	,969**	,926**	,805*	1
Condition	**Tr. 1.5 Km/h**	**Tr. 2.0 Km/h**	**Tr. 2.5 Km/h**	**Lo. 1.5 Km/h 20% GF**	**Lo. 2.0 Km/h 20% GF**	**Lo. 2.5 Km/h 20% GF**	**Lo. 1.5 Km/h 40% GF**	**Lo. 2.0 Km/h 40% GF**	**Lo. 2.5 Km/h 40% GF**	**Lo. 1.5 Km/h 70% GF**	**Lo. 2.0 Km/h 70% GF**	**Lo. 2.5 Km/h 70% GF**	**Lo. 1.5 Km/h 100% GF**	**Lo. 2.0 Km/h 100% GF**	**Lo. 2.5 Km/h 100% GF**

* Correlation is significant at the 0.05 level (2-tailed).
** Correlation is significant at the 0.01 level (2-tailed).

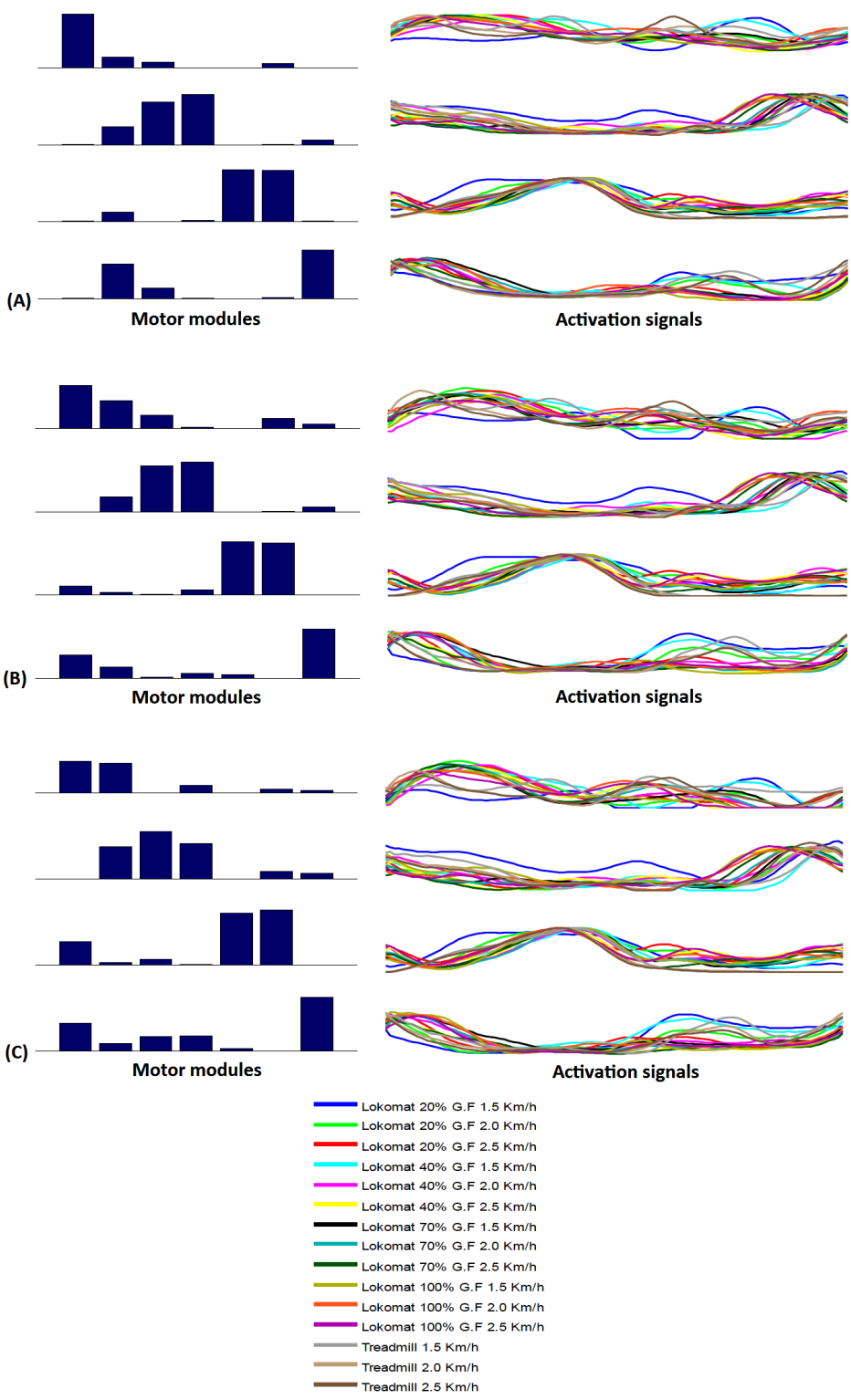

Figure 8.7: Analysis of the computed activation signals for all conditions of guidance force and speed using the motor modules obtained on (A) Treadmill at 2.5 Km/h, (B) Treadmill at 2.0 Km/h and (C) Treadmill at 1.5 Km/h. The same motor modules were used for all conditions.

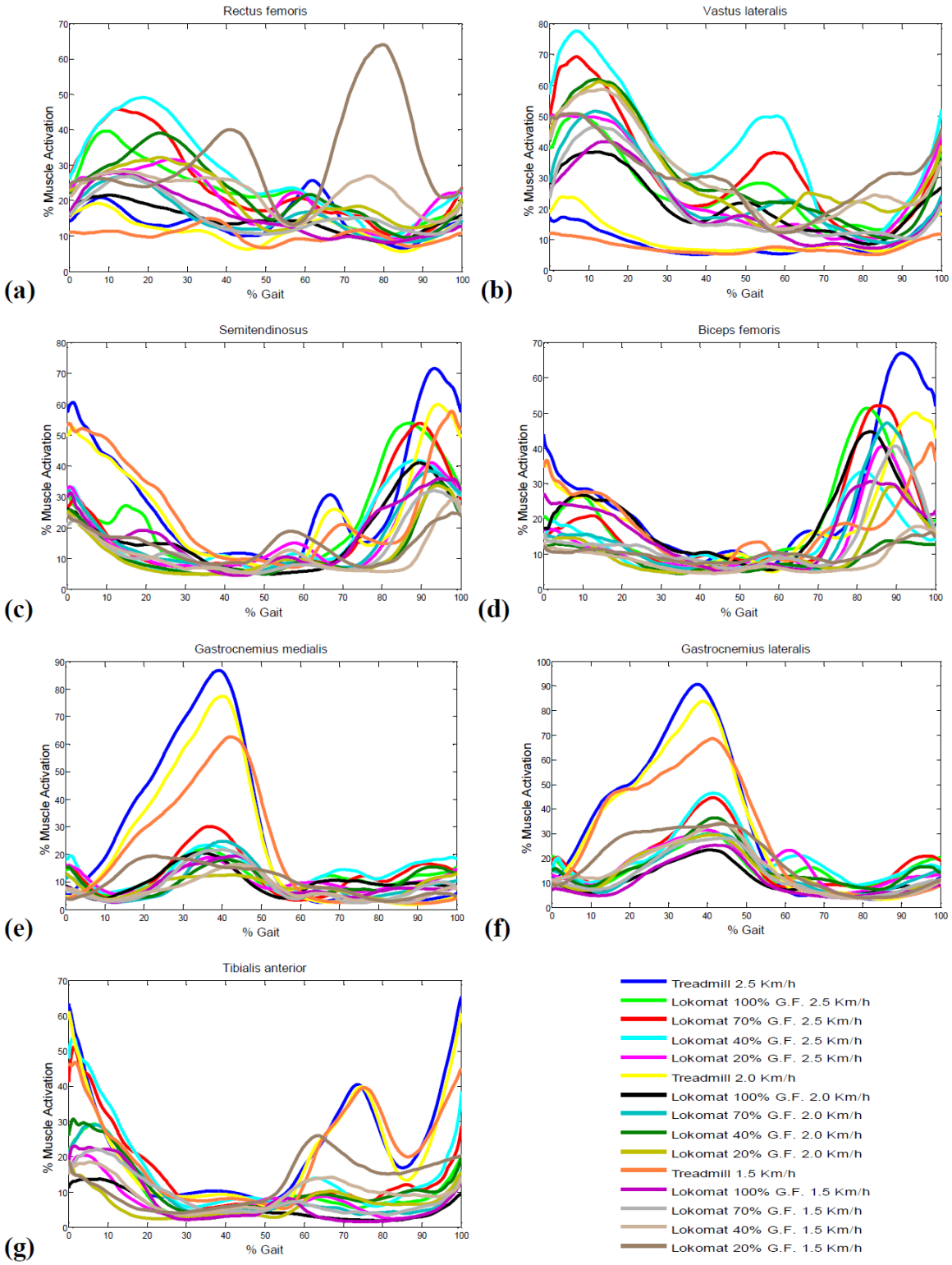

Figure 8.8: Average envelope signals of Rectus femoris (a), Vastus lateralis (b), Semitendinosus (c), Biceps femoris (d), Gastrocnemius medialis (e), Gastrocnemius lateralis (f) and Tibialis anterior, for all the conditions of guidance force and speed (all subjects).

Table 8.12: Variability (mean ± SD) of some gait parameters across different conditions of walking within the group of participants.

	Gait cycle time (s)	Stance time (s)	Swing time (s)	Stance ratio (%)	Swing ratio (%)
Treadmill 2.5 Km/h	1,45 ± 0,11	0,90 ± 0,02	0,55 ± 0,01	62,29 ± 1,55	37,71 ± 0,77
Treadmill 2.0 Km/h	1,57 ± 0,15	0,99 ± 0,02	0,58 ± 0,01	62,85 ± 1,14	37,15 ± 0,95
Treadmill 1.5 Km/h	1,81 ± 0,17	1,19 ± 0,02	0,61 ± 0,02	65,95 ± 1,15	34,05 ± 1,05
Lokomat 100% G.F. 2.5 Km/h	1,77 ± 0,20	1,18 ± 0,05	0,59 ± 0,05	66,84 ± 2,82	33,16 ± 2,82
Lokomat 100% G.F. 2.0 Km/h	2,36 ± 0,26	1,62 ± 0,05	0,74 ± 0,06	68,70 ± 2,26	31,30 ± 2,38
Lokomat 100% G.F. 1.5 Km/h	3,16 ± 0,31	2,17 ± 0,09	0,98 ± 0,09	68,83 ± 2,99	31,17 ± 2,85
Lokomat 70% G.F. 2.5 Km/h	1,89 ± 0,21	1,22 ± 0,08	0,67 ± 0,08	64,55± 4,22	33,81 ± 4,23
Lokomat 70% G.F. 2.0 Km/h	2,34 ± 0,26	1,51 ± 0,1	0,83 ± 0,09	64,53 ± 4,27	35,47 ± 3,85
Lokomat 70% G.F. 1.5 Km/h	3,16 ± 0,32	2,00 ± 0,11	1,16 ± 0,10	63,26 ± 3,34	36,74 ± 3,04
Lokomat 40% G.F. 2.5 Km/h	1,89 ± 0,19	1,15 ± 0,07	0,74 ± 0,06	60,84 ± 3,70	39,15 ± 3,17
Lokomat 40% G.F. 2.0 Km/h	2,37 ± 0,22	1,45 ± 0,09	0,92 ± 0,11	61,18 ± 3,97	31,73 ± 4,57
Lokomat 40% G.F. 1.5 Km/h	3,15 ± 0,27	1,92 ± 0,13	1,23 ± 0,14	60,97 ± 3,97	39,03 ± 4,35
Lokomat 20% G.F. 2.5 Km/h	1,87 ± 0,18	1,13 ± 0,07	0,75 ± 0,10	60,15 ± 3,97	39,85 ± 5,46
Lokomat 20% G.F. 2.0 Km/h	2,37 ± 0,30	1,47 ± 0,06	0,89 ± 0,05	62,28 ± 2,66	37,72 ± 2,30
Lokomat 20% G.F. 1.5 Km/h	3,16 ± 0,28	1,94 ± 0,12	1,21 ± 0,10	61,57 ± 3,80	38,43 ± 3,27

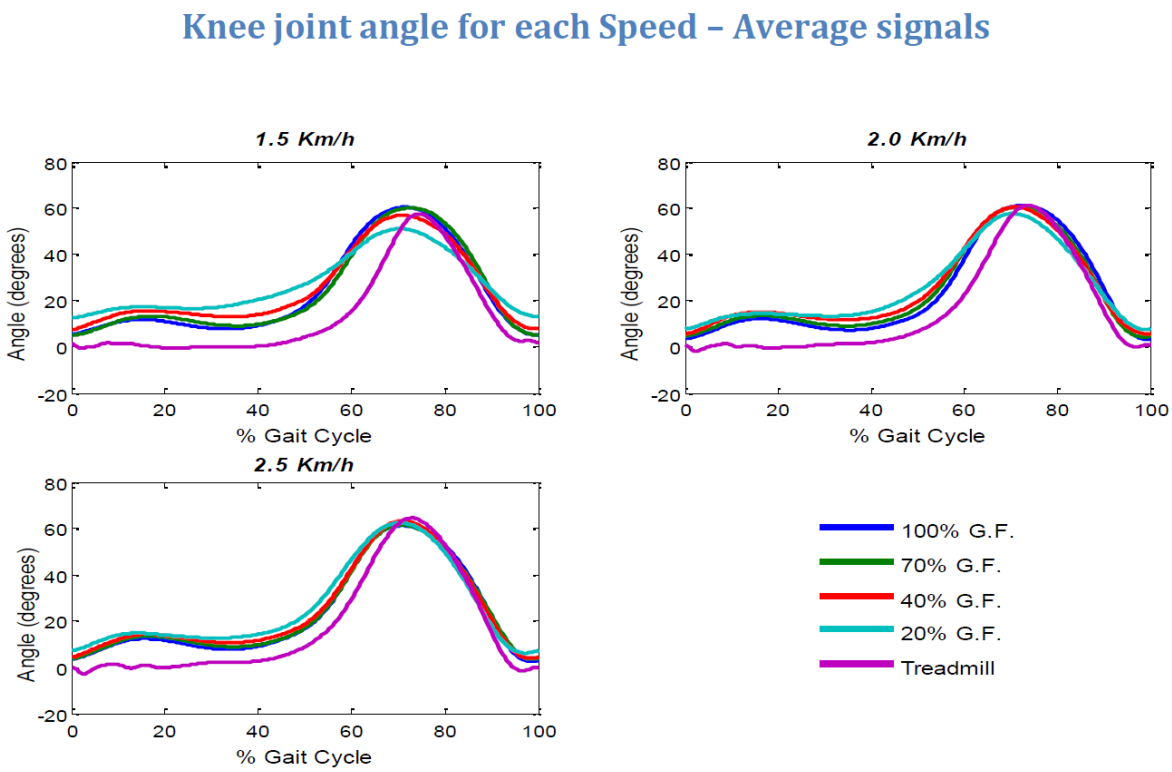

Figure 8.9: Mean kinematic trajectories of the knee joint (sagittal plane) during the gait cycle comparing both types of walking, in relation to the same speed.

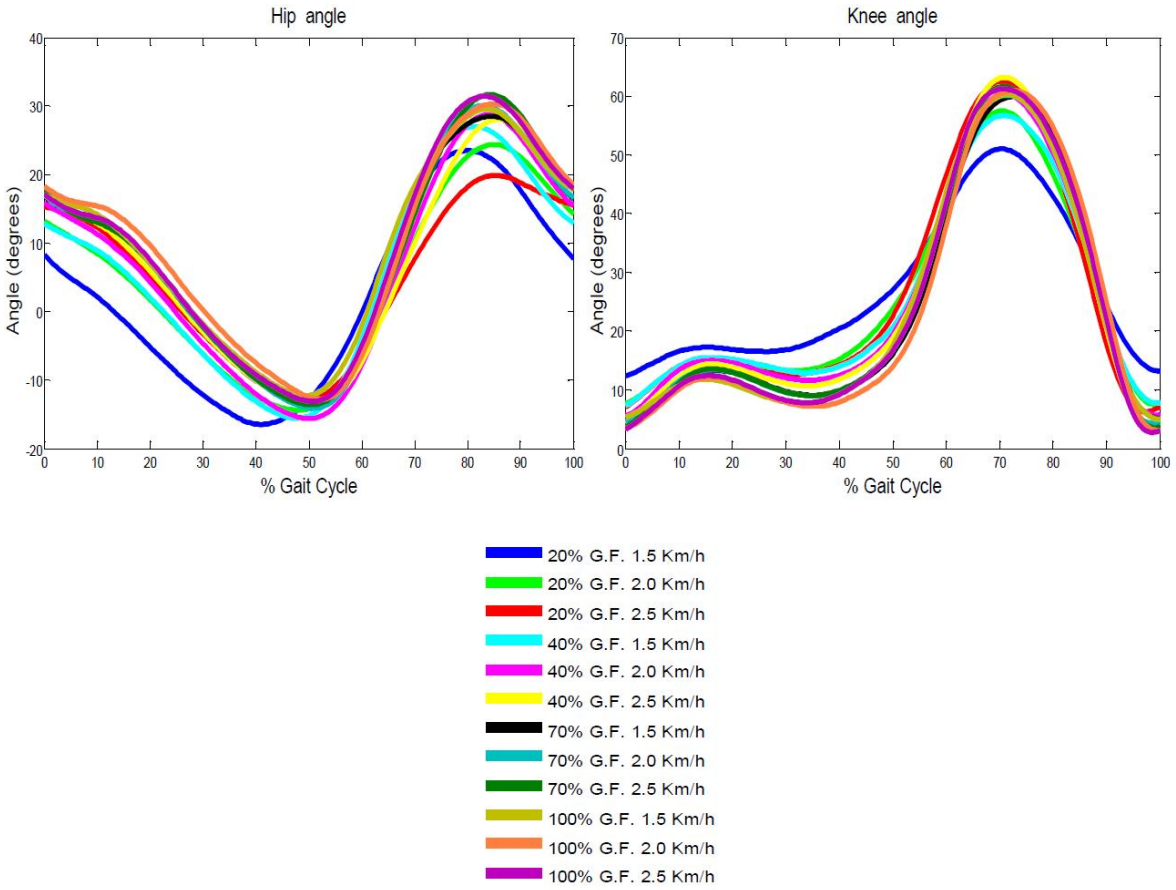

Figure 8.10: Mean kinematic trajectories of the hip and knee joints (sagittal plane) during the gait cycle in the robotic-aided walking condition.

Table 8.13: Kinematic patterns of the hip and knee joints in the sagittal plane during Lokomat walking. Results of the group average for all conditions of guidance force and speed. Representation of the minimum and maximum angle of the gait cycle, the range of motion, the standard deviation and the correspondent moments of gait cycle when the minimum and maximum angles are obtained, for both joints.

Kinematics

		Hip						Knee					
		Min (1)	Max (2)	ROM (3)	SD (4)	Time (Min) (5)	Time (Max) (6)	Min (1)	Max (2)	ROM (3)	SD (4)	Time (Min) (5)	Time (Max) (6)
20% G.F.	1.5 Km/h	-16,47	23,49	39,96	14,10	41,20	80,40	12,40	51,02	38,62	11,76	0,40	70,40
	2.0 Km/h	-14,37	24,38	38,75	11,64	48,40	85,20	7,56	57,52	49,96	13,29	99,20	70,80
	2.5 Km/h	-13,01	19,86	32,87	8,42	49,20	85,60	6,25	62,52	56,27	15,07	97,60	70,80
40% G.F.	1.5 Km/h	-15,55	26,99	42,53	10,91	48,00	81,60	7,33	56,68	49,35	11,21	0,40	71,20
	2.0 Km/h	-15,60	28,77	44,36	7,91	50,40	84,40	5,67	60,39	54,72	12,27	0,40	71,20
	2.5 Km/h	-13,79	28,07	41,85	5,78	51,20	86,40	3,99	63,24	59,26	11,23	98,80	71,20
70% G.F.	1.5 Km/h	-13,90	28,48	42,38	6,27	51,60	84,80	5,02	59,97	54,95	9,82	0,40	73,20
	2.0 Km/h	-14,12	30,00	44,12	5,06	51,20	83,20	4,31	60,18	55,86	9,12	98,80	71,60
	2.5 Km/h	-13,60	31,67	45,28	6,54	50,80	84,80	3,52	61,65	58,13	10,23	99,20	71,20
100% G.F.	1.5 Km/h	-12,29	29,54	41,83	7,13	49,60	84,00	4,97	60,32	55,35	11,42	100,40	72,00
	2.0 Km/h	-12,80	30,28	43,08	3,92	52,80	85,60	3,11	60,92	57,81	7,04	100,00	72,80
	2.5 Km/h	-13,08	31,44	44,52	2,42	51,20	83,60	2,75	61,26	58,51	5,99	98,80	71,20

(1) **Minimum angle**

(2) **Maximum angle**

(3) **Range of motion ((2) - (1))**

(4) **Standard deviation**

(5) **Correspondent % Gait cycle of the minimum**

(6) **Correspondent % Gait cycle of the maximum**

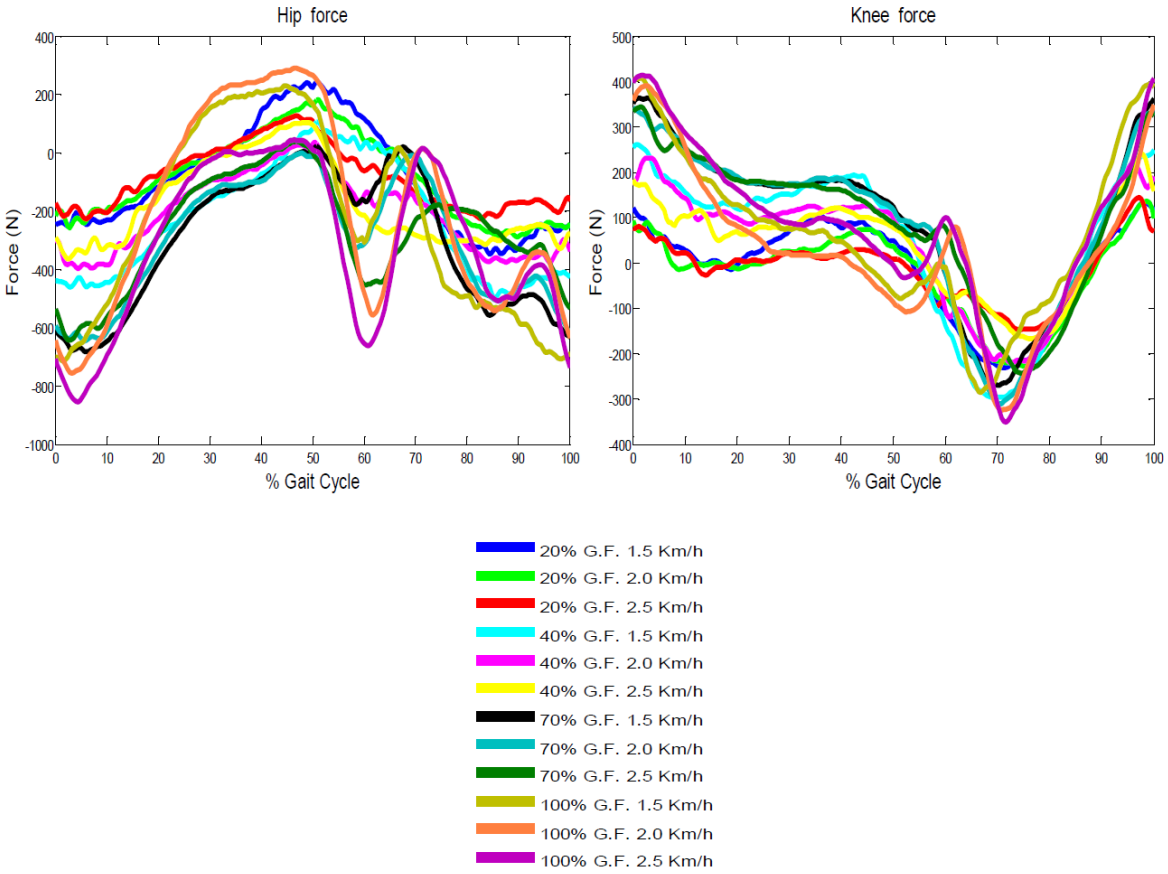

Figure 8.11: Mean interaction joint forces between the participants and Lokomat during the gait cycle.

Table 8.14: Kinetic values obtained in the (A) hip and (B) knee joints in the sagittal plane during Lokomat walking. Results of the group average for all conditions of guidance force and speed and for the seven phases of gait cycle. Representation of the minimum and maximum forces obtained in each gait phase of for each condition, for both joints. For each condition, it is also referred the ROF (range of forces) values.

A) Hip Kinetics - Forces actuating in Lokomat hip joint

		Phase 1 Initial double support (0-10% GC)		Phase 2 Mid stance (10-30% GC)		Phase 3 Terminal stance (30-50% GC)		Phase 4 Preswing (50-60% GC)		Phase 5 Initial swing (60-73% GC)		Phase 6 Mid swing (73-87% GC)		Phase 7 Terminal swing(87-100% GC)		ROF (1)
		Min.	Max.	Min.	Max.	Min.	Max.	Min.	Max.	Min.	Max.	Min.	Max.	Min.	Max.	
20% G.F.	1.5 Km/h	-252	-206	-229	-12	-9	240	117	244	-194	110	-349	-202	-340	-245	593
	2.0 Km/h	-257	-193	-195	-18	-11	172	41	182	-126	45	-287	-130	-288	-238	470
	2.5 Km/h	-228	-173	-200	-1	3	129	-61	96	-171	-43	-226	-161	-204	-153	357
40% G.F.	1.5 Km/h	-460	-428	-444	-160	-155	85	13	107	-184	37	-497	-195	-483	-410	604
	2.0 Km/h	-397	-298	-384	-95	-93	31	-171	36	-191	-134	-374	-200	-377	-296	433
	2.5 Km/h	-364	-290	-324	-22	-20	104	-214	89	-292	-221	-315	-287	-328	-246	468
70% G.F.	1.5 Km/h	-683	-610	-639	-158	-151	6	-177	24	-168	21	-557	-165	-632	-485	707
	2.0 Km/h	-645	-592	-601	-133	-130	0	-325	-6	-304	-9	-508	-98	-615	-423	645
	2.5 Km/h	-643	-535	-551	-94	-90	39	-453	-11	-454	-190	-287	-178	-533	-295	682
100% G.F.	1.5 Km/h	-714	-518	-507	152	160	232	-306	157	-316	18	-535	-336	-707	-536	946
	2.0 Km/h	-756	-591	-572	185	195	291	-479	261	-559	14	-541	-17	-636	-339	1046
	2.5 Km/h	-854	-694	-680	-25	-21	45	-654	7	-662	15	-507	-18	-738	-385	899

B) Knee Kinetics - Forces actuating in Lokomat knee joint

		Phase 1 Initial double support (0-10% GC)		Phase 2 Mid stance (10-30% GC)		Phase 3 Terminal stance (30-50% GC)		Phase 4 Preswing (50-60% GC)		Phase 5 Initial swing (60-73% GC)		Phase 6 Mid swing (73-87% GC)		Phase 7 Terminal swing(87-100% GC)		ROF (1)
		Min.	Max.	Min.	Max.	Min.	Max.	Min.	Max.	Min.	Max.	Min.	Max.	Min.	Max.	
20% G.F.	1.5 Km/h	28,4	121	-14	70,3	47,1	103	-110	45,4	-232	-116	-225	-33	-27	135	367
	2.0 Km/h	-14	93,2	-13	27	24,1	74,6	-77	31,1	-221	-79	-227	-47	-42	136	363
	2.5 Km/h	20,3	80,3	-27	23,1	7,53	30,2	-95	8,08	-138	-62	-148	-35	-30	144	292
40% G.F.	1.5 Km/h	156	262	118	152	102	195	-138	94,2	-297	-150	-283	8,94	24,9	249	559
	2.0 Km/h	143	232	86,5	139	97,1	127	-105	89	-219	-101	-218	-12	0,22	220	451
	2.5 Km/h	83,5	185	49,4	117	77,6	121	-66	75,4	-152	-61	-168	-18	-8,8	242	410
70% G.F.	1.5 Km/h	251	364	169	246	124	183	-25	117	-270	-37	-240	-8,5	1,09	362	633
	2.0 Km/h	250	343	173	243	116	187	-23	109	-311	-42	-286	6,97	13,2	333	654
	2.5 Km/h	248	344	172	249	87,7	172	49,9	84,5	-226	68,3	-244	-36	-26	330	588
100% G.F.	1.5 Km/h	236	408	74,6	229	-68	76,9	-79	-2,6	-286	-23	-165	50,7	62,5	394	695
	2.0 Km/h	256	392	19,9	243	-88	17,9	-108	37,4	-324	79,7	-308	-12	-5,4	348	716
	2.5 Km/h	286	415	88,2	281	-5,4	98,5	-33	101	-351	98	-324	33,9	43,2	407	766

(1) ROF is the range of forces

Chapter 9

Conclusions

Evidences show that motor rehabilitation should be performed with the aim of improving some damaged gait tasks, so that these tasks can be relearned [93] [21]. Future exoskeletons used in gait training will certainly present a control strategy based on this principle. Robotic training should be as intensive as possible (providing only the amount of assistance as needed) and begin as soon as possible. Thus, it is more likely to obtain the necessary cortical arrangement responsible for improving the damaged walking tasks [5].

It is fundamental to understand how the nervous system coordinates the muscular activity during robotic-guided walking in order to design new robotic therapy for post-stroke patients. Our study evaluated the effects of robotic-aided walking in healthy participants. We developed a protocol to analyze the differences in the modular organization of the nervous system, in the muscular activation, in the gait parameters, as well as the kinematic and kinetic differences between normal walking and walking assisted by an exoskeleton, changing the guidance force and the speed. The results of our study are very important, because they provide a baseline for comparison with future studies about motor rehabilitation in post-stroke patients during robotic therapy, as well as to develop new rehabilitation methods.

9.1 Discussion of the Work

Our work had three main goals: to study the muscular electric activity during walking in Lokomat, by varying the total assistance provided by the device, as well as the walking speed; to analyze the kinematic changes obtained during Lokomat-assisted walking, as well as the interaction forces between each user and the robotic device; to understand how the

nervous system synchronizes the muscular activity during walking assisted by robotic devices. All these three major goals were completely achieved.

A very difficult task of this study was the acquisition of muscle activity during Lokomat walking. In some trials of the individuals not included in this study, we noticed contact between sEMG electrodes and the Lokomat's cuffs, which could influence the results. Therefore, the results of those individuals were not considered for this study. We developed a final protocol for the acquisition of electromyographic signals in robotic-aided locomotion, taking into account the resting time the individuals need and the correct position of the electrodes based on the cuffs location. Throughout all the steps of walking, we had to observe carefully the position of the electrodes and the quality of the EMG signals. Finally, we had to motivate the individuals during the 120 minutes they participated in the experience.

We should also take into account the possible existence of delays between the detection of contact by the footswitches in relation to the real contact time. Those possible delays are usually ignored in scientific papers and, therefore, not mentioned.

There is more than one computational decomposition technique to extract motor modules and activation signals. We decided to use NNMF for this study, which may influence the quantitative results of the analysis in comparison with other methods, but it is unlikely that those differences qualitatively change the results. Besides, the most recent studies seeking for new modules during different motor tasks have been using NNMF methods as well [11] [12] [28].

The main characteristic roles of motor modules and activation signals during robotic-guided walking were identified in our study. Four modules were sufficient to reconstruct every phases of all gait cycles. Fewer modules were insufficient to correctly reconstruct the gait cycles. Module 1 mainly provides body support during the early stance phase. This module increases its contribution in response to increased robotic guidance. Module 2 is a major responsible of leg movement during late swing and preparation towards early stance. This module decreases its contribution (decrease activity of the hamstrings) in response to increased robotic guidance. Module 3 mainly contributes to control the propulsion of the foot during the last part of the stance phase. Module 4 provides mainly contribution to control

the ankle during early stance and early swing. Modules 3 and 4 contribute less significantly to the generation of torque during the tested conditions.

We verified that if the biomechanical requirements had changed during Lokomat walking, then the modular activation would also change. Motor modules were very similar among conditions and across individuals, whereas the activation signals varied much more according to the conditions of guidance force and speed. The computed motor modules and activation signals support the idea of a modular organization of the nervous system to produce walking and that a flexible modulation of this organization is sufficient to explain the walking under variations of robotic guidance force and speed. We believe that neuronal signals select, activate and combine in a flexible way (activation signals) specified by networks with constant motor modules in the spinal cord or in the brain stem.

The motor responses among different conditions of guidance force and speed can be described by the correlation values. High correlation values indicate a similar motor response between conditions and low correlation values indicate a different motor response between conditions. For rehabilitations purposes, we believe that future design and control strategies should induce similar synergistic activation patterns with the normal walking obtained in healthy subjects. Therefore, control strategies inducing different synergistic activation can have negative consequences for motor learning.

The modular control of the nervous system produced variations in muscular activation as a result of the type of robotic assistance. It is remarkable that in the present study is confirmed that robot-aided walking in general induces significantly different muscle activation patterns if compared to treadmill walking, in line with the results obtained by McGowan [59]. The reduced degrees of freedom on Lokomat are believed to be the reason to induce different muscular activation between Treadmill and Lokomat walking, especially when using higher guidance forces. Maybe the use of more degrees of freedom that allow pelvis and abduction movement, as well as the control of ankle movement could introduce new advantages to rehabilitation purposes. An electromyographic study of the walking in a rehabilitation device presenting those features could guide further development in robotic devices for gait training.

The biomechanical results gave us the basis to compare future biomechanical data of

post-stroke patients during robotic-aided walking, in comparison with healthy subjects. Future therapy design will be done based on these results.

The conclusions of this study with healthy subjects cannot be extrapolated to people with neurologic damages. We assume that those individuals exhibit different modular organization due to the injuries in some motor commands. Nevertheless, this study can be a basis of comparison between healthy subjects and individuals with neurologic injuries.

One of the contributes of our study is to have proposed a method to generate a motor control template for robotic-based rehabilitation of walking. Future design control strategies to be implemented in robotic gait trainers might be directed to promote similar modular control to the obtained in this study. Robotic devices to retrain human gait after brain damage should be adapted to train the nervous system to induce the required timing of activity generated by central pattern generator neurons that is directed to the motorneurons.

We also pretend to analyze the activity of more muscles simultaneously in order to verify more accurately the possible existence of more modules and how they act according to the amount of assistance provided by the exoskeleton. If researches identify which modules are affected post-stroke, it will be possible to develop focused therapies to retrain those modules. To achieve this goal, it is necessary to perform much more studies about the working of the modules in post-stroke patients during robotic-assisted walking, by testing many different therapies.

Finally, we believe that future directions on the rehabilitation orthoses field are the addition of more degrees of freedom to the individual's leg, as well as the implementation of complex control strategies to guide leg movements such as the 'assistance-as-needed' control algorithm. The addition of more degrees of freedom will allow more natural motion at later stage of rehabilitation. On the other hand, therapists can lock come joints if the patient is not sufficiently prepared to perform some movements without those joints being locked. Each exoskeleton should be capable of customize the training for every patient, according to their modular organization and kinematic/kinetic patterns. Assistance-as-needed should be controlled according to each gait phase and for all the joints. Each of these features mentioned above may result in more normative muscle activation patterns and provide new challenges

to the patient during the training, which can add more benefits to the recovery of people with neurologic injuries.

9.2 Future Work

Rehabilitation of gait disorders requires a step-forward to intervene with more accurate actions that rely on objective assessment of the patients' performance and recovery. This requires improvement in two key aspects:

- The assessment of pathologic gait in terms of biomechanics and neuromuscular performance in realistic conditions;
- Training of movement with feedback that is designed based on targeted neuromuscular and biomechanical patterns.

In the future, we pretend to develop novel means to ambulatory monitor and rehabilitate gait in stroke survivors by means of improved wearable sensing and exoskeletons technologies that are suitable for gait retraining in stroke, spinal cord and Parkinson disease (PD) patients and to gain a new insight into cognitive human-robot interface systems (Brain-neuronal computer interaction). Innovation comes from the hypothesis of a TOP-DOWN robotic approach for walking: neuro-physiological signals originated in the neural system can be used to complement biomechanical signals for both monitoring and control technologies used for neuro-rehabilitation. The PhD project is to be fitted in the framework of the HYPER (Spanish) and BETTER (European) projects coordinated by CSIC's Bioengineering Group. At the final, our results should include:

- New rehabilitation tools for future treatment and research.
- Advancement in current concepts of motor control of walking.
- Improved neuro-rehabilitation, involving enhanced motor learning in stroke survivors, spinal cord injured and/or PD patients.

Bibliography

[1] Paul Allard, Régis Lachance, Rachid Aissaoui, and Morris Duhaime. Simultaneous bilateral 3-d able-bodied gait. *Human Movement Science*, 15(3):327–346, 1996.

[2] K. Aminian, B. Najafi, C. Bula, P. F. Leyvrazc, and P. Robert. Spatio-temporal parameters of gait measured by an ambulatory system using miniature gyroscopes. *Journal of Biomechanics*, 35(5):689–699, May 2002.

[3] D. Aoyagi, W. E. Ichinose, S. J. Harkema, D. J. Reinkensmeyer, and J. E. Bobrow. A Robot and Control Algorithm That Can Synchronously Assist in Naturalistic Motion During Body-Weight-Supported Gait Training Following Neurologic Injury. *Neural Systems and Rehabilitation Engineering, IEEE Transactions on [see also IEEE Trans. on Rehabilitation Engineering]*, 15(3):387–400, 2007.

[4] F. Barroso, A. Frizera, C. Santos, and R. Ceres. Revisão crítica das ortóteses activas para membros inferiores. *VI Congresso Iberoamericano de Tecnologías de Apoyo a la Discapacidad*, 2:369–377, 2011.

[5] Nestor A. Bayona, Jamie Bitensky, Katherine Salter, and Robert Teasell. The Role of Task-Specific Training in Rehabilitation Therapies. *Topics in Stroke Rehabilitation*, 12(3):58–65, June 2005.

[6] N. Bernstein. *The Coordination and Regulation of Movements*. Oxford, UK: Pergamo, 1967.

[7] R.S. Bogey, L.A. Barnes, and J. Perry. Computer algorithms to characterize individual subject emg profiles during gait. *Arch Phys Med Rehabil*, 73:835–841, 1992.

[8] A Burden and R Bartlett. Normalisation of emg amplitude: an evaluation and comparison of old and new methods. *Med Eng Phys*, 21(4):247–57, 1999.

[9] Stephen M Cain, Keith E Gordon, and Daniel P Ferris. Locomotor adaptation to a powered ankle-foot orthosis depends on control method. *Journal of NeuroEngineering and Rehabilitation*, 4:13, 2007.

[10] G. Cappellini, Y. P. Ivanenko, R. E. Poppele, and F. Lacquaniti. Motor patterns in human walking and running. *J Neurophysiol*, 95(6):3426–3437, June 2006.

[11] V. C. Cheung, L. Piron, M. Agostini, S. Silvoni, A. Turolla, and E. Bizzi. Stability of muscle synergies for voluntary actions after cortical stroke in humans. *Proc Natl Acad Sci U S A*, 106:19563Ű–19568, 2009.

[12] David J. Clark, Lena H. Ting, Felix E. Zajac, Richard R. Neptune, and Steven A. Kautz. Merging of healthy motor modules predicts reduced locomotor performance and muscle coordination complexity post-stroke. *J Neurophysiol*, 103(2):844–857, February 2010.

[13] G. Colombo, M. Joerg, R. Schreier, and V. Dietz. Treadmill training of paraplegic patients using a robotic orthosis. *J Rehabil Res Dev*, 37(6):693–700, 2000.

[14] P.M. Conn. *Neuroscience in medicine*. Humana Press, 2008.

[15] ©Noraxon. Inline foot contact sensor. `http://www.noraxon.com/products/sensors/footswitch.php`. Accessed August 8, 2011.

[16] P.P. Correia and P. Mil-Homens. *A electromiografia no estudo do movimento humano*. FMH Edições, 2004.

[17] J.R. Cram and E. Criswell. *Introduction to Surface Electromyography*. Jones and Bartlett, 2011.

[18] T. DŠAlessio and S. Conforto. Attempting to solve estimation problems with an adaptive procedure for dynamic protocols. *IEEE Engineering in Medicine and Biology*, pages 55–61, 2001.

[19] Andrea D'Avella, Philippe Saltiel, and Emilio Bizzi. Combinations of muscle synergies in the construction of a natural motor behavior. *Nature Neuroscience*, 6(3):300–8, 2003.

[20] B. L. Davis and C. L. Vaughan. Phasic behavior of EMG signals during gait: Use of multivariate statistics. *J EMG Kinesiol*, 3:51–60, 1993.

[21] B.H. Dobkin. Strategies for stroke rehabilitation. *Lancet Neurol*, 3(9):528–36, 2004.

[22] Aaron M Dollar and Hugh Herr. Active orthoses for the lower-limbs: Challenges and state of the art. *2007 IEEE 10th International Conference on Rehabilitation Robotics*, 1(c):968–977, 2007.

[23] F.F. Evans-Martin and D.A. Cooley. *The Nervous System*. The Human Body, How It Works. Facts on File, 2009.

[24] E. Fernández-Peña, E. Lucertini, and M. Ditroilo. A maximal isokinetic pedalling exercise for emg normalization in cycling. *Journal of Electromyography and Kinesiology*, 19:162Ű–170, 2009.

[25] Daniel P Ferris and Cara L Lewis. Robotic lower limb exoskeletons using proportional myoelectric control. *Conference Proceedings of the International Conference of IEEE Engineering in Medicine and Biology Society*, pages 2119–2124, 2009.

[26] Society for Neuroscience. Tourette syndrome. `http://www.sfn.org/index.aspx?pagename=brainBriefings_tourette`. Accessed August 19, 2011.

[27] A.M. Gilroy, B.R. MacPherson, and L.M. Ross. *Atlas of anatomy*. Thieme Anatomy. Thieme, 2008.

[28] L. Gizzi, J.F. Nielsen, F. Felici, Y.P. Ivanenko, and D. Farina. Impulses of activation but not motor modules are preserved in the locomotion of subacute stroke patients. *J Neurophysiol*, 106(1):202–210, 2011.

[29] J. Hamill and K.M. Knutzen. *Biomechanical Basis of Human Movement*. Lippincott Williams & Wilkins, 2010.

[30] L.A. Harris. *CliffsAP Psychology*. CliffsAP Series. Wiley Pub., 2005.

[31] H. Hermens. Development of recommendations for SEMG sensors and sensor placement procedures. *Journal of Electromyography and Kinesiology*, 10(5):361–374, October 2000.

[32] H.J. Hermens, B. Freriks, and R. Merletti. *European recommendations for surface electromyography: results of the SENIAM project*. Biomedical and health research program. Roessingh Research and Development, 1999.

[33] J.A. Herring and M.O. and Tachdjian. *Tachdjian's pediatric orthopaedics from the Texas Scottish-Rite Hospital for Children*. W.B. Saunders, 2002.

[34] S. Hesse and D. Uhlenbrock. A mechanized gait trainer for restoration of gait. *Journal of rehabilitation research and development*, 37(6):701–708, 2000.

[35] J. Hidler, W. Wisman, and N. Neckel. Kinematic trajectories while walking within the Lokomat robotic gait-orthosis. *Clinical Biomechanics*, 23(10):1251–1259, December 2008.

[36] J. M. Hidler and A. E. Wall. Alterations in muscle activation patterns during robotic-assisted walking. *Clin Biomech (Bristol, Avon)*, 20(2):184–193, February 2005.

[37] A L Hof, H Elzinga, W Grimmius, and J P K Halbertsma. Speed dependence of averaged emg profiles in walking. *Gait & Posture*, 16(1):78–86, 2002.

[38] Jeffrey F. Israel, Donielle D. Campbell, Jennifer H. Kahn, and George T. Hornby. Metabolic costs and muscle activity patterns during robotic- and therapist-assisted treadmill walking in individuals with incomplete spinal cord injury. *Phys. Therapy*, 86(11):1466–1478, November 2006.

[39] Y. P. Ivanenko, R. E. Poppele, and F. Lacquaniti. Five basic muscle activation patterns account for muscle activity during human locomotion. *J Physiol*, 556(Pt 1):267–282, April 2004.

[40] Y.P. Ivanenko, G. Cappellini, N. Dominici, R.E. Poppele, and F. Lacquaniti. Coordination of locomotion with voluntary movements in humans. *The Journal of Neuroscience*, 25(31):7238–7253, 2005.

[41] Y.P. Ivanenko, R. Grasso, M. Zago, M. Molinari, G. Scivoletto, V. Castellano, V. Macellari, and F. Lacquaniti. Temporal components of the motor patterns expressed by the human spinal cord reflect foot kinematics. *J Neurophysiol*, 90(5):3555–65, 2003.

[42] J.W. Kalat. *Biological Psychology*. Wadsworth, Cengage Learning, 2008.

[43] J.J. Kaneko, J.W. Harvey, and M.L. Bruss. *Clinical Biochemistry of Domestic Animals*. Academic Press. Academic Press/Elsevier, 2008.

[44] P. Kao, C.L. Lewis, and D.P. Ferris. Invariant ankle moment patterns when walking with and without a robotic ankle exoskeleton. *J Biomech*, 43:203–209, 2010.

[45] P. Kao, C.L. Lewis, and D.P. Ferris. Joint kinetic response during unexpectedly reduced plantar flexor torque provided by a robotic ankle exoskeleton during walking. *J Biomech*, 43:1401–1407, 2010.

[46] C. Kirtley. *Clinical gait analysis: theory and practice*. Elsevier, 2006.

[47] Taryn Klarner, Henry K Chan, James M Wakeling, and Tania Lam. Patterns of muscle coordination vary with stride frequency during weight assisted treadmill walking. *Gait & Posture*, 31(3):360–365, 2010.

[48] T. S. Kuan, J. Y. Tsou, and F. C. Su. Hemiplegic gait of stroke patients: the effect of using a cane. *Archives of physical medicine and rehabilitation*, 80(7):777–784, July 1999.

[49] D. K. Kumar, N. D. Pah, and A. Bradley. Wavelet analysis of surface electromyography to determine muscle fatigue. *IEEE Transactions on Neural Systems and Rehabilitation Engineering*, 11(4):400–406, December 2003.

[50] Daniel D. Lee and H. Sebastian Seung. Learning the parts of objects by non-negative matrix factorization. *Nature*, 401(6755):788–791, October 1999.

[51] C.L. Lewis and D.P. Ferris. Walking with increased ankle pushoff decreases hip muscle moments. *Journal of Biomechanics*, 41:2082–2089, 2008.

[52] Chih J. Lin. Projected Gradient Methods for Non-negative Matrix Factorization. *Neural Comput.*, 19(10):2756–2779, October 2007.

[53] Hui-Ting Lin, Ar-Tyan Hsu, Jia-Hao Chang, Chi-Sheng Chien, and Guan-Liang Chang. Comparison of emg activity between maximal manual muscle testing and cybex maximal isometric testing of the quadriceps femoris. *Journal of the Formosan Medical Association Taiwan yi zhi*, 107(2):175–180, 2008.

[54] L. Lünenburger, G. Colombo, R. Riener, and V. Dietz. Biofeedback in gait training with the robotic orthosis lokomat. *Proceedings of the 26th Annual International Conference of the IEEE EMBS*, pages 4888–4891, 2004.

[55] Lars Lünenburger, Gery Colombo, and Robert Riener. Biofeedback for robotic gait rehabilitation. *Journal of NeuroEngineering and Rehabilitation*, 4(1):1+, January 2007.

[56] Laura Marchal-Crespo and David J. Reinkensmeyer. Review of control strategies for robotic movement training after neurologic injury. *Journal of NeuroEngineering and Rehabilitation*, 6(1):6–20, June 2009.

[57] N. Massó, F. Rey, D. Romero, G. Gual, L. Costa, and A. Germán. Surface electromyography applications in the sport. *Apunts Medicina de l'Esport*, 45(165):121–130, 2010.

[58] S. Mazzoleni, G. Stampacchia, E. Cattin, E. Bradaschia, M. Tolaini, B. Rossi, and M. C. Carrozza. Effects of a robot-mediated locomotor training on emg activation in healthy and sci subjects. *2009 IEEE 11th International Conference on Rehabilitation Robotics*, pages 378–382, 2009.

[59] Craig P. McGowan, Richard R. Neptune, David J. Clark, and Steven A. Kautz. Modular control of human walking: Adaptations to altered mechanical demands. *Journal of Biomechanics*, 43(3):412–419, February 2010.

[60] H. Mitsumoto. *Amyotrophic Lateral Sclerosis: A Guide for Patients and Families*. Demos Health Series. Demos Health, 2009.

[61] Juan C Moreno, Fernando Brunetti, Eduardo Rocon, and José Luis Pons. Immediate effects of a controllable knee ankle foot orthosis for functional compensation of gait in patients with proximal leg weakness. *Med Biol Eng Comput*, 46(1):43–53, 2008.

[62] Preeti M Nair, Kelly L Rooney, Steven A Kautz, and Andrea L Behrman. Stepping with an ankle foot orthosis re-examined: a mechanical perspective for clinical decision making. *Clin Biomech (Bristol, Avon)*, 25(6):618–622, 2010.

[63] R. R. Neptune and C. P. McGowan. Muscle contributions to whole-body sagittal plane angular momentum during walking. *J Biomech*, 44(1):6–12, January 2011.

[64] Richard R Neptune, David J Clark, and Steven A Kautz. Modular control of human walking: a simulation study. *Journal of Biomechanics*, 42(9):1282–1287, 2009.

[65] E. Newsholme and A. Leech. *Functional Biochemistry in Health and Disease*. John Wiley & Sons, 2009.

[66] Y. Nishijima, T. Kato, M. Yoshizawa, M. Miyashita, and H. Iida. Application of the segment weight dynamic movement method to the normalization of gait emg amplitude. *J Electromyogr Kinesiol*, 20:550–557, 2009.

[67] Marc F Norcross, J Troy Blackburn, and Benjamin M Goerger. Reliability and interpretation of single leg stance and maximum voluntary isometric contraction methods of electromyography normalization. *J Electromyogr Kinesiol*, 20(3):420–5, 2010.

[68] Jennifer R Nymark, Suzanne J Balmer, Ellen H Melis, Edward D Lemaire, and Shawn Millar. Electromyographic and kinematic nondisabled gait differences at extremely slow overground and treadmill walking speeds. *J Rehabil Res Dev*, 42(4):523–34, 2005.

[69] K. S. Olree and C. L. Vaughan. Fundamental patterns of bilateral muscle activity in human locomotion. *Biol Cybern*, 73(5):409–414, 1995.

[70] A. Parent and M.B. Carpenter. *Carpenter's human neuroanatomy*. Williams & Wilkins, 1996.

[71] S. H. Park and S. P. Lee. Emg pattern recognition based on artificial intelligence techniques. *IEEE Trans Rehabil Eng*, 6(4):400–405, 1998.

[72] A. E. Patla. Some characteristics of EMG patterns during locomotion: implications for the locomotor control process. *J Mot Behav*, 17:443–461, 1985.

[73] J. Perry. *Gait analysis: normal and pathological function*. SLACK, 1992.

[74] Victor R. Preedy and T.J. Peters. *Skeletal muscle: pathology, diagnosis and management of disease*. Greenwich Medical Media, 2002.

[75] M. B. Raez, M. S. Hussain, and Mohd F. Yasin. Techniques of EMG signal analysis: detection, processing, classification and applications. *Biological procedures online*, 8:11–35, 2006.

[76] J. A. Rathelot and P. L. Strick. Subdivisions of primary motor cortex based on cortico-motoneuronal cells. *Proc Natl Acad Sci U S A*, 106:918–23+, 2009.

[77] W.O. Reece. *Functional Anatomy and Physiology of Domestic Animals*. Wiley-Blackwell, 2009.

[78] R. Riener, L. Lünenburger, S. Jezernik, M. Anderschitz, G. Colombo, and V. Dietz. Patient-cooperative strategies for robot-aided treadmill training: first experimental results. *IEEE Trans Neural Syst Rehabil Eng*, 13(3):380–394, September 2005.

[79] Benjamin J. Sadock and Virginia A. Sadock. *Kaplan and Sadock's Synopsis of Psychiatry: Behavioral Sciences/Clinical Psychiatry*. Lippincott Williams & Wilkins, tenth edition edition, November 2008.

[80] G. Sawicki and D. Ferris. A pneumatically powered knee-ankle-foot orthosis (kafo) with myoelectric activation and inhibition. *J Neuroeng Rehabil*, 6(1):16, 2009.

[81] J. D. Schaechter. Motor rehabilitation and brain plasticity after hemiparetic stroke. *Prog Neurobiol*, 73(1):61–72, May 2004.

[82] Anne Schmitz, Amy Silder, Bryan Heiderscheit, Jane Mahoney, and Darryl G Thelen. Differences in lower-extremity muscular activation during walking between healthy older and young adults. *Journal of Electromyography and Kinesiology*, 19(6):1085–1091, 2009.

[83] L. Sherwood. *Fundamentals of physiology: a human perspective*. Brooks/Cole, 2006.

[84] L. Sherwood. *Human physiology: from cells to systems*. Human Physiology. Brooks/Cole, Cengage Learning, 2008.

[85] G. L. Soderberg. *Selected topics in surface electromyography for use in the occupational setting: expert perspectives*. U.S. Department of Health and Human Services, 1992.

[86] E.P. Solomon, L.R. Berg, and D.W. Martin. *Biology*. Brooks/Cole Thomson Learning, 2004.

[87] L H Ting and J M Macpherson. A limited set of muscle synergies for force control during a postural task. *Journal of Neurophysiology*, 93(1):609–613, 2005.

[88] Lena H H. Ting and J Lucas L. McKay. Neuromechanics of muscle synergies for posture and movement. *Curr Opin Neurobiol*, February 2008.

[89] Gelsy Torres-Oviedo and Lena H. Ting. Muscle synergies characterizing human postural responses. *Journal of Neurophysiology*, 98(4):2144–2156, 2007.

[90] Gerard J. Tortora and Bryan. *Principles of anatomy and physiology*. Wiley & Sons,, 11th ed. edition, 2006.

[91] M. C. Tresch, P. Saltiel, and E. Bizzi. The construction of movement by the spinal cord. *Nat Neurosci*, 2(2):162–167, February 1999.

[92] E. H. F. van Asseldonk, J. F. Veneman, R. Ekkelenkamp, J. H. Buurke, F. C. T. van der Helm, and H. van der Kooij. The Effects on Kinematics and Muscle Activity of Walking in a Robotic Gait Trainer During Zero-Force Control. *IEEE Trans. Neural Syst. Rehabil. Eng.*, 16(4):360–370, 2008.

[93] R. P. Van Peppen, G. Kwakkel, S. Wood-Dauphinee, H. J. Hendriks, P. J. Van der Wees, and J. Dekker. The impact of physical therapy on functional outcomes after stroke: what's the evidence? *Clin Rehabil*, 18(8):833–862, December 2004.

[94] James Watkins. *Structure and Function of the Musculoskeletal System*. Human Kinetics, 1999.

[95] A. Wernig, A. Nanassy, and S. Müller. Laufband (treadmill) therapy in incomplete paraplegia and tetraplegia. *J Neurotrauma*, 16(8):719–26, 1999.

[96] Kelly Westlake and Carolynn Patten. Pilot study of Lokomat versus manual-assisted treadmill training for locomotor recovery post-stroke. *Journal of NeuroEngineering and Rehabilitation*, 6(1), June 2009.

[97] W.C. Whiting and S. Rugg. *Dynatomy: dynamic human anatomy*. Number v. 10 in Dynatomy: dynamic human anatomy. Human Kinetics, 2006.

[98] D.A. Winter. *Biomechanics and Motor Control of Human Movement*. Wiley, 2009.

Appendix A

Pocket EMG Features

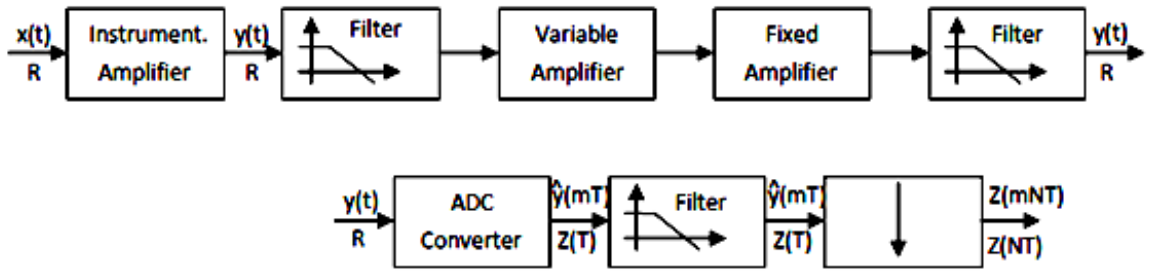

Figure A.1: Block Diagram of the components implemented in Pocket EMG. Courtesy of BTS

Instrumentation amplifier:

- Gain: fixed, selectable between 1 and 10000
- CMRR: 110 dB
- Noise Voltage: 10 nV/ Hz with frequencies up to 1 KHz
- Input resistance: $10^{10}\Omega$
- Common Mode Input Capacity: 4pF
- Differential Input Capacity: 1pF

Analog Filter:

- Type: High Pass
- Fcutoff: 15.7 Hz

Variable amplifier:

- Gain: variable between 0 and 255/256 in 256 steps

- Noise Voltage: 29 nV

Fixed Amplifier:

- Gain: fixed, 120
- CMRR: 95 dB
- Noise Voltage: 8 nV
- Common Mode Input Capacity: 8.8 pF
- Differential Input Capacity: 2.59 pF

Filter:

- Type: Analogic -20dB/dec
- Fcutoff: 1000 Hz

ADC Converter:

- Resolution: 16 bit
- Sampling frequency: up to 100 KHz. Standard = 20 KHz

Antialiasing Filter:

- Type: Digital, FIR lowpass (Kaiser Window), 16 tap.
- Fcutoff: 450 Hz with sampling frequency up to 1KHz, 750 Hz up to 2KHz and 1000 Hz for Fs= 2KHz

Decimation:

- 1, 2, 5, 10 KHz of the signal sampled at 20 KHz, according to the choosen sampling frequency

Appendix B

Electrodes location

It is necessary to place the participant in a starting posture to determine the correct location of the electrodes on each muscle (figure B.1), based in relative distances between anatomical landmarks (represented in figure 4.11). Finally, there were performed tests to check if the electrodes were effectively well fitted. All the procedures performed for each muscle are detailed in table B.1 and they were done according to the SENIAM recommendations [32].

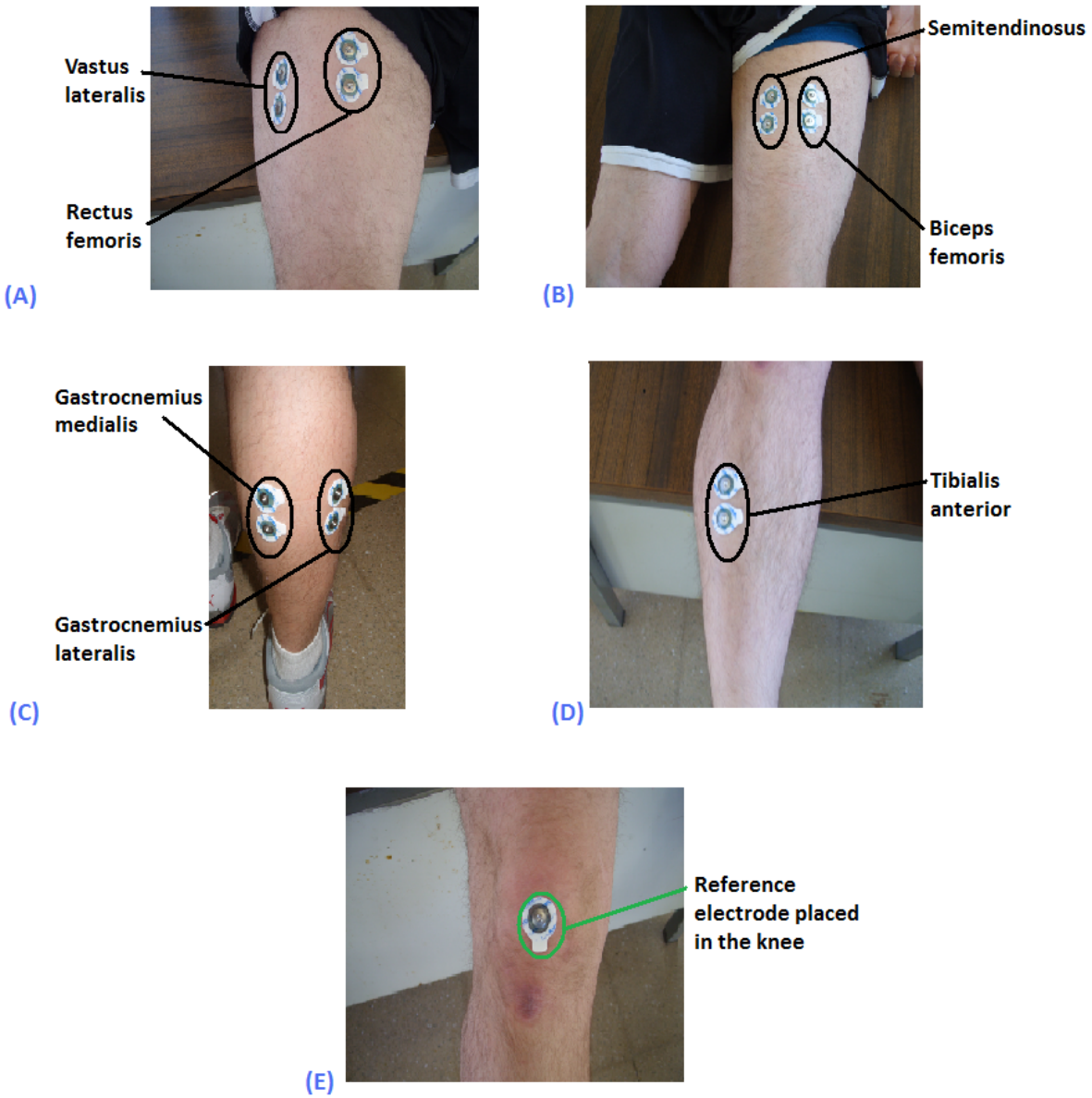

Figure B.1: Electrodes location in the seven muscles studied: (A) Rectus femoris and Vastus laterais, (B) Semitendinosus and Biceps femoris, (C) Gastrocnemius medialis and Gastrocnemius lateralis, (D) Tibialis anterior. (E) Reference electrode is placed in the knee.

Table B.1: Recommendations for the starting posture, electrodes location and tests of activity of the seven studied muscles on this work. Adapted from SENIAM [32]

Rectus femoris	
Starting posture	Sitting on a table with the knee in slight flexion and the upper body bend backward
Electrodes location	At the middle of the line between anterior superior iliac spine and the patella
Test	Extend the knee while applying force against the leg in the direction of flexion

Vastus lateralis	
Starting posture	Sitting on a table with the knee in slight flexion and the upper body bend backward
Electrodes location	At 2/3 on the line between anterior superior iliac spine and the lateral side of patella
Test	Extend the knee while applying force against the leg in the direction of flexion

Semitendinosus	
Starting posture	Lying on a table with the face down , the thigh touching on the table and the knee flexed approximately 45 degrees
Electrodes location	In the middle of the line between the Ischial tuberosity and the medial epycondyle of the tibia
Test	Press the leg in the direction of knee extension

Biceps femoris	
Starting posture	Lying on a table with the face down , the thigh touching on the table and the knee flexed approximately 45 degrees
Electrodes location	In the middle of the line between the Ischial tuberosity and the lateral epycondyle of the tibia
Test	Press the leg in the direction of knee extension

Gastrocnemius medialis	
Starting posture	Standing, with the ankle joint in plantarflexion
Electrodes location	On the most prominent bulge of the muscle
Test	Standing, in plantarflexion, with a bar or some other fixed platform making pressure against the shoulder

Gastrocnemius lateralis	
Starting posture	Standing, with the ankle joint in plantarflexion
Electrodes location	At 1/3 of the line between the head of the fibula and the heel
Test	Standing, in plantarflexion, with a bar or some other fixed platform making pressure against the shoulder

Tibialis anterior	
Starting posture	Sitting
Electrodes location	At 1/3 of the line between the tip of the fibula and the tip of medial malleolus
Test	Apply pressure against the medial side, dorsal surface of the foot, in the direction of plantarflexion of the ankle joint

Appendix C

Matlab functions to implement NNMF

```
function [W,H] = nmf(V,Winit,Hinit,tol,timelimit,maxiter)

% NMF by alternative non-negative least squares using projected gradients
% Author: Chih-Jen Lin, National Taiwan University

% W,H: output solution
% Winit,Hinit: initial solution
% tol: tolerance for a relative stopping condition
% timelimit, maxiter: limit of time and iterations

W = Winit; H = Hinit; initt = cputime;

gradW = W*(H*H') - V*H'; gradH = (W'*W)*H - W'*V;
initgrad = norm([gradW; gradH'],'fro');
fprintf('Init gradient norm %f\n', initgrad);
tolW = max(0.001,tol)*initgrad; tolH = tolW;

for iter=1:maxiter,
  % stopping condition
  projnorm = norm([gradW(gradW<0 | W>0); gradH(gradH<0 | H>0)]);
  if projnorm < tol*initgrad | cputime-initt > timelimit,
    break;
  end

  [W,gradW,iterW] = nlssubprob(V',H',W',tolW,1000); W = W'; gradW =
gradW';
  if iterW==1,
    tolW = 0.1 * tolW;
  end

  [H,gradH,iterH] = nlssubprob(V,W,H,tolH,1000);
  if iterH==1,
    tolH = 0.1 * tolH;
  end

  if rem(iter,10)==0, fprintf('.'); end
end
fprintf('\nIter = %d Final proj-grad norm %f\n', iter, projnorm);
```

Figure C.1: Function nmf (). Used with permission from [52]

```
function [H,grad,iter] = nlssubprob(V,W,Hinit,tol,maxiter)

% H, grad: output solution and gradient
% iter: #iterations used
% V, W: constant matrices
% Hinit: initial solution
% tol: stopping tolerance
% maxiter: limit of iterations

H = Hinit; WtV = W'*V; WtW = W'*W;

alpha = 1; beta = 0.1;
for iter=1:maxiter,
  grad = WtW*H - WtV;
  projgrad = norm(grad(grad < 0 | H >0));
  if projgrad < tol,
    break
  end

  % search step size
  for inner_iter=1:20,
    Hn = max(H - alpha*grad, 0); d = Hn-H;
    gradd=sum(sum(grad.*d)); dQd = sum(sum((WtW*d).*d));
    suff_decr = 0.99*gradd + 0.5*dQd < 0;
    if inner_iter==1,
      decr_alpha = ~suff_decr; Hp = H;
    end
    if decr_alpha,
      if suff_decr,
    H = Hn; break;
      else
    alpha = alpha * beta;
      end
    else
      if ~suff_decr | Hp == Hn,
    H = Hp; break;
      else
    alpha = alpha/beta; Hp = Hn;
      end
    end
  end
end

if iter==maxiter,
  fprintf('Max iter in nlssubprob\n');
end
```

Figure C.2: Function nlssubprob (). Used with permission from [52]